UNIVERSITÀ POLITECNICA DELLE MARCHE

Department of Agricultural, Food and Environmental Sciences

Doctoral School in Agricultural, Food and Environmental Sciences

20th cycle (2018-2021)

Detection and effects of climate extremes on Mediterranean forests

Doctoral final dissertation

PhD candidate
Dott. Enrico Tonelli (LM)

Supervisors
Prof. Carlo Urbinati, PhD

Dott. Alessandro Vitali, PhD

Ancona, February 28th, 2022

Table of contents

Abstract

Research on occurrence and effects of natural and anthropogenic disturbances on forests is largely widespread around the globe. The Mediterranean basin due to its geographic but also socio-economic features, is one of the regions where climate changes are expected to affect the most forests and ecosystems in general. With this research we have integrated different methodologies to study the effects of climate induced disturbances on different Mediterranean forests. In particular, we focused on the detection and the intensity, of climatic stress on tree growth in some deciduous forests. We conducted analyses at population and individual tree-level using mainly tree-ring series to assess the species and individual sensitivity to spring frost (Central and Southern Apennines, Italy) and to summer drought (and thinnings) (Sub-Pyrenees, Spain), detecting occurrence of extreme events and post-disturbance radial growth recovery and resilience. Within a sub-sample (Central Apennines) we also analysed time series of wood anatomical traits to extract possible alteration signals on tree inner structure. Finally, we applied remote sensing analysis for the spatio-temporal detection of late frost effects on forest cover. We also checked how reliable are short tree-ring series for assessing climate-growth relationship.

This report, after an overall introduction, is organized as a compilation of: one published article (Chapter 2), one manuscript under review (Chapter 3), one in preparation (Chapter 4) and one ready for submission (Chapter 5). Each chapter stands alone, containing its own introduction, materials and methods, results, discussion, conclusions (and eventually supplementary materials). A short general conclusion chapter and a general reference list are closing the report.

Chapter 2 is a dendrochronological study conducted on naturally regenerating European black pines (*Pinus nigra* J.F.Arnold) aimed to identify the potential and limitations of young trees in recording climate signals. The results confirm the presence of individualistic growth trends in many studied trees, but also the ability of the population to respond uniformly following particularly favourable or unfavourable growing seasons.

Chapter 3 is a study on European beech (*Fagus sylvatica* L.) sensitivity to spring frosts in the Apennines forests, in collaboration with the University of Padova (UNIPD, Italy), the University of Basilicata (UNIBAS, Italy) and the Pyrenean Institute of Ecology (IPE,

Zaragoza, Spain). Here we combined tree-ring and remote-sensing data to assess the vulnerability and the recovery capacity of beech populations to late frosts. Late frost occur in spring and defoliation rates are strictly related to the forest leaf phenology and stand elevation. Mature beech trees revealed to be resilient and to recover rapidly their growth trends, showing no legacy effects.

Chapter 4 presents the preliminary results of an ongoing study aimed to search the effects of late frost events on fine wood anatomical traits in beech tree-rings. We conducted the anatomical slide preparation in the laboratories of the Department of Land, Agriculture and Forestry Systems (TESAF) at UNIPD. Frost events do not seem to affect the plasticity of vessel traits, which could be more related to the tree size (especially tree height) and to stand elevation.

Chapter 5 is a study in collaboration with IPE Zaragoza, Spain for assessing the radial growth response to thinning and drought of *Quercus subpyrenaica*. Drought events limit the radial growth of trees, and the effects are clear when the trees are in a release phase, for example after thinning. Trees in thinned plots have higher basal area increment (BAI) even in co-occurrence of drought events, and recovery periods do not differ between thinned and unthinned plots.

Trees change their phenotypic traits in response of extreme climate condition, not only in terms of vegetation greenest or leaf area but also in inner structure (e.g. tree rings and xylem anatomical traits). For this reason, only a multiscale and multidisciplinary approaches allow to identify all the impact of the ongoing climate variability. The resulting information can guide sylvicultural strategies to better adapt forests to climate change.

Chapter 1

General introduction and research aim

Climate change affects forest ecosystem differently, and in some cases in opposite ways. For instance, boreal forests are likely to feature transitory beneficial effects, with an increase of productivity due to raising CO_2 concentration and warming that directly improve use efficiencies of plants (Bussotti et al. 2015, D'Orangeville et al. 2018). In Mediterranean forests effects are predominantly negative, with projected increase in frequency of climate-change induced disturbances, mostly fires, droughts, pests, and windstorm (Maracchi et al. 2005; Tuel and Eltahir 2020; Carnicer et al., 2013, Vayreda et al., 2016). In addition, tree spring phenology is largely influenced by climate warming which could induce an earlier leaf unfolding and increase sensitivity to abrupt frost damage (Čufar et al. 2008, Menzel et al. 2011). In Europe, the ongoing climate variability also significantly increased the frequency of late (spring) frosts (Augspurger 2013; Zohner et al. 2020), that can reduce tree growth and productivity of widely distributed forest tree species.

For years, the forests played relevant socio-economic roles in Mediterranean countries, but since the early 19th century forests were gradually but largely abandoned. In this context, sustainable forest management is a key forestry issue, especially in the Mediterranean countries where scenarios of warmer and drier climate conditions are forecasted (Vila-Viçosa et al. 2020). Forest management strategies such as thinning or understory treatments induce short-term benefits but may not result in long-term adaptation to global change, that can be achieve promoting mixed forests or changes in species or genetic composition (Vilà-Cabrera et al. 2018).

In this dissertation, the forest disturbances caused by spring frost and drought conditions will be specifically treated, studying their carry over effects and the interaction of management practices.

In temperate forests, late frosts, occurring in spring, consist of extreme and abrupt temperature drops within a period of mild climate conditions (Augspurger 2009). In European hardwood species such as beech (*Fagus sylvatica* L.) below-zero temperatures in early spring can damage recently unfolded leaves causing leaf shedding, and limit radial growth (Dittmar et al. 2003, 2006, Gazol et al. 2019, Vitasse et al. 2019, Sangüesa-

Barreda et al. 2021). Late frosts frequency and their effects on beech forests pose several questions concerning post-disturbance recovery. In mature beech trees, old carbohydrates can rapidly be mobilized to produce a second cohort of leaves after damage (D'Andrea et al. 2019). Beech leaf defoliation after late frosts is commonly reported both in central Europe (e.g., Dittmar et al. 2006, Vitasse et al. 2019) and in Mediterranean mountains at the southernmost species distribution limit (Gazol et al 2019), causing abrupt reduction in tree stem growth. In 2016 and 2017 two extended late frost events occurred in the Central and Southern Apennines (Italy) approximately affecting 5,000 km^2, one third of the beech forest surface area in Italy (Nolè et al. 2018, Bascietto et al. 2018, 2019). Effects of late frost events vary on beech stands depending on site elevation and ongoing phenology. Remote-sensing data show that trees at high-elevation with a later leaf unfolding can be less affected than those at mid- and low-elevation (Nolè et. al 2018).

In southern Europe growth and productivity of the same forests (beech but also oak forests) can also be severely constrained by summer drought (Piovesan et al. 2008, Geßler et al. 2007, Gazol et al. 2019, Tognetti et al. 2019), a key factor determining the southernmost or xeric edge of many broadleaf and conifer species (Jump et al. 2006, Bolte et al. 2007, Serra-Maluquer et al. 2019). Tree growth rates are related to climate conditions, and each species has specific temperature and precipitation ranges. Under climate warming conditions there is an increasing probability that air temperatures and evapotranspiration rates could exceed the relative optimum thresholds. In the past decades, Europe has experienced a substantial increase of shorter warm-season droughts together with an increase in potential evapotranspiration that have also caused socioeconomic losses and environmental impacts (Markonis et al 2021, Vicente-Serrano et al. 2021, Büntgen et al. 2021). Individual tree growth responses to drought events can vary according to tree size and forest spatial and chronological structure (D'Amato et al. 2013; Schwarz & Bauhus 2019, Bottero et al. 2017; Andrews et al. 2020). Trees feature different sensitivity to dry conditions in sites with different soil water holding capacity, stand density and slope (Zalloni et al. 2019). Trees in dense forests are more water stressed and show lower radial growth, suggesting greater vulnerability to drought (Moreno-Gutiérrez et al. 2012). Selective thinning targeting larger trees could not only reduce competition for residual trees but also increase their resistance to upcoming severe drought events (Bose et al. 2021).

Detection of these climate induced disturbances can occur in different ways according to the observation scale and the details we need to provide. In this research we used a combination of tree-ring analysis and remote sensing.

The specific spectral signature of brown-colored foliage after disturbance events such as late frost or summer droughts can be detected by satellite multispectral imagery and used to assess the geographic extension and the severity of such disturbances at broad spatial scales and in remote sites (Allevato et al. 2019, Decuyper et al. 2020, Olano et al. 2021). Multispectral satellite images are widely used in vegetation studies. Satellite-based sensors such as MODIS (Moderate Resolution Imaging Spectroradiometer) provide images at moderate spatial resolution (250m) and a revisiting time of globe in 1 – 2 days and they are particularly performing for the study of disturbances affecting large forest areas. Other satellite products such as Sentinel and Landsat images, allow the study of vegetation at regional or population scale. Commercial satellite imagery can go as far as sub-meter resolutions and provide more detailed information up to individual responses. From the multispectral satellite images, it is also possible to derive vegetation indices, which are very useful for quantifying the intensity and duration of stress. NDVI (Normalized Difference Vegetation Index) is the most widely used vegetation index and is not only related to canopy structure and LAI, but also to canopy greenness and cover (Xue and Su 2017). NDVI uses NIR and Red ranges of the spectrum and its values are between -1 and 1 (Rouse et al. 1974). Positive NDVI values between 0.3 and 0.8 usually refer to vegetation canopy with a high cover and greenness values. However, since NDVI is sensitive to soil brightness and atmosphere conditions, the use of EVI (Enhanced Vegetation Index) can simultaneously correct these noises (Liu and Huete 1995, Huete et al. 2002). EVI includes a gain factor, soil adjustment parameters, two correcting coefficients for aerosol influences in the red band, and reflection in the blue band (Henrich et al. 2009).

Growth limitation caused by late frost or drought events can also be investigated with multiple methods of tree-ring analysis. Dendroecology is a scientific approach based on dendrochronological methods to study ecological processes related to forest ecosystems (Fritts & Swetnam 1989). One of the most important postulates in dendrochronology is the principle of aggregate tree growth, where the total seasonal growth is the result of many interacting factors (tree age, climate, endogenous and exogenous disturbance, annual variability in nutrient availability and carbon allocation and random error).

Intensity and duration of the effects of a predominant limiting growth factor vary annually until it is no longer limiting. The rate of plant processes will increase until another factor becomes limiting (Fritts 1976). Tree age cause a low frequency variation in tree ring series, also known as age related trend. To enhance the contribution of climate in ring formation, low frequency variance could be removed. This detrending (Bontemps & Esper, 2011) or standardization (Fritts, 1976; Briffa & Melvin, 2011) of the tree-ring series transforms raw data into indexed time series including only the high frequency variance. In most dendroecological studies ring-width indices are averaged for many trees to reduce the "noise" of random errors and non-climatic variations in growth. However, in ecologically based climate sensitivity studies the individual growth variability is another important information to be considered (Carrer 2011), which becomes fundamental for assessing the impacts of extreme events in forest trees. Tree-ring research has recently expanded in the science of wood anatomy (Büntgen 2019). The integration of wood anatomical parameters in time series analyses allow to use several proxies for assessing study disturbances in tree species, increasing the resolution of climate-growth analysis (Carrer et al., 2015).

The cumulative effects of disturbance events on trees and forests can be assessed through their resilience changes. In ecological studies, resilience is defined as the capacity of a natural ecosystems, communities, or individuals to recover after disturbance and regain its pre-disturbance structure and function (Scheffer et al. 2001, Folke et al. 2004, Lloret et al 2011). In this regard, tree-rings series represent one of the most effective proxies for the study of post disturbance legacy effects on trees. Lloret et al (2011) proposed different indices (resilience components) to quantify how tree growth in a forest system respond to a disturbance event: i) Resistance, the ratio between the performance during and before the disturbance, ii) Recovery, the ratio between performance after and during disturbance and iii) Resilience, the ratio between the performance after and before disturbance.

The main aim of this research is to integrate different methodologies to study the effects of climate induced disturbances on Mediterranean forests. Detection, intensity and legacy effects of spring frost and summer drought on tree growth disturbances were studied applying dendrochronology, quantitative wood anatomy and remote sensing derived data. Analyses were at different temporal and spatial scales focusing both on population and individual tree-level responses.

In detail, (i) we aimed to identify the potential and limitations of young trees in recording climate signals in a dendrochronological study conducted on naturally regenerating European black pines (*Pinus nigra* J.F.Arnold). Then, (ii) we assessed spring frosts sensitivity of European beech (*Fagus sylvatica* L.) in Mediterranean mountain forests. We used satellite imagery analysis to detect and quantify frost events occurred in the Apennines, and after appropriate site selection we applied dendroecological analysis to discriminate between affected and non-affected populations and assessing their resilience at stand scale along an altitudinal gradient. In one of the sites, (iii) we used the dendroanatomy to search frost signals within the annual ring microstructure of selected individuals. Finally (iv) we assessed the summer drought impact on tree growth in a mixed *Quercus subpyrenaica* forest in the pre-Pyrenees (Spain) that was also subjected to previous thinning. We focused on post thinning legacies in trees sensitivity to summer dry periods. We used dendroecology to quantify the resistance, recovery, and resilience of thinned and unthinned stands.

Our hypotheses are that: (i) despite individualistic growth trends linked to microsite characteristics, young trees respond uniformly to unfavorable climatic conditions; (ii) the spring frosts do not have uniform effects on the beech forests with intensities that depend on the elevation and bud burst timing; (iii) the anatomical features of the xylem provide additional indications for detecting climatic disturbances and (iv) thinning can increase the resistance and resilience of forest stands to drought disturbances.

Chapter 2

Are young trees suitable for climate-growth analysis? A trial with *Pinus nigra* in the central Apennines treelines

This chapter has been revised and accepted for publication on 22nd May 2020:

Tonelli, E.[a], Vitali, A.[a], Piermattei, A.[b], & Urbinati, C.[a] (2020). Are young trees suitable for climate-growth analysis? A trial with Pinus nigra in the central Apennines treeline. Dendrochronologia, 62, 125720. https://doi.org/10.1016/j.dendro.2020.125720

[a]Department of Agricultural, Food and Environmental Sciences, Marche Polytechnic University, Via Brecce Bianche 10, 60131 Ancona, Italy

[b]Department of Geography, University of Cambridge, Downing Place, CB2 3EN Cambridge, United Kingdom

Abstract

In the context of ecological research, growth-ring analysis often deals with short time series (< 30 years). Their crossadting and averaging can be difficult but crucial to use such data for ecological modelling, multivariate statistics and climate-growth analysis. Several studies were conducted in the Central Apennines (Italy) on recent encroachment of European black pine (*Pinus nigra* J.F. Arnold) on treeless areas above the current forestline. Growth of young trees is mainly controlled by endogenous or microclimatic factors making usual dendrochronology methods less applicable and crossdating very difficult or even impossible. The ecological information potential deriving from tree-ring growth in short series is therefore severely limited by this methodological bias. The aim of this study is to test suitable methods for optimizing the use of short ring series for further analytical use. A dataset of 734 tree-ring series of young European black pine (mean cambial age of 15 years) all growing at high altitude was used in this analysis. At each site the growth-ring series were divided in two groups: the crossdated or selected series (SEL), and non-crossdated or rejected ones (REJ). At each site the following dendrochronological parameters were calculated for SEL and REJ series: mean tree-ring width (TRW), mean sensitivity (MS), Gini coefficient (G), first order autocorrelation (AC1), interseries correlation (Rbar) and Gleichläufigkeit (glk). Two methods of pointer years analysis were tested in order to detect years with synchronous growth: i) Normalization in a moving Window (NW) and ii) the RElative growth change method (RE). The two methods were applied to the raw series varying the proposed standard thresholds, in order to detect synchronous growth-years in SELs and REJs groups. A sensitivity analysis was included to assess how the thresholds choice in the analysis could affect the results obtained. 47% of all trees were classified as SEL. The term "common" was used to indicate years with similar tree growth response. Differences in the detected number of common (*sensu* pointer) years within SEL and REJ were found changing the time windows in the RE and NW methods. The SEL series have more common years than the REJ series, but the same occurs considering all the series together without SEL/REJ discrimination. In general, a significant occurrence of common years could be a tool to select series to be averaged for a site mean chronology. These are preliminary but encouraging results contributing to a more efficient use of the ecological information provided by short time series from young trees.

Keywords: European black pine; Italy; dendrochronology; short growth series; crossdating; pointer years

1. Introduction

Growth-ring series are among the most accessible and reliable ecological proxies. They occur worldwide in woody species, have an annual (also sub-annual) resolution, and are very sensitive to many ecological and environmental processes (Fritts,1976; Schweingruber, 1996; Speer,2010; Zhang, 2015). In dependence of cambial age at the date of sampling and on the size and integrity of wood in archaeological finds, the length of growth-ring series can vary from very few to thousands of years. In time series analysis, the minimum number of observations, regardless of the field of application (ecology, climatology, earth or life sciences, etc.) depends on different features such as the temporal resolution of the data (daily, monthly, yearly, decadal), the number of variables involved and the purpose of the analysis. The "magic" number of 30 observations, commonly considered as minimum threshold, is not proven to be always applicable and some authors suggest using at least 60 (or even 100) observations, that would be 60 years for annually resolved data but 5 years for monthly data. Dendroclimatology requires long tree-ring series for climate reconstruction but most of the climate records around the world are about 60-70 years long (Zhang, 2015) and only a limited number extend over 100 years (Auer et al., 2007; Camuffo et al., 2010). In dendroecological studies long-lived species and individuals are usually preferred especially when the aim is to detect specific disturbance return intervals or to assess their spatio-temporal regimes (Copenheaver and Abrams, 2003).

Nonetheless, there are several studies demonstrating the variability of the climate-growth relationships in trees of different cambial age or stadial stage (Sczeic and MacDonald, 1994; Carrer and Urbinati, 2004; He et al., 2005; Campelo et al., 2013; Sanchez-Salguero et al., 2018; Hanna et al., 2019; Piermattei et al. 2020). For instance, trees at juvenile stages have a reduced and shallower root system than adult trees and their development is more likely influenced by microclimate and site-specific variables than by regional climate patterns (Thomas et al., 2002; Chhin and Wang, 2008). If growing in the understory layer inside forests, juvenile trees likely feature a more beneficial micro-climate which makes them less susceptible to extreme climatic conditions respect to

isolated individuals in open areas (Aussenac, 2000; Kovács et al., 2017; De Frenne et al., 2019; Zellweger et al., 2019) but, at the same time, they experience stronger competition by dominant tree layer and understory vegetation (Bigler and Bugman, 2003; De Lombaerde et al., 2019).

However, most of these cited studies refer to consolidated forest environments where it is possible to compare growth responses of trees at different life stages (seedling, sapling, adult or senescent) or growing in different canopy layers. Nonetheless in more dynamic contexts, such as the initial seral stages after ecological disturbances, there is a scarce or no occurrence of multi-aged cohorts of trees (e.g. seral stages of ecological succession such as formation of new forests in fallow lands, treeline upshift, pioneer vegetation in geomorphic active fluvial vegetation, etc.) (Bätz et al., 2016; Piermattei et al., 2016; Vitali et al., 2017). In these cases, growth-ring analysis can often be performed mainly with tree-ring series shorter than 30 years. Given the above-mentioned specific growth conditions, juvenile trees often feature ring-width characteristics that make series crossdating and averaging very challenging, if not impossible.

Moreover, it is difficult to detect missing rings or match event years when chronologies of neighbouring older stands are not available. On the other hand, short series synchronization and averaging is mandatory for applying growth data to ecological modelling, multivariate statistics and climate-growth analysis. The outlined problems associated with crossdating juvenile trees result in a potential underrepresentation of studies on recent vegetation dynamics, particularly in areas where longer reference chronologies are missing, e.g. tree-line ecotones.

This question arose repeatedly throughout recent studies conducted in the Central Apennines in Italy, where European black pine (*Pinus nigra* J.F. Arnold) has naturally expanded on treeless areas above the closed forest limit (Fig. S1), with several cohorts of seedlings, saplings and young trees unexpectedly reaching high elevations (Piermattei et al., 2016; Vitali et al., 2017).

The main scope of this study was to test a suitable and objective method to discriminate among the most and the least fitted short growth-ring series based on interseries correlation, using the suitable ones for commonly applied chronology building. We proposed a pointer years analysis to detect years of synchronous growth and to check if rejected series retain ecological information.

2. Material and methods

2.1 Tree ring dataset

To demonstrate the performance of the proposed method, we used 734 tree-ring series of European black pine collected at eight sites across the central Apennines (Italy) (Fig. 1, Tab.1) (Piermattei et al., 2013; 2014; 2016; Vitali et al., 2017). All sampled individuals were naturally encroached at eight mountain treeline ecotones, ranging from 1800 and 2100 m a.s.l.. They originated from *Pinus nigra* stands extensively planted during the 20th century at lower altitude (1500-1600 m a.s.l.). This species was selected for its pioneering and rapid land covering capacity to reduce the severe slope erosion originated by former deforestation and intensive pastoral use (Isajev et al., 2004; Vitali et al., 2017). Tree-ring series span the period 1960-2015 with a common overlap period from 1994-2008 and a mean cambial age of 15.3 years (SD = 6.8) (Fig. S2). For all individuals, in addition to an increment core extracted at the stem base, basal diameter and total height were measured, with resulting mean values of 12.7 cm and 2.13 m, respectively (Tab. 1).

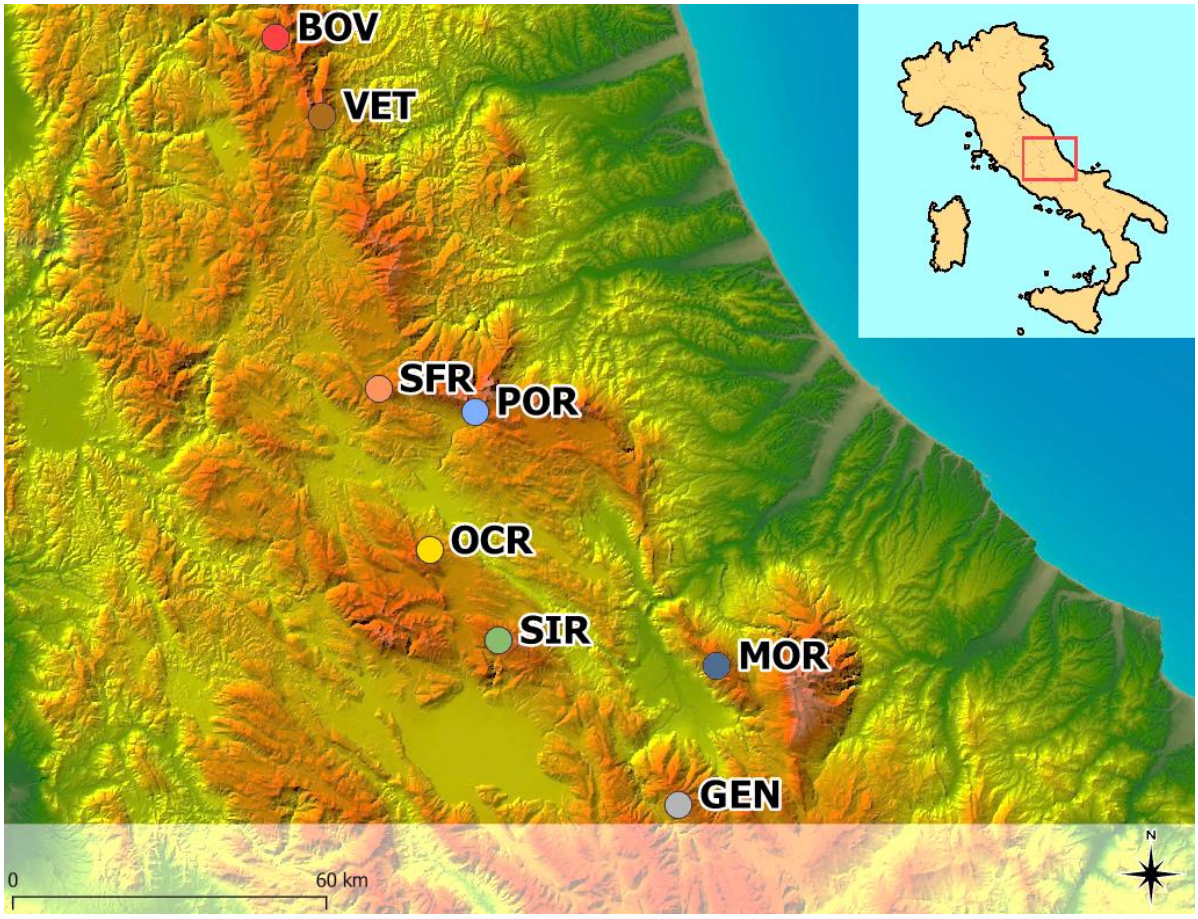

Figure 1 – Location of the eight black pine sites at high elevation in the central Apennines (Italy): BOV (Mt. Bove); VET (Mt. Vettore); SFR (Mt. San Franco); POR (Mt. Portella); OCR (Mt. Ocre); SIR (Mt. Sirente); MOR (Mt. Morrone) and GEN (Mt. Genzana). Forestline elevations are reported in Table 1.

Table 1 - Main features of the sampled trees in the eight study sites. For each site is reported the amount of sampled trees (N. TREES), the average tree-ring width (TRW), the basal stem diameter (Bd), the total height (H), the sampling year, the average cambial age, the main aspect, the average slope, the forest line elevation, and the geographical coordinates (Lat./Long.). The standard deviations are in brackets.

SITE	N. TREES	Avg. TRW (±SD) [mm]	Avg. Bd (±SD) [cm]	Avg. H (±SD) [cm]	Sampling year	Avg. AGE (±SD) [years]	Main aspect	Avg. elope [%]	Forestline elevation [m a.s.l.]	Lat./Long.
BOV	71	3.4 (1.25)	13 (8.2)	241 (176)	2015	12 (6)	SW	49	1715	42°54'/13°11'
VET	149	1.89 (1.03)	10 (7.3)	169 (142)	2008	14 (7)	SE	35.8	1600	42°81'/13°26'
SFR	108	2.36 (0.93)	12.6 (7.3)	204 (132)	2011	14 (7)	SW	32	1500	42°45'/13°38'
POR	20	2.31 (0.97)	11.9 (4.9)	192 (98)	2014	12 (3)	SW	53	1740	42°26'/13°31'
OCR	134	1.8 (1.00)	10.6 (5.2)	168 (100)	2012	15 (5)	NE	54	1635	42°15'/13°27'
SIR	133	2.8 (1.16)	16.7 (8.3)	282 (153)	2012	17 (7)	SW	19	1650	42°15'/13°60'
MOR	84	2.41 (0.93)	13.4 (5)	217 (90)	2014	15 (4)	SW	32	1542	42°06'/13°57'
GEN	35	2.51 (1.22)	14.5 (8.4)	271 (260)	2014	18 (6)	SW	30	1705	41°56'/13°53'

All cores were mounted on wooden supports and thoroughly polished with progressively finer sandpaper. Tree-ring width measurements, at 0.01 mm accuracy, were provided by the semi-automatic LINTAB system WinTSAP (Rinntech). Crossdating was attempted both visually and with COFECHA software, comparing each series with the relative mean site chronology. Then, critical Pearson correlation coefficients (one tail) at 95% confidence level, variable with series lengths (Tab. S1) were used as a threshold to discriminate in each site between: i) the synchronized (SEL - selected) and ii) the non-synchronized (REJ - rejected) time series. We decided to use the critical values corresponding to the 95% confidence level as thresholds because 99% confidence level were too selective (Tab. S2). Correlation coefficients were calculated between mean site chronologies and raw series without autoregressive model and logarithms transformation.

2.2 Statistical and pointer year sensitivity analysis

For each series the following dendrochronological parameters were calculated: mean tree-ring width (TRW), mean sensitivity (MS), Gini coefficient (G), first order autocorrelation (AC1), interseries correlation (Rbar) and Gleichläufigkeit (glk). Cambial age, tree height and basal stem diameter were compared between the SEL and REJ groups using a two-sided Wilcoxon test. Statistical analyses were run using the R "stats" package (R Core Team, 2018). Two different methods to detect pointer years were compared and assessed using the R package PointRes (van der Maaten-Theunissen et al., 2015): the Normalization in a moving Window (NW) (Cropper, 1979) and the RElative growth change method (RE) (Schweingruber et al., 1990). The NW method delivers Cropper values (*zi*) series by normalizing tree-ring series in moving windows, whereas RE method is based on the calculation of the individual relative radial growth variation by comparison of ring-width of a particular year with the average ring width of the preceding years. NW and RE methods were applied to raw series changing the proposed standard thresholds in order to detect synchronous growth-years in SELs and REJs groups. Different threshold of Cropper values (*zi*) or growth changes, proportion of trees to be considered for pointer years and window size were compared in a sensitivity analysis to provide a more objective series selection (Tab. 2). In NW method we considered $|zi|$ of 0.60, 0.75, 0.85 and 1 as event years. We tested the NW method using a 5-years (NW5) and a 3-years moving window (NW3). We decided to consider the 3-year moving window to carry out the analysis over as many years as possible even in the shortest series. With RE method we defined an event year when the growth variation (30%, 40%, 50% and 60% increase or 20%, 25%, 30% and 40% decrease respectively) occurred in a given year compared to the previous one (RE1) or to the four preceding years (RE4). With all methods (NW3, NW5, RE1, RE4) we retained a "common" year when the event year occurs in 50%, 60% or 75% of the series (series threshold). Some of the thresholds tested in the sensitivity analysis are generally less conservative as commonly used for pointer years analysis. Indeed, our goal was to detect in each study site those years when most of the series had a similar growth (positive or negative). The rings corresponding to the years detected were not always neither very narrow nor very wide, so we decided to use the term "common years" (CY) instead of pointer years. The occurrence of CY was then visually compared at different sites and between SEL and REJ groups.

Table 2: Methods and thresholds used in sensitivity analysis. *Zi* is the Cropper value and the sample depth is the minimum number of series required.

Methods	Window width (yrs)	|*zi*| threshold	Growth change threshold (positive and negative)	Series threshold (%)	Sample depth
NW	3/ 5	0.60/0.75 /0.85/1	-	50/60/75	10 series
RE	1/ 4	-	30-20/40-25/50-30/60-40	50/60/75	10 series

3. Results

3.1 Statistics of selected and rejected series

Globally, 47% of the tree-ring series have been classified as SEL, with site shares ranging between 37-65%. The number of REJ series is relatively high and in 5 sites of 8 exceeds that of SEL series. The average ring widths at two study sites were significantly higher ($\alpha = 0.05$) in the SEL group but not statistically different in the other sites (Tab. 2). At three sites Gini coefficients were significantly higher ($\alpha = 0.05$) for REJ, whereas MS showed a similar response only in GEN site. Autocorrelation (AC) was significantly higher in SEL series of three sites except for SFR site, where it was higher in REJ series. At three sites diameters and heights were significantly different between SEL and REJ series with higher values in SELs. However, at only one (GEN) of these three sites tree age was also statistically higher in selected trees. SEL series shown a greater and significantly different global glk in all sites.

Table 3: SEL and REJ series statistics, TRW: tree-ring width, MS: mean sensitivity, AC1: first order autocorrelation, Rbar:interseries correlation, Glk: global *Gleichläufigkeit*. The statistics are in bold characters when significant different between SEL and REJ group in the same site ($\alpha<0.05$).

Site Group	n° SERIES	Mean TRW (mm)	Gini	MS	AC1	Rbar	Glk	Mean cambial age (years)	Mean diameter (cm)	Mean height (m)
BOV										
SEL	46	3.51	0.24	0.24	**0.516**	**0.731**	**0.625**	11.5	12.9	2.40
REJ	25	3.22	0.21	0.30	**0.275**	**0.141**	**0.535**	13.0	13.4	2.45
VET										
SEL	61	1.98	0.26	0.32	**0.487**	**0.659**	**0.597**	15.2	10.5	1.82
REJ	87	1.83	0.26	0.36	**0.347**	**0.100**	**0.514**	14.7	9.8	1.63
SFR										
SEL	45	**2.64**	**0.24**	0.33	**0.318**	**0.653**	**0.610**	13.1	13.7	2.27
REJ	62	**2.14**	**0.29**	0.37	**0.416**	**0.143**	**0.562**	15.7	11.1	1.88
POR										
SEL	8	2.10	0.24	0.28	**0.562**	**0.691**	**0.555**	14.0	12.3	2.04
REJ	12	2.45	0.22	0.31	**0.301**	**-0.064**	**0.475**	12.0	11.7	1.86
OCR										
SEL	52	1.76	0.25	0.37	0.338	**0.664**	**0.688**	**16.0**	10.6	1.71
REJ	82	1.83	0.25	0.36	0.405	**0.126**	**0.554**	**14.5**	10.8	1.67
SIR										
SEL	72	2.87	**0.23**	0.32	0.426	**0.593**	**0.652**	17.6	**16.9**	**2.87**
REJ	61	2.71	**0.26**	0.33	0.446	**0.129**	**0.553**	17.9	**10.8**	**1.67**
MOR										
SEL	47	2.57	0.29	0.35	0.464	**0.654**	**0.591**	16.0	**14.8**	**2.41**
REJ	37	2.23	0.29	0.40	0.379	**0.103**	**0.544**	15.3	**11.6**	**1.87**
GEN										
SEL	13	**3.11**	**0.20**	**0.25**	0.478	**0.545**	**0.626**	**23.2**	**21.9**	**4.60**
REJ	22	**2.16**	**0.28**	**0.35**	0.477	**-0.048**	**0.520**	**15.3**	**10.2**	**1.60**

3.2 Sensitivity analysis

With the sensitivity analysis, two methods (NW and RE) for detecting the common years were compared using different time-windows and thresholds for a total of 48 possible combinations (24 per method) (Figs. 2-3; Figs. S3-S4). With the NW method the highest number of CYs is detected both with 5 and 3-year window and the lowest series threshold (50%) and Cropper $|zi|$ value (0,6) (Fig. 2). The number decreases with increasing series thresholds (60% and 75%) and with Cropper values up to 1. All combinations except two (Fig. 2, solid lines) bring the CY values to less than 10% at 0,75 $|zi|$. At this regard the best performing method with all Cropper values is the one with 5yrs window and 30% of series, whereas the least performing one is that with 3yrs and 75% series. The RE method

is more performing and provides globally a higher percentage of CYs compared to the NWs. The decrease of all curves is less steep than in NW and minimum values never reach the 0 as it occurred in previous case (Fig. 3). RE4 provides higher shares than RE1 especially with 50 and 60% series thresholds that allow to detect 36-52% of CYs. RE1(50%) and RE4 (60%) share the same values at the various thresholds of growth responses.

As expected, with the methods and parameters used (Table 4), more CYs were detected within SEL than REJ series (Fig.4b,c). The CYs found in SEL have a very similar occurrence to those obtained using all series together, especially in 1999 and 2011 (positive) and 1998 and 2004 (negative) occurring in at least 4 study sites. The year 2004 is a CY also in REJ series at four sites (Fig.4a,b). Several of the CYs counted in REJ occurred also in SEL, like at SIR where, despite the lower intercorrelation values, 1998 and 2004 are negative years both in SEL and REJ series (Fig. 5).

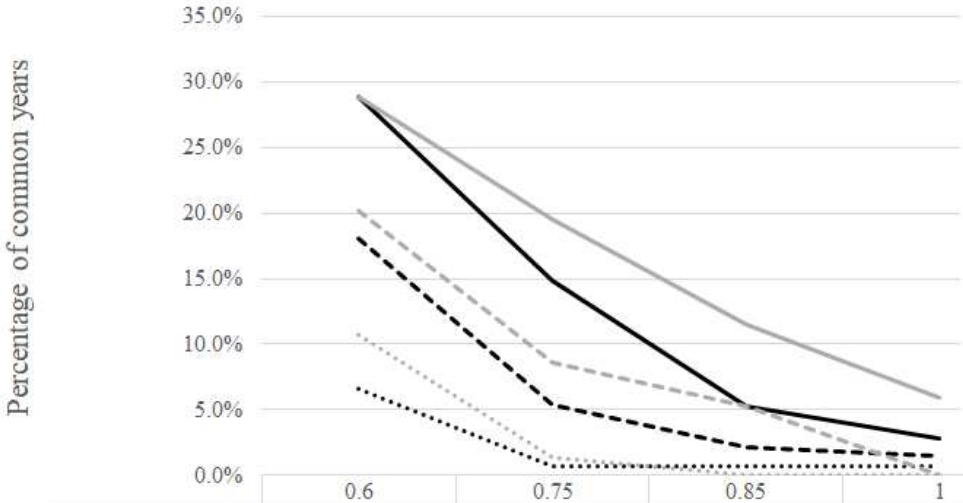

	0.6	0.75	0.85	1	m
3yrs 50% series	28.9%	14.8%	5.3%	2.9%	-0.67
3yrs 60% series	18.0%	5.4%	2.1%	1.4%	-0.41
3yrs 75% series	6.6%	0.7%	0.7%	0.7%	-0.14
5yrs 50% series	28.9%	19.5%	11.5%	5.9%	-0.59
5yrs 60% series	20.2%	8.6%	5.2%	0.0%	-0.50
5yrs 75% series	10.7%	1.3%	0.0%	0.0%	-0.26

Figure 2: Percentage of Common Years (CY, positive or negative) in SEL series detected by the NW method (Normalization in a moving window) using a three (3yrs – black lines) and five-years (5yrs – gray lines) windows. On X axis different % thresholds of Cropper values are reported. Sample depth is always of 10 series. Values in "m" column are the trendline slope angles.

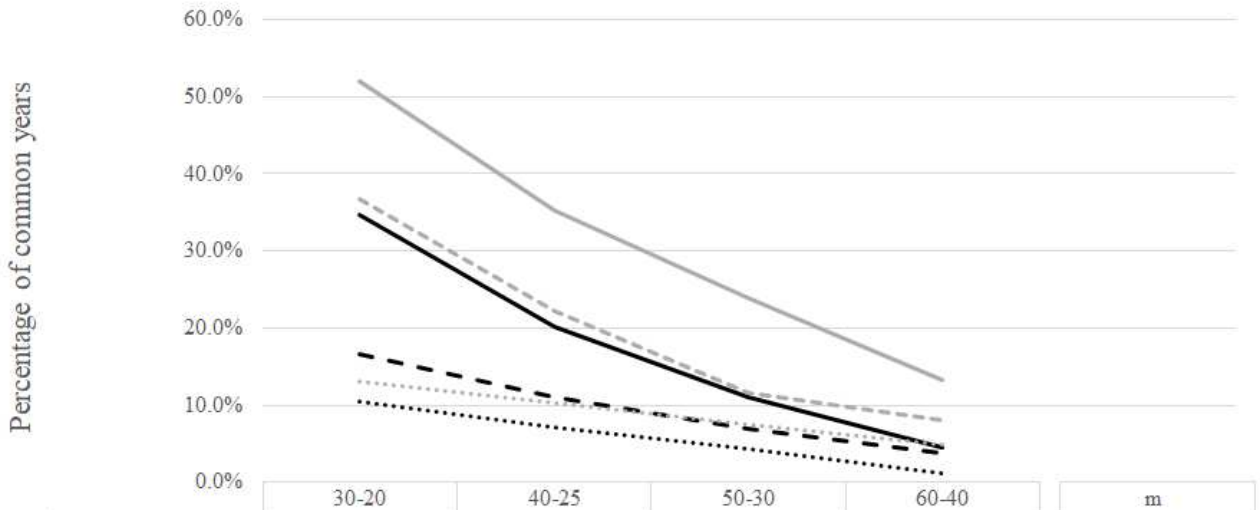

	30-20	40-25	50-30	60-40	m
1yrs 50% series	34.6%	20.2%	11.1%	4.6%	-1.18
1yrs 60% series	16.7%	11.1%	6.9%	3.8%	-0.51
1yrs 75% series	10.4%	7.1%	4.4%	1.1%	-0.37
4yrs 50% series	52.0%	35.2%	23.9%	13.3%	-1.53
4yrs 60% series	36.7%	22.3%	11.6%	8.0%	-1.15
4yrs 75% series	13.1%	10.3%	7.5%	4.9%	-0.33

Figure 3: Percentage of CY (positive or negative) for SEL series detected by the RE method (Relative growth change) using one (1yrs – black lines) and four-year (4yrs – gray lines) windows. On X axis different % threshold combinations of positive and negative growth responses in individual series are reported. Values in "m" column are the trendline slope angles.

Table 4: Number (#) of common years detected with NW3, NW5, RE1 and RE4 methods, considering a series threshold of 50% and a minimum sample depth of 10 series. The symbols "+" and "–" indicate positive and negative years respectively.

Method		NW3		NW5		RE1		RE4	
Parameters		3 years window $\|zi\| > 0.6$		5 years window $\|zi\| > 0.6$		1 previous year, growth change threshold 30% (positive) and 20% (negative)		4 previous years, growth change threshold 40% (positive) and 25% (negative)	
Site	Groups	+	–	+	–	+	–	+	–
BOV	SEL	1	1	0	1	3	1	2	0
	REJ	1	1	1	0	0	0	0	0
VET	SEL	4	1	2	0	7	2	4	3
	REJ	2	2	1	0	1	1	0	0
SFR	SEL	1	3	1	3	4	1	2	2
	REJ	2	2	1	1	6	2	1	1
POR	SEL	1	1	1	1	2	0	2	0
	REJ	1	0	1	0	0	0	0	0
OCR	SEL	5	3	3	3	5	5	4	4
	REJ	4	5	1	2	5	3	1	0
SIR	SEL	3	4	7	5	7	4	4	4
	REJ	1	3	3	3	2	3	1	1
MOR	SEL	1	2	0	2	3	1	3	4
	REJ	1	1	0	1	1	1	1	1
GEN	SEL	3	4	1	3	2	3	0	2
	REJ	1	1	0	2	1	2	0	0
Total	SEL	19	19	15	18	33	17	21	19
	REJ	13	15	8	9	16	12	4	3

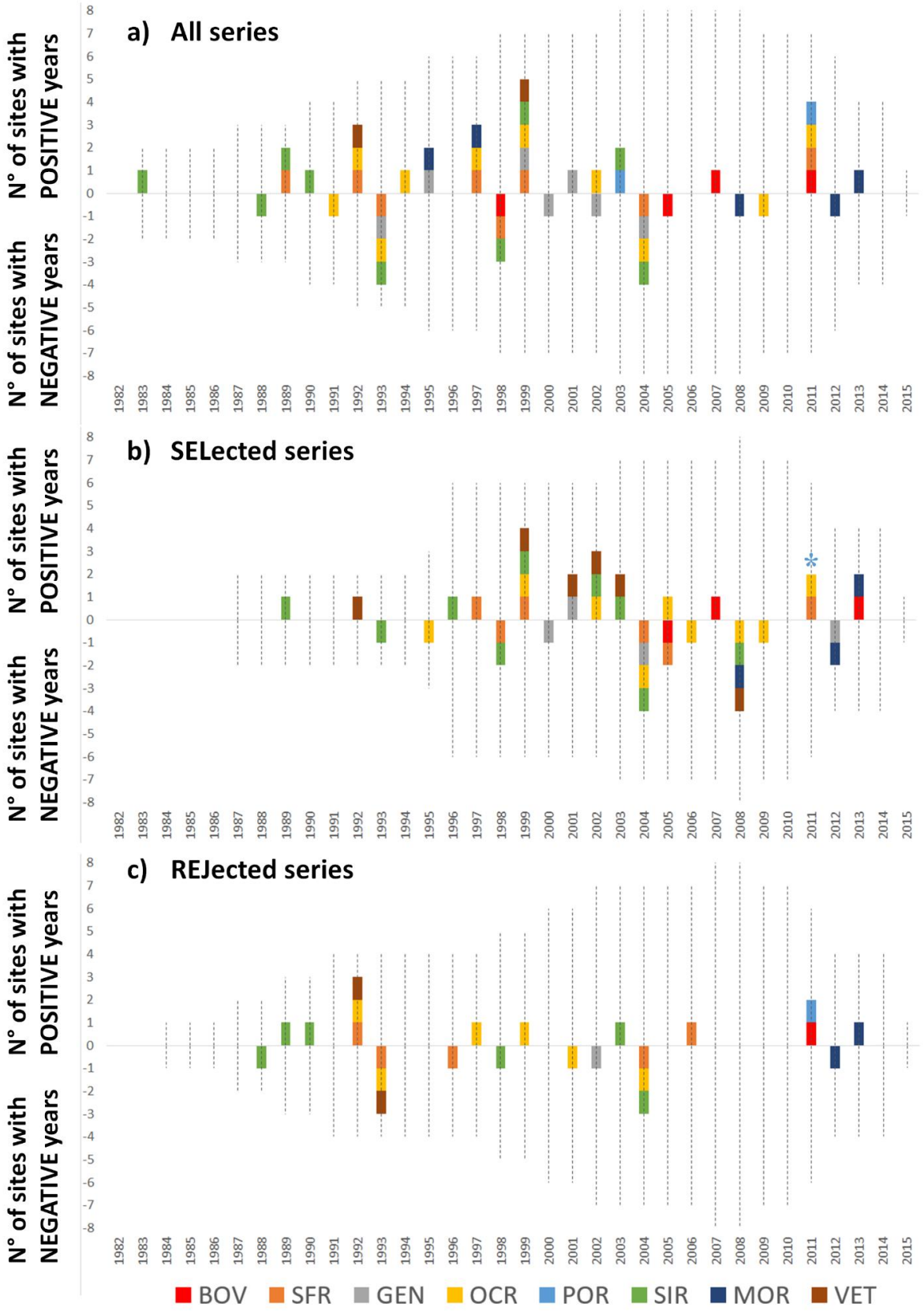

Figure 4 – Common years detected with at least two of the four methods used (Table 4). Acronyms correspond to the study sites. The dotted vertical lines indicate the potential total number of sites available each year. At POR there are only 8 selected series (*) indicate higher synchrony detected with 8 instead of 10 series.

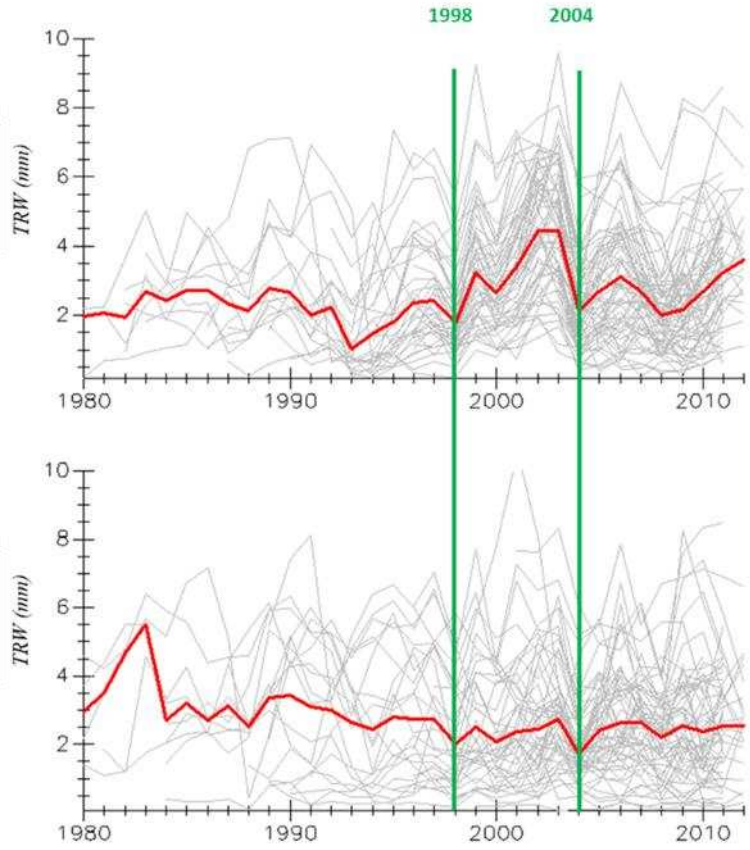

Figure 5 - Individual tree-ring width (TRW) series (grey lines) and averaged series (red lines) at the SIR site. Green vertical lines highlight two common years (1998 and 2004) detected in SEL (top) and REJ (bottom) series.

4. Discussion

The risk to discard many specimens because of their poor intercorrelation is rather high when working with growth-ring series from juvenile trees. Our results show that a relevant number of young trees (63%) cannot be used for dendroclimatic analysis due to their poor crossdating. In a study on riparian vegetation (Bätz et al., 2016) with young trees and shrub of willow species the mean chronology after crossdating was built with only 60% of the collected individual series. This could suggest that, when studying recent ecological processes were young trees are involved, it is advisable to sample a higher number of individuals compared to what it usually done when dealing with mature trees. For example, in this study, the number of collected specimens varied at all sites between 35 and 149 except POR where only 20 young pines were sampled. This number is usually considered suitable for adult trees in order to obtain a mean chronology to perform further analysis, but not in our case, since only 8 series have been selected and finally crossdated

in that site. Collecting stem discs rather than increment cores in adult trees increases the number of available individual series and facilitates the missing rings and the pointer year detection (Kirdyanov et al., 2018) but the benefits for short series should still be tested. In addition, in Italy as in other European countries, it is infrequent to obtain sampling permission for felling large number of trees even at their young life stages. In our study using the NW methods, the number of CYs decreased with the time window lag (5 or 3 years), whereas with RE method it decreased with the number of preceding years (1 or 4 yrs) used for the analysis (Jetschke et al., 2019). With less conservative thresholds, as used here, when series exhibited a growth depression or increase immediately before or after a distinctive growth, both years were identified as CY. Some common years identified in SEL series occur at several sites (e.g. 1993 and 2004 as negative years and 1999 as positive year). Considering the 8 study sites, crossdating of all tree-ring series was mainly based on the same regional CYs (1999, 2004 and 2008), whereas in REJ series their occurrence appeared more related to site specific events. Less common years were detected in the REJ series, but most of them were present also in SEL series, in a limited number of sites. This suggested that even in the series with a more individualistic growth, like REJ, certain years are still climate sensitive and could provide relevant information. This is also evident when looking at the common years for all the series, being very similar to those of the SEL series. Since REJ series exhibited a growth response similar to that of more climate-coupled trees, it should be recommended to not discard them but simply to process them differently.

The dataset used seemed also influenced by the specific environmental conditions of the treeline ecotones where young trees often feature complete or partial missing rings and enhanced eccentricity due to slope inclination, snow accumulation and/or wind. This may result in poor series crossdating and low correlation with the mean chronology, particularly when only one core per tree is available. In our case, the limitation effect due to microsite factors (e.g. type of micro-habitat, niche micro-topography, etc.) on young encroaching treeline pines could have altered, positively or negatively, the detection of common years. Young and isolated growing trees are mainly dependent on microsite factors showing smaller growth increments, higher Gini coefficients and mean sensitivities. The availability of suitable regeneration niches (Grubb, 1977) is a crucial issue for tree encroachment and development, especially on open areas without the facilitation effects provided by adult trees or deadwood. In our study sites the main land cover types were classified as grass, debris and bedrock, excluding shrubs for providing

their possible facilitation effect on seedlings and saplings. Based both on land cover and on mid-resolution topography, microsites with debris and on steeper slopes hosted the highest number of pines, but the larger size trees were mainly founded on grass cover and gentler slope (Vitali et al., 2017; Vitali et al., 2019), suggesting that the more crossdatable series could be collected on these land cover conditions.

5. Conclusions

Here we used short growth series from young *P. nigra* trees encroaching above the central Apennines treelines to test methods for selecting suitable series for tree-ring analysis, since intercorrelation is usually much lower in young than in adult trees. Climate-coupling signals expressed by good series crossdating are more difficult to find here than in trees of older forest stands. In fine-scale vegetation dynamics, the availability of micro-topography (high resolution) information, through remote and proximal sensing data, could enhance the knowledge of the facilitation effect provided by concave and/or wind-sheltered lee slopes, that can promote the formation of thick and long-lasting snowpack (Hagedorn et al., 2014; Kullman and Öberg, 2009). Furthermore, combining remote/proximal sensing data and microsite meteorological field measurements (e.g. temperature, humidity, etc.) could allow a better understanding of the processes involved, providing useful information about their effects on tree growth dynamics and resulting proportions of SEL/REJ trees. Further studies on different species should be tested in order to improve the SEL/REJ discrimination, especially focusing on tree microsite differentiation.

Supplementary material

Associated with: Enrico Tonelli, Alessandro Vitali, Alma Piermattei, Carlo Urbinati: Are young trees suitable for climate-growth analysis? A trial with *Pinus nigra* in the central Apennines treelines.

Figure S1: View of a slope with *Pinus nigra* encroachment at OCR (Mt. Ocre) site, Central Italy.

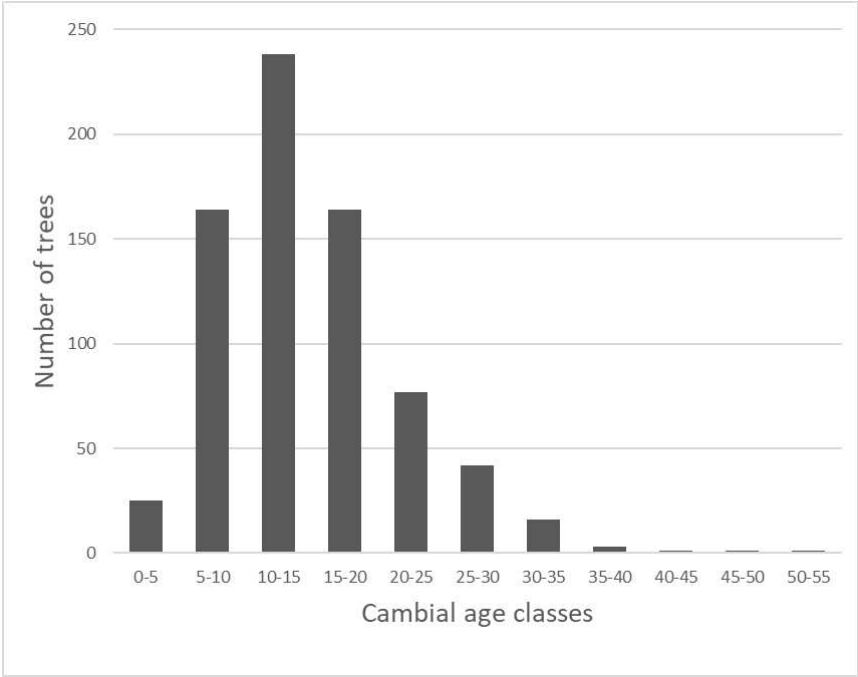

Figure S2: Frequency distribution of cambial age classes of the entire dataset (734 trees). Mean cambial age is 15.3 years, the median is 14 years and the standard deviation 6.8 years.

Table S1: Critical values for Pearson's correlation coefficient and length of series.

DF	Length of Series	Correlation at 95% Confidence Level	Correlation at 99% Confidence Level
1	3	0.9877	0.9995
2	4	0.9000	0.9800
3	5	0.8054	0.9343
4	6	0.7293	0.8822
5	7	0.6694	0.8329
6	8	0.6215	0.7887
7	9	0.5822	0.7498
8	10	0.5494	0.7155
9	11	0.5214	0.6851
10	12	0.4973	0.6581
11	13	0.4762	0.6339
12	14	0.4575	0.6120
13	15	0.4409	0.5923
14	16	0.4259	0.5742
15	17	0.4124	0.5577
16	18	0.4000	0.5425
17	19	0.3887	0.5285
18	20	0.3783	0.5155
19	21	0.3687	0.5034
20	22	0.3598	0.4921
21	23	0.3515	0.4815
22	24	0.3438	0.4716
23	25	0.3365	0.4622
24	26	0.3297	0.4534
25	27	0.3233	0.4451
26	28	0.3172	0.4372
27	29	0.3115	0.4297
28	30	0.3061	0.4226
29	31	0.3009	0.4158
30	32	0.2960	0.4093
31	33	0.2913	0.4032
32	34	0.2869	0.3972
33	35	0.2826	0.3916
34	36	0.2785	0.3862
35	37	0.2746	0.3818
36	38	0.2709	0.3760
37	39	0.2673	0.3712
38	40	0.2638	0.3665
39	41	0.2605	0.3621
40	42	0.2573	0.3578
41	43	0.2542	0.3536
42	44	0.2512	0.3496
43	45	0.2483	0.3457
44	46	0.2455	0.3420
45	47	0.2429	0.3384
46	48	0.2403	0.3348
47	49	0.2377	0.3314
48	50	0.2353	0.3281
49	51	0.2329	0.3249
50	52	0.2306	0.3218

Table S2: Percentage comparison of SEL series using the 95% and the 99% critical values for Pearson's correlation coefficient. Column ">0.4" indicates the percentage of series which has a correlation coefficient greater than 0.4.

Site	**95%**	**99%**	**>0.4**
BOV	64.8	40.8	38.0
VET	41.2	22.3	38.5
SFR	42.1	16.8	65.4
POR	40.0	30.0	30.0
OCR	38.8	24.6	58.2
SIR	54.1	24.8	61.7
MOR	56.0	33.3	57.1
GEN	37.1	22.9	51.4
Average	**46.8**	**26.9**	**50.0**

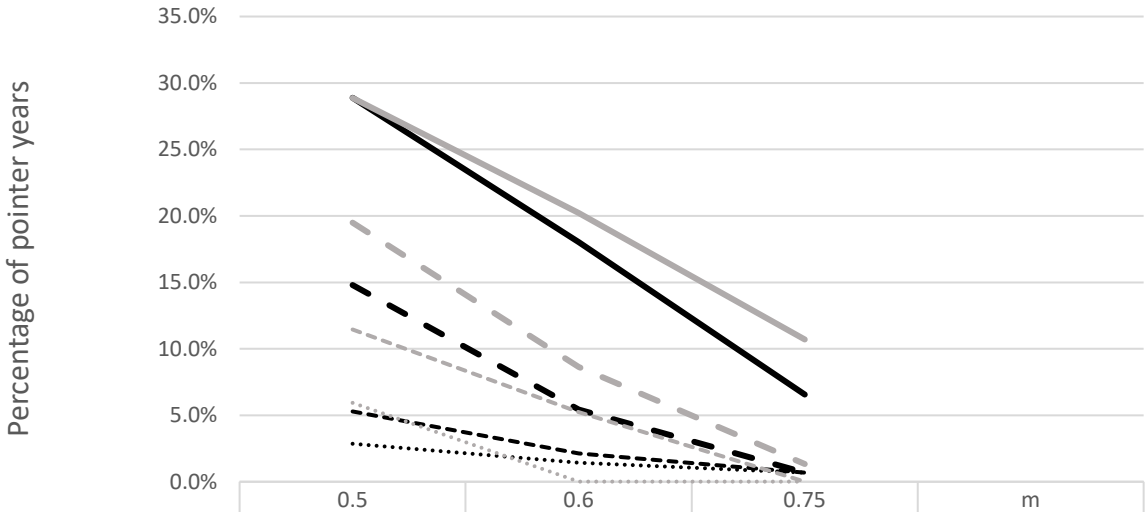

	0.5	0.6	0.75	m
3yrs |zi|= 0.6	28.9%	18.0%	6.6%	-0.88
3yrs |zi|= 0.75	14.8%	5.4%	0.7%	-0.54
3yrs |zi|= 0.85	5.3%	2.1%	0.7%	-0.18
3yrs |zi|= 1	2.9%	1.4%	0.7%	-0.08
5yrs |zi|= 0.6	28.9%	20.2%	10.7%	-0.72
5yrs |zi|= 0.75	19.5%	8.6%	1.3%	-0.71
5yrs |zi|= 0.85	11.5%	5.2%	0.0%	-0.45
5yrs |zi|= 1	5.9%	0.0%	0.0%	-0.22

Figure S3: Percentage of common years (positive or negative) for SEL series detected by method NW (Normalization in a moving window) using a three (3yrs – black lines) and five-years (5yrs – gray lines) windows. Lines represent different combinations of window width and |zi| value. In abscissa axis, different threshold of series showing event year. In all cases, we consider a sample depth of 10 series. In "m" column the trendline slope has reported.

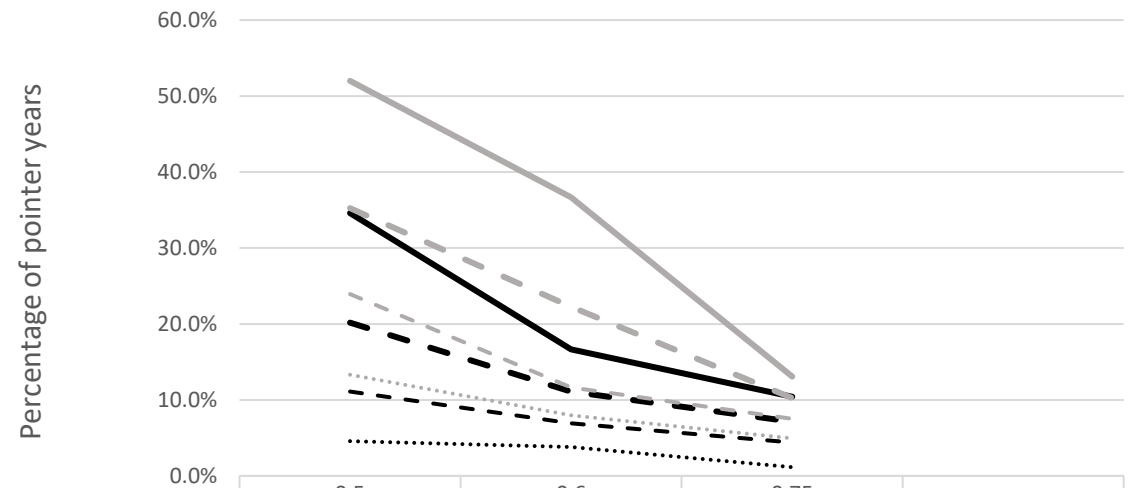

	0.5	0.6	0.75	m
1yrs rgc: 30-20	34.6%	16.7%	10.4%	-0.92
1yrs rgc: 40-25	20.2%	11.1%	7.1%	-0.50
1yrs rgc: 50-30	11.1%	6.9%	4.4%	-0.26
1yrs rgc: 60-40	4.6%	3.8%	1.1%	-0.14
4yrs rgc: 30-20	52.0%	36.7%	13.1%	-1.56
4yrs rgc: 40-25	35.2%	22.3%	10.3%	-0.98
4yrs rgc: 50-30	23.9%	11.6%	7.5%	-0.63
4yrs rgc: 60-40	13.3%	8.0%	4.9%	-0.33

Figure S4: Percentage of common years (positive or negative) for SEL series detected by method RE (Relative growth change) using a one (1yrs – black lines) and four-years (4yrs – gray lines) windows. Lines represent different combinations of window width and relative growth change. In abscissa axis, different threshold of series showing event year. In all cases, we consider a sample depth of 10 series. In "m" column the trendline slope has reported.

Chapter 3

Tree-ring and remote sensing analyses for assessing the role of elevation on European beech sensitivity to late spring frost

This chapter has been submitted to Agricultural and Forest Meteorology on 25th November 2021 and is currently under review.

Authors: **Enrico Tonelli**[1], Alessandro Vitali[1], Francesco Malandra[1], Julio J. Camarero[2], Michele Colangelo[2,3], Angelo Nolè[3], Francesco Ripullone[3], Marco Carrer[4] and Carlo Urbinati[1]

[1]Department of Agricultural, Food and Environmental Sciences, Marche Polytechnic University, Ancona, Italy.

[2]Instituto Pirenaico de Ecología (CSIC). Apdo. 202, 50192 Zaragoza, Spain.

[3]School of Agricultural, Forest, Food and Environmental Sciences (SAFE), University of Basilicata, 85100 Potenza, Italy.

[4]Universitá degli Studi di Padova, Dipartimento Territorio e Sistemi Agro-Forestali (TeSAF), Viale dell'Università 16 - 35020 Legnaro, Italy

Abstract

Extreme weather events such as late spring frosts (LSFs) negatively affect productivity and tree growth in temperate beech forests. However, detailed information on how these forests recover after such events are still missing. We investigated how LSFs affected forest cover and radial growth in European beech (*Fagus sylvatica* L.) populations located at different elevations at four sites in the Italian Apennines, where LSFs have been recorded. We combined tree-ring and remote-sensing data to analyse the sensitivity and recovery capacity of beech populations to LSFs. We quantified climate-growth relationships at population and individual levels to test if LSFs affected the growth response to climate. Using daily temperature records, we reconstructed LSF events and assessed legacy effects on growth. We also evaluated the role played by elevation and stand structure as modulators of LSFs impacts. Finally, using satellite images we computed Normalized Difference Vegetation Index (NDVI), Enhanced Vegetation Index (EVI) and LAI (Leaf Area Index) to evaluate the post-LSF canopy recovery. The growth reduction in LSF-affected trees ranged from 36% to 84%. We detected a negative impact of LSF on growth only during the LSF year, with growth recovery occurring within 1-2 years after the event. Water deficit during summer and cold spring temperatures are the main factors limiting beech growth. LSF-affected stands featured low vegetation indices until late June, i.e. on average 75 days after the frost events. We found a higher frequency of frost rings at mid than at low or high elevations, related to spring leaf unfolding. Our findings indicate a high recovery capacity and no legacy effects of LSFs.

Key words: Apennines, Fagus sylvatica, dendrochronology, canopy defoliation, resilience.

Highlights

- We assessed the impact of late spring frost on beech at different elevations
- We apply tree-rings and remote sensing analysis
- The impact of late spring frost on beech growth depends on site elevation
- Radial growth recovers after canopy damage without noticeable legacies
- Remote sensing data show post-frost canopy recovery after two months

1. Introduction

In temperate forests, a late spring frost (hereafter LSF) is an abrupt and severe temperature drop during a period of mild weather (also known as false spring) which negatively impact tree productivity and growth (Augspurger 2009, Chamberlain et al. 2020). In European hardwood species such as European beech (*Fagus sylvatica* L.) below-zero temperatures during spring can damage the recently unfolded leaves and cause a radial growth reduction (Dittmar et al. 2003, 2006, Gazol et al. 2019, Vitasse et al. 2019, Sangüesa-Barreda et al. 2021). In Europe, the recent climate variability significantly increased the frequency of extreme weather events such as LSFs (Augspurger 2013, Bigler & Bugmann 2018, Zohner et al. 2020, Lamichhane 2021), summer droughts (Spinoni et al. 2018, Gazol & Camarero 2022, Dukat et al. 2022), and their combined effects pose several questions about forest productivity, tree growth and post-disturbance recovery in widely distributed species such as beech (Gazol et al. 2019, Vitasse et al. 2019, D'Andrea et al. 2020).

In mature beech trees, old carbohydrates can rapidly be mobilized to produce a second cohort of leaves after LSF induced defoliations (D'Andrea et al. 2019). However, new leaves and twigs of affected trees may be smaller and less productive than in undamaged individuals (Rubio-Cuadrado et al. 2021b). Moreover, LSFs occurring in two consecutive years may hamper growth resilience (Rubio-Cuadrado et al. 2021a). Even if

beech trees are very vulnerable in their juvenile phase, compensatory effects were observed in beech seedlings that survived to a LSF and featured an increased in autumn photosynthetic activity (Zohner et al. 2018).

LSFs induced defoliations largely depend on the timing of the event occurrence and of the leaf unfolding. In beech, bud burst timing is mainly controlled by chilling and forcing temperatures and influenced by the photoperiod (Heide 1993; Vitasse et al. 2014). Due to this interaction beech, compared to other co-occurring species, features different timing in leaf upfolding according to the site elevation: later at lower altitude and earlier at higher altitude (Vitasse et al. 2009). Climate warming also affects tree phenology especially at high elevation sites, turning beech forest canopies more prone to LSFs (Čufar et al. 2008, Menzel et al. 2011).

Leaf shedding after LSF is commonly reported in the beech distribution core area, in central Europe (e.g., Dittmar et al. 2006, Vitasse et al. 2019) and, in recent years, also in Mediterranean mountains at the southernmost beech distribution limit (Gazol et al 2019). Recent studies, based on remote-sensing and tree-ring data, showed that LSF defoliation events on southern European beech forests were frequent from 1990 onwards (Olano et al. 2021, Sangüesa-Barreda et al 2021). However, this information could be biased by the availability or quality of satellite images. We need complementary information on how LSF affected beech radial growth in the last decades and across extended ecological gradients, i.e. in sites at different altitudes or with different soil water availability. The Italian Apennines range provides a valuable setting for such research because its NW-SE slope orientation, where beech forests receive different precipitation amounts and along altitudinal gradients, spanning from the sub-montane belt up to the upper treeline even at 1900 m a.s.l. (Vitali et al. 2018, Malandra et al. 2019).

In 2016 and 2017 two large-scale LSF events occurred along the Central and Southern Apennines affecting approximately 5,000 km^2 of forested area, around one third of the beech forests extension in Italy (Nolè et al. 2018, Bascietto et al. 2018, 2019). LSFs can differently affect beech canopies depending on site elevation and their phenology. A remote-sensing study in Italy indicate that due to later leaf unfolding high-elevation beech forests are less defoliated than mid- and low-elevation stands (Nolè et. al 2018). However, high elevation stands could be more affected if a late frost occurs at the time of emerging leaves, while at lower sites leaves would be mature enough and more frost resistant.

Lacking a clear relationship between beech forest elevation and occurrence of LSF defoliations, we could not accept the hypotheses that: i) the forests located at higher elevations are more sensitive to LSF disturbance and ii) their increased frequency may in the longer term jeopardize the presence of beech from high-altitude sites in Mediterranean mountains. We therefore tested this hypothesis by combining short-term remote sensing information with long-term, retrospective tree-ring analyses at four sites, two located on the wetter central Apennines and two on the drier southern Apennines. The specific multispectral signature of brown-coloured affected foliage after LSF can be detected by satellite imagery and used to assess the geographic extension and the severity of such disturbances at broad spatial scales and in remote sites (Allevato et al. 2019, Decuyper et al. 2020, Olano et al. 2021). With tree-ring measurements and climatic data, we reconstructed some past LSFs and assessed their impacts on beech radial growth. We aimed (i) to detects the effects of LSF on tree growth along altitudinal gradients, and (ii) to assess the European beech post-LSF recovery and resilience in terms of productivity and canopy greenness with remote sensed imagery.

2. Material and methods

2.1. Study sites

We studied four locations (Figure 1) located in central and southern Italy, all within the European beech distribution range (Pott 2000). In this mountainous region, beech is the most frequent species of the upper treeline ecotones ranging between 1600 and 1900 m a.s.l. (Vitali et al. 2018).

Study sites were selected combining documental evidence of LSF events (e.g., forest reports) with satellite imagery verification (Figure 1c). Two sites are in the central (Mt. Acuto -ACU and Mt. dei Fiori - MDF), and two in the southern Apennines (Mt. Volturino - VOL and Mt. Pollino - POL), (Table 1, Figure 1a). At all sites, pure beech forests extend continuously for at least 300-400 m along an elevation gradient from mid-slope to the upper forestline.

Mean annual temperatures range from 8.4 °C (ACU) to 5.0 °C at the coldest location (POL), whereas annual precipitation varies from 754 mm in VOL to 1330 mm in ACU (Table S1). According to the *Ecopedologic map of Italy* all sites are located on calcareous substrates and share the same basic and deep soils (Italian Ministry for the Environment, Land and Sea, http://www.pcn.minambiente.it/viewer). Slope steepness ranges between 20 to 40%, and it increases upwards.

2.2. Field data collection

Between 2019 and 2020, in each study site, at high, mid, and low altitude we placed two concentric circular sampling plots (Figure 1c). Along the slopes sampling plots have been located assuring an elevation difference of at least 100 m between one another. At each location we sampled beech trees within a larger plot with variable radius between 20 and 30 m to guarantee the presence of at least 20 evenly distributed dominant

healthy trees, with ⩾30 cm diameter at breast height (DBH) and without crown damage. The inner plot radius was fixed at 10 m.

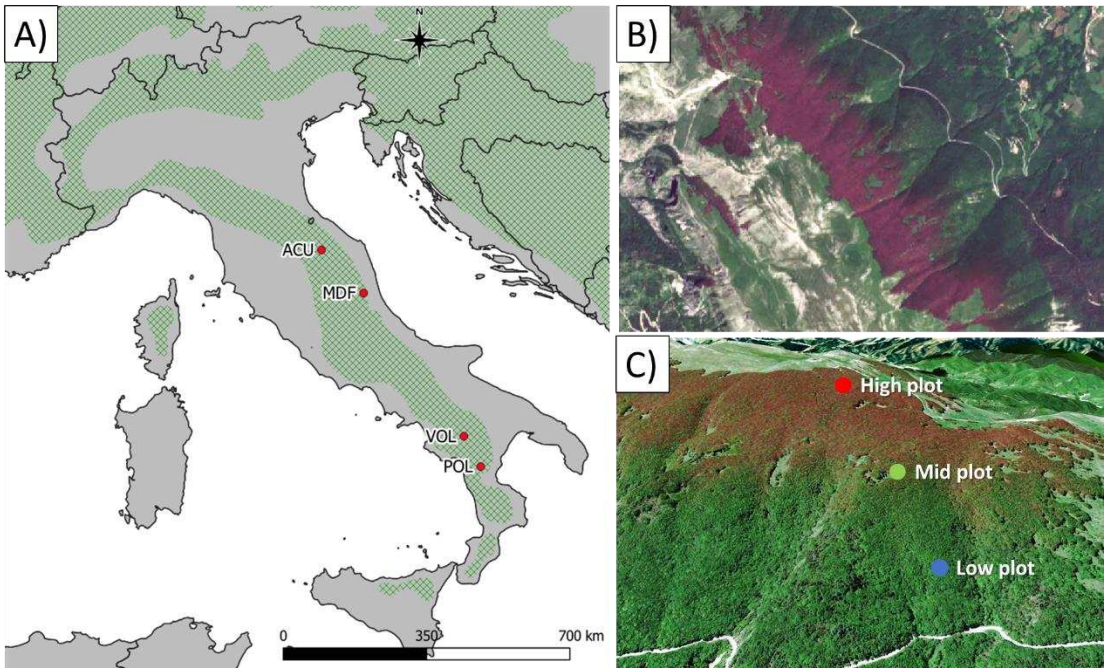

Figure 1. (A) Location of the four study sites in central and southern Apennines (Italy) within the *Fagus sylvatica* distribution range (green area) (Caudullo et al. 2017). (B) A true-colour Sentinel 2A satellite image (May 26th, 2016) showing the beech forest sectors affected by a spring frost at MDF site. (C) Distribution of plot areas along the altitude gradient at MDF, (Google earth Pro V 7.3.4.8248; May 22nd, 2016).

Table 1. Geographic settings of the study sites and their forest structure variables.

Site	Lat (°N)	Long (°E)	Plot	Elevation	Forest structure	Tree density (No stems ha^{-1})	Basal area (m^2 ha^{-1})	DBH (cm)	Height (m)
ACU	43.48	12.68	High	1375	OC	7417	56.47	9.8	13.2
			Mid	1245	CC	1146	44.70	22.3	16.5
			Low	1080	HF	382	77.39	50.8	22.0
MDF	42.79	13.59	High	1584	OC	4170	51.68	12.6	14.9
			Mid	1423	OC	4520	53.98	12.3	15.2
			Low	1159	OC	3342	55.94	14.6	17.3
VOL	40.43	15.79	High	1600	CC	1401	54.69	22.3	21.8
			Mid	1405	CC	1655	49.75	19.6	25.3
			Low	1300	CC	1910	31.72	14.5	20.0
POL	39.93	16.16	High	1890	OC	4010	55.69	13.3	18.8
			Mid	1590	CC	2769	60.30	16.6	20.5
			Low	1450	HF	923	73.35	31.8	29.3

In the inner plots we measured the DBH (minimum threshold 2.5 cm) of all standing and living stems. In the larger plots we measured DBH and total height of the dominant individuals with a laser clinometer and rangefinder (TruPulse 360B, Laser Technology, Inc.). We extracted wood cores at breast height (1.3 m) orthogonally to the slope from 20 dominant trees with a Pressler increment borer. Basal area ranged from 31 to 77 m^2 ha^{-1} and tree height from 13 to 29 m (Table 1). Values variability is partly related to different management systems: overaged coppices (e.g., ACU-high plot) have higher tree density and lower tree size (DBH, height) than high forests (e.g., POL-low plot). Coppices in conversion feature intermediate density values (e.g., VOL-mid plot).

2.3. Cores processing and tree-ring width series

We mounted all cores on wooden supports and polished them with progressively finer sandpaper. We visually cross-dated each core and then measured ring widths using a semi-automatic system (LINTAB-TSAP) at 0.01 mm accuracy. We used the COFECHA software to check the visual cross-dating (Holmes 1983). Then we detrended the tree-ring width series by fitting cubic spline functions to remove the age- and disturbance-related trends and to emphasize the high-frequency growth variability (Cook et al. 1990). We set the smoothing spline's rigidity at 25 years and its wavelength cut-off value at 50%. We detrended all measured series dividing observed by fitted values to obtain dimensionless ring-width indices. We averaged individual tree-ring indexed series using a bi-weight robust method to develop a mean chronology and obtained 12 mean plot chronologies (Figure 2).

We compared the mean chronologies by calculating descriptive statistics both on single raw series, such as the first-order autocorrelation (AC) and the Gini coefficient (Gini), and on indexed series as inter-series correlation (Rbar) and Expressed Population

Signals (EPS). The AC describes the influence of the previous growth on the current year growth, and the Gini coefficient accounts for the percentage of variability in the widths from one year to the next (Biondi and Qeadan 2008), similarly to the mean sensitivity (MS) (Fritts 1976). Rbar and EPS assess respectively the mean correlation between the series and the similarity degree of a given chronology with a correct reference chronology (Briffa and Jones 1990; Wigley et al. 1984). We processed the raw series with the "dplR" package (Bunn 2008) of R software (R Development Core Team, 2020). To assess the similarity among plots' indexed chronologies we calculated their Pearson correlations, and performed a Principal Component Analysis (PCA) on the covariance matrix.

2.4. Climate-growth relationships

We assessed the climate sensitivity of beech growth at population and individual levels with Pearson correlation analyses. We used the mean monthly series of minimum and maximum temperatures (Tmin and Tmax) and monthly precipitation (Prec) of the daily E-OBS V 22.0e gridded datasets at 0.1° spatial resolution (Cornes et al 2018). For each study site we selected the climate time series at the closest grid point. At population scale, we considered the mean standard chronologies of each elevation plot and the monthly climatic variables covering a window from May of the year prior to growth ($t-1$) to September of the growth year (t) for the reference period 1950–2019. At tree level, we used individual tree-ring indexed series and a selection of monthly or seasonal climatic variables that turned out significant from previous analyses. Since some tree-ring series did not extend back to 1950, for the individual level analysis we investigated only the 1960–2019 interval. The significance of correlations and confidence intervals were computed with a bootstrap approach with 1000 iterations (Politis and Romano 1994). We run climate-growth analyses within the R package treeclim (Zang and Biondi 2015).

2.5. Inferring frost events from climate records

To detect the potential LSF years, we used daily climate data from the E-OBS gridded dataset, interpolating the temperatures records from the grid elevation to the plot location considering a mean lapse rate of −6.5 °C km^{-1}. We used the accumulated degree-days (ΣT) as a proxy of leaf phenology and the spring daily temperature anomalies (ΔT) to quantify the severity of the events. ΣT is the cumulated daily mean temperature above a 5°C threshold from January 1st (Day Of the Year - DOY 1) to the date of the minimum temperature recorded between DOY 111 and 131 (approximately from April 20th to May 10th). This method slightly differs from the one in the literature (Vitasse et al. 2019), where accumulated degree-days are accounted to the date of the last late frost day (≤ -2°C). Yet, to avoid influences related to temperature interpolation in gridded datasets, which are prone to large errors, especially in daily records and across topographically complex areas, we decided to consider the day with minimum temperatures rather than the temperature threshold of – 2°C.

As a second indicator for the LSF detection, we computed spring temperature anomalies (ΔT) or the difference between the mean minimum temperature from March 1st to April 30th and the minimum temperature from April 20th to May 10th for each year. High values of ΣT and ΔT mean higher sensitivity of beech to LSF events (Gazol et al. 2019, Vitasse et al. 2019). We defined years with the highest risk of severe LSF when both ΣT and ΔT exceeded the 3rd quartile computed for the reference period 1951–1990.

We then compared these two meteorological indices and validated them with available daily data collected by local meteorological stations (Table S2). Again, temperature records were interpolated from station elevation to the plot location considering a mean lapse rate of −6.5 °C km^{-1}. Local stations provide the daily absolute

minimum temperatures that we used to validate the calculated ΔT values considering only the frost events (temperature < 0°C).

2.6. Quantifying frost impacts on tree growth

In dendrochronology an event year is a dated tree-ring considerably wider or narrower with respect to prior or subsequent rings, whereas a pointer year refers to several trees that display synchronously an event year within the series (Schweingruber et al. 1990). If LSFs are sufficiently severe, they can affect the cambial activity of trees and induce the formation of narrow rings detectable as negative event years and possibly as pointer years. We computed pointer years of all indexed individual tree-ring width series with the "Normalization in a moving Window" method (Cropper, 1979) using the R package PointRes (van der Maaten-Theunissen et al. 2015). This method delivers Cropper values (*zi*) series by normalizing tree-ring width series in moving windows. We considered event years |*zi*| values of 0.75 in a 5-year moving window. We retained a pointer year when the event year occurred in 75% of the plot series. Then, we selected the negative pointer years (nPYs) matching with a LSF year, hereafter abbreviated as LSF ring.

We estimated the recovery time after the selected years on indexed tree-ring width series using the Superposed Epoch Analysis (SEA), with a time lag of 4 years and bootstrapped resampling (Lough and Fritts 1987, Rao et al. 2019), using the "sea" function of the "dplR" package (Bunn 2008). Then, we averaged and plotted the departures from the mean SEA value of each core for the 4 years prior to, and immediately after each LSF nPY, to determine the occurrence of significant growth deviations. This analysis allows detecting post-frost carryover or legacy effects on radial growth. For the SEA over recent LSFs occurring in 2016 and 2017 we considered only one or two years

after each event, since tree-ring series end in 2018 (MDF site) or 2019 (ACU, VOL and POL sites).

As an additional analysis to assess the impact of LSF in nPY, we calculated resistance (*Rt*), recovery (*Rc*) and Resilience (*Rs*) indices following Lloret et. al (2011):

$$\text{Resistance (Rt)} = \text{Ring width index}_{t} / \text{Ring width index}_{t-2} \quad [1]$$

$$\text{Recovery (Rc)} = \text{Ring width index}_{t+2} / \text{Ring width index}_{t} \quad [2]$$

$$\text{Resilience (Rs)} = \text{Ring width index}_{t+2} / \text{Ring width index}_{t-2} \quad [3]$$

We computed these indices using standard tree-ring width series and a 2-year lag to avoid recovery underestimation due to consecutive LSFs, and to study the most 2016 and 2017 LSFs.

2.7. *Tree variability to frost sensitivity*

The effect of various drivers of individualistic tree growth on frost sensitivity was analysed at tree level. We assumed that beech sensitivity to spring frost could be explained by individual tree characteristics, such as cambial age and topographic elevation that could play an important role. The total number of LSF rings obtained by climate data analysis were considered as an indicator of frost sensitivity. We fitted Generalized Linear Models (GLMs) for predicting at each site the number of LSF rings formed by each tree as a function of the following variables: cambial age, mean tree-ring width, basal area increment (BAI), mean sensitivity and Gini index computed for the 1950-2019 time interval, and the growth trend in the period 1990–2019. This trend was based on the slope of BAI for that period. From the matrix we removed the heavily correlated predictors showing a high (≥4) Variance Inflation Factor to avoid

multicollinearity. We rescaled all the predictors to account for differences on measurement scale and we used a Poisson distribution family for the response count variable (LSF rings). For each model, we also used the plot elevation as fixed factor to search for different responses among plots.

We fitted two GLMs for modelling the presence/absence of LSF rings in each series in 1957 and 2016, the years with more trees affected by frost, as a function of cambial age, mean tree-ring width, mean sensitivity, and Gini index. We used plots nested in sites to focus on the explained variance. We rescaled all the predictors to account for differences on measurement scale and we used a binomial distribution family for the response variable (presence/absence of LSF rings). We performed all statistical analyses within the R environment (R Development Core Team, 2020), using the "glm" function of "stats" package (version 4.0.3) and the "glmer" function of "lme4" package (Bates et al., 2015). BAI was calculated using the "bai.out" function of the "dplR" package (Bunn 2008).

2.8. Frost events detected through remote sensed imagery

We used multispectral satellite Copernicus Sentinel-2 imagery to estimate the incidence of late frost and the recovery time of beech at the different plots. We used images from the twin satellites Sentinel-2A and Sentinel-2B. These platforms carry a Multi-Spectral Instrument (MSI) that samples thirteen spectral bands (Drusch et al. 2012). The EO Browser service (https://www.sentinel-hub.com/explore/eobrowser/) allowed satellite images selection with cloud-free areas over the study sites for the time interval ranging from March 2016 to December 2018. We selected images only for ACU and VOL sites due to (i) the least cloud contamination over their plots, and (ii) the occurrence of two consecutive LSF events in 2016 and 2017. We collected 62 images of the same time

interval and downloaded the corresponding products from the Copernicus Scientific Data Hub (https://scihub. copernicus.eu/) as a Level-1C (Top-of-atmosphere reflectance – orthoimage products) and Level-2A (Bottom-of-atmosphere reflectance – atmospherically corrected), when available (Table S3).

We processed twenty-six Sentinel-2 Level-1C images performing the atmospheric corrections using the SNAP 8.0 and Sen2Cor V2.8 software provided by the European Space Agency. We used the classification mask, built from the scene classification layer produced by Level 2A-processing, or provided in the level 2 product acquired, to remove pixels classified specifically as cloud shadows, water, intermediate and high-probability of cloud cover, thin cirrus, and snow. All images were calibrated to convert Digital Number into units of surface reflectance applying their respective scale factor. Then we calculated three vegetation indices: (i) Normalized Difference Vegetation Index (NDVI), (ii) Enhanced Vegetation Index (EVI), and (iii) Leaf Area Index (LAI). NDVI is the most widely used vegetation index and it is not only related to canopy structure and LAI, but also to canopy cover and greenness (Xue and Su 2017). NDVI ranges between -1 and 1 (Rouse et al. 1974) and is computed as follows:

$$NDVI = (NIR – Red) / NIR + Red \quad [4]$$

where NIR and Red are reflection values in the near-infrared and red ranges of the electromagnetic spectrum. Positive NDVI values between 0.3 and 0.8 usually refer to vegetation canopy with a high cover and greenness values. Since NDVI is sensitive to soil brightness and atmosphere conditions, EVI can simultaneously correct these noises (Liu and Huete 1995, Huete et al. 2002). EVI is expressed as:

$$EVI = G * (NIR – Red) / (NIR + C1* Red – C2 * Blue + L) \quad [5]$$

Where G is the gain factor, L the soil adjustment parameters, C1 and C2 are the coefficients used to correct the aerosol influences in the red band, and Blue are reflection

values from the blue band. For the Sentinel 2 products, we adopted the following coefficients: L=1, C1 = 6, C2 = 7.5, and G = 2.5 (Henrich et al. 2009).

For each selected image, we computed NDVI and EVI in a 40-m radius buffer zone from each plot centroids. A minimum of 30 pixels falling within the 40-m buffer were used to extract NDVI and EVI mean values for each low, mid, and high elevation plots at both ACU and VOL sites.

Finally, effective Leaf Area Index (LAI_{eff}) was estimated from satellite observations using the biophysical processor in SNAP 8.0. This function is proposed to use neural networks for the estimation of biophysical variables (Weiss and Baret 2016). We calculated the LAI_{eff} at ACU and VOL sites on the date of maximum LSF severity and on the date of the following full recovery time.

3. Results

3.1. Tree growth

Mean tree age varied from 61 years to 132 years, with the oldest tree (216 years) sampled at the VOL-high plot (Table 2). The mean tree-ring width ranged from 1.39 to 2.10 mm. At ACU, trees at low elevation showed the highest mean growth rate, but the rate decreased with increasing elevation (Table 2, Figure S1). The MDF, VOL and POL plots have similar growth rates within each site with no evident effects due to elevation, although the POL-low showed lower growth rates after 1990 (Figure S1). At MDF, we found wider rings in the lowest plot, whereas in VOL and POL at the mid-elevation plots.

First order autocorrelation values (AC1) in tree-ring width series are similar and ranging between 0.51 and 0.74 (Table 2). High Gini coefficients indicate sensitive series with high year-to-year growth variability. The EPS and Rbar values are high at all sites suggesting a large inter-annual growth variation and synchrony, i.e., a common growth

signal shared among trees. Tree-rings chronologies developed at each site at different elevations are well intercorrelated with high and significant ($p < 0.01$) values (Table S4). The PCA discriminates two groups of plots mean chronologies corresponding to the central and southern Apennines (Figure S2). Their yearly interquartile range (IQR) reached the highest values in years of LSF occurrence, such as 2016 and 2017 (Figure 2). In these two years, very cold spring temperatures reduced growth rates of several trees. We observed other abrupt growth reductions in most trees related to LSFs in 1957, 1986–1987 and 2013 (Figure 2).

Table 2. Dendrochronological statistics of sampled trees. First-order autocorrelation (AC1) and Gini (Gini) coefficients refer to the raw series, whereas inter-series correlation (Rbar) and Expressed Population Signal (EPS) refer to indexed ring-width series. Values are means ± SD.

Site plot	No. trees	Series length (yrs.)	Ring width (mm)	AC1	Gini	Rbar	EPS
ACU-High	23	75 ± 11	1.03 ± 0.48	0.51	0.25	0.50	0.94
ACU-Mid	18	85 ± 14	1.51 ± 0.66	0.57	0.25	0.34	0.88
ACU-Low	17	104 ± 14	2.18 ± 0.93	0.61	0.24	0.37	0.90
MDF-High	18	75 ± 19	1.56 ± 0.66	0.50	0.23	0.43	0.90
MDF-Mid	20	71 ± 8	1.42 ± 0.65	0.57	0.25	0.43	0.92
MDF-Low	20	61 ± 6	1.80 ± 0.82	0.63	0.25	0.44	0.93
VOL-High	26	120 ± 46	1.66 ± 0.80	0.62	0.28	0.35	0.88
VOL-Mid	27	75 ± 28	2.10 ± 1.08	0.62	0.28	0.34	0.86
VOL-Low	26	111 ± 58	1.54 ± 0.86	0.69	0.32	0.37	0.87
POL-High	25	108 ± 48	1.59 ± 0.81	0.67	0.29	0.35	0.88
POL-Mid	27	84 ± 33	1.87 ± 0.81	0.55	0.25	0.40	0.90
POL-Low	22	133 ± 30	1.39 ± 0.77	0.74	0.31	0.32	0.88

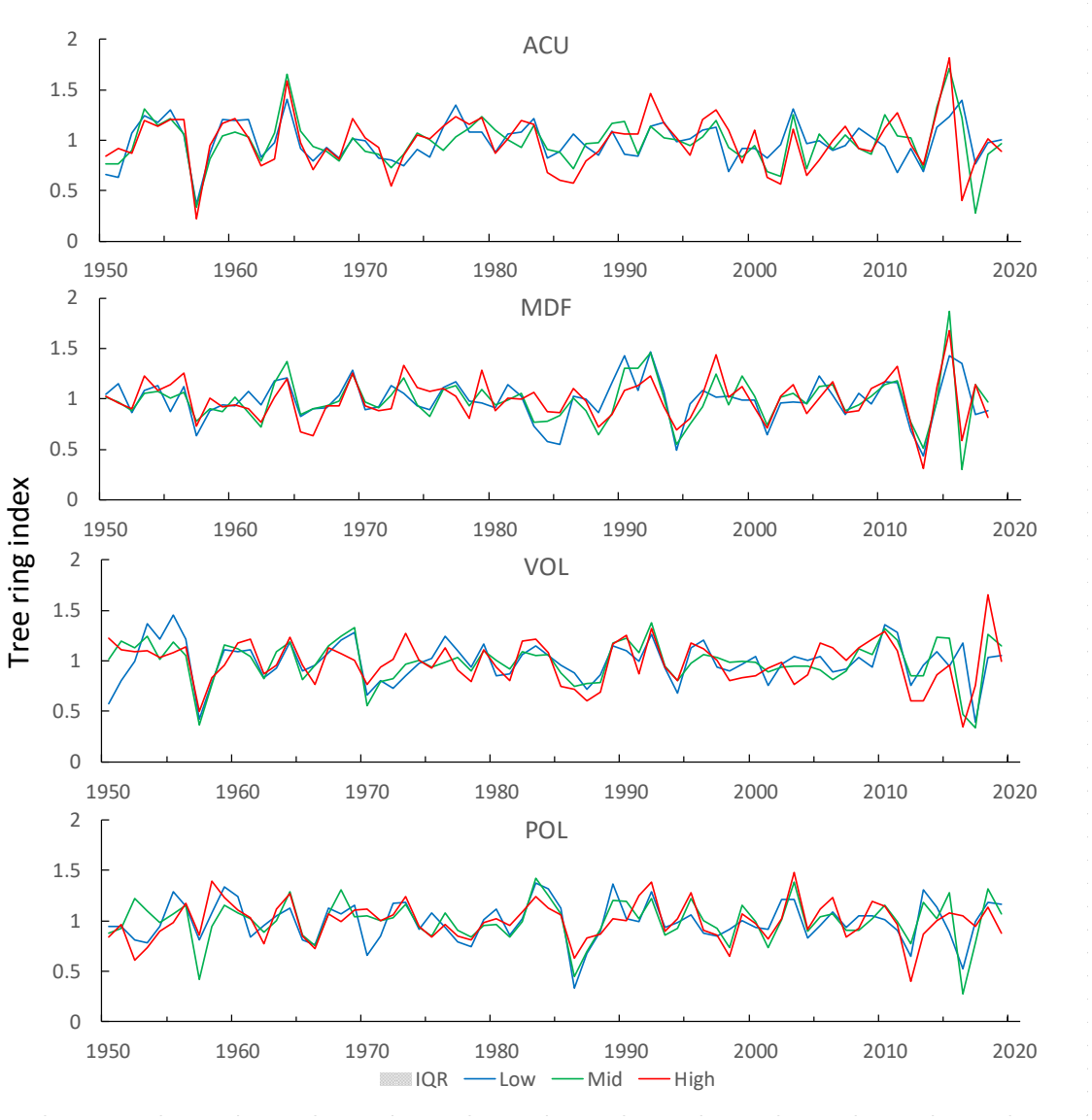

Figure 2. Mean indexed, ring-width chronologies at high (red), mid (green) and low (blue) elevation plots at the four study sites. The grey shadow is the interquartile range (IQR) of each site series. Chronologies are truncated in 1950, for matching the common time interval used in climate-growth analysis (1950–2019).

3.2. Climate-growth relationships

Beech growth series showed (i) a negative relationship with summer temperatures in both current and previous years, and (ii) a positive relationship with prior summer and winter and current summer precipitation. May is a key month for radial growth causing distinctive responses compared to prior and following months. Positive effects correspond to warm minimum May temperature, whereas negative correlations appeared

in response to moister conditions (Figure 3). Some differences emerged between the central and southern Apennines, but the role of elevation within each site was not straightforward. Growth at MDF-high plot is positively correlated with maximum and minimum May temperatures, whereas at ACU-low plot is positively correlated with May minimum temperatures. At four plots (MDF-low and high, POL-low and high), beech growth was negatively correlated with April minimum temperatures. We also detected negative correlations with prior and current summer temperatures, particularly at low and mid elevation. There is also evidence of a positive effect of precipitation on growth indices, also in the summer prior to growth, especially in ACU site. At this more mesic site, the positive effect of summer precipitation during the growing season decreased upwards. Similarly, at the VOL site the positive influence of June precipitation decreased upwards.

We then selected a few representative climatic variables to assess the climate-growth relationships at individual tree level: (i) summer (June to August) maximum temperatures and mean precipitation of current (t) and previous year (t-1), and (ii) mean minimum May temperature of current year (Table 3). Most individual ring-width series (37%) were positively correlated with current summer precipitation, and a few series (4%) were positively correlated with May temperature. Most of the ACU series were positively correlated with summer precipitation and maximum temperatures of previous year except for the low plot where most series positively correlated with current summer precipitation. In this site only few series (5-6%) at low and high plots are positively correlated with May minimum temperature. At MDF results are similar, but more series at mid- (16%) and high-elevation (14%) plots are positively correlated with minimum May temperatures. Growth series from the VOL and POL sites correlated well with current year precipitation.

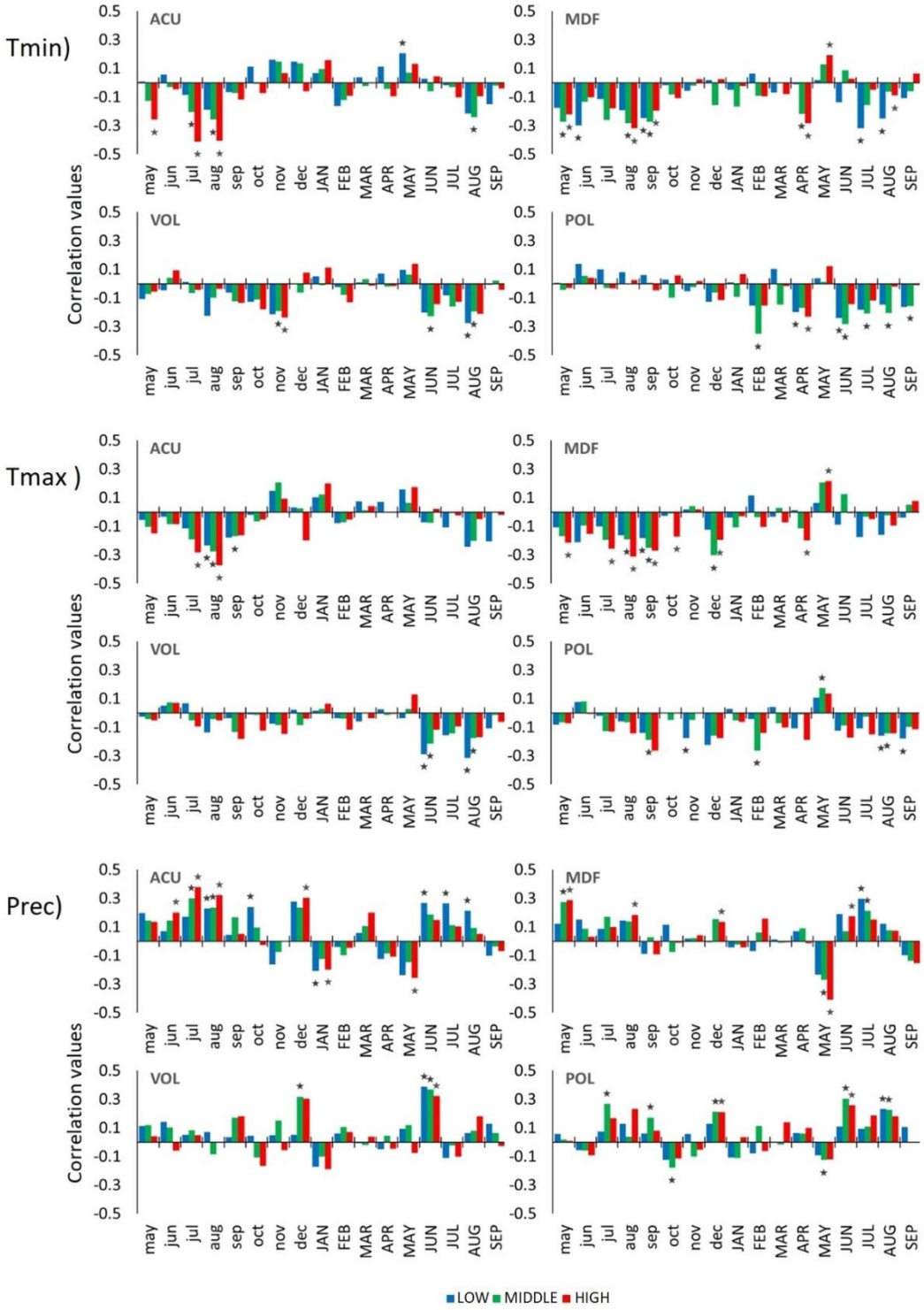

Figure 3. Bootstrapped correlation values calculated with indexed chronologies and monthly minimum (Tmin), maximum (Tmax) temperatures and total precipitation (Prec) for the 1950–2019 period. Blue, green, and red bars refer to low, mid, and high elevation plots respectively. Stars indicate significant correlation values ($p < 0.05$). Months in lowercase and uppercase letters correspond to the previous and current years, respectively.

Table 3. Percentage of indexed ring-width series with a significant ($p < 0.05$) correlation (**positive** in bold, *negative* in italic) with monthly or seasonal climate variables. Abbreviations: Prec, total precipitation; Tmax and Tmin, mean maximum and minimum temperatures, respectively; (t-1), year before the tree-ring formation; NS, percentage of individual series without a significant correlation with climate variables.

Site	Plot	Climate variables					NS
		Summer Prec (t-1)	Summer Prec	JJA Tmax (t-1)	Summer Tmax	May Tmin	
ACU	High	**84**	**11**	*68*	*0*	**5**	16
	Mid	**47**	**0**	*47*	*6*	**0**	41
	Low	**6**	**35**	*0*	*12*	**6**	53
MDF	High	**21**	**21**	*43*	*7*	**14**	36
	Mid	**32**	**26**	*26*	*0*	**16**	21
	Low	**27**	**67**	*13*	*20*	**0**	7
VOL	High	**0**	**50**	*6*	*13*	**0**	38
	Mid	**7**	**29**	*14*	*21*	**0**	57
	Low	**28**	**33**	*0*	*39*	**0**	33
POL	High	**33**	**67**	*25*	*8*	**0**	0
	Mid	**17**	**72**	*0*	*11*	**0**	22
	Low	**6**	**41**	*0*	*0*	**0**	53
All		**27**	**37**	*20*	*11*	**4**	32

3.3. Detection of LSF years using temperature data

The analysis of climate records revealed eleven potential LSF years (1955, 1957, 1962, 1967, 1970, 1977, 1989, 1991, 2001, 2016 and 2017). In these years, accumulated degree days (ΣT) and spring temperature anomalies (ΔT) exceeded the threshold values of the third quartile computed for the 1951–1990 reference period (Figure S3, Table S5). In four years (1957, 1991, 2016 and 2017) there is documented evidence of frost events, and local climate records confirm the abrupt drop of temperatures (Table S6). In 1957,

1991 and 2017, high temperature anomalies were recorded at all sites, whereas in 2016 E-OBS data underestimated the frost risk for the southern VOL and POL sites. Above average ΣT and ΔT values following the LSF events in years 1957, 2016 and 2017 are recorded in most sites and plots, whereas in 1991 high ΣT and ΔT occurred only at ACU site.

3.4. Impact of LSF on radial growth

Within the common time interval (1950–2019) we detected 56 nPYs distributed in 21 different calendar years (Figure 4). In particular, 19 nPYs were associated to LSF events detected in previous analyses. LSF rings occurred in 1957, 1970, 1991, 2001, 2016 and 2017. All trees from ACU and VOL sites showed the 1957 nPY, as well as the MDF-high, POL-low and POL-mid plots. The LSF events in 1970 and 1991 lead to nPYs only in POL-low and ACU-low plots, respectively. All MDF plots shared a LSF ring in 2001, as well as VOL-mid and POL-mid plots. According to local weather station data, the mean values of ΣT and absolute minimum temperatures in years of LSF ring occurrence were 302°C and -3.9 °C respectively (Figure S4).

The SEA of ring-width indexed series revealed a significant ($p < 0.05$) growth reduction in 71% of the series during the LSF year (Figure 5). One year after each LSF event growth was recovering since reduction occurred in only 4.9 % of the trees. In affected trees average growth was 54 and 84 % lower than the two preceding years (Table S7). At all plots, growth series showed high levels of recovery. Two years after (t_{+2}) the LSFs, tree rings were 2.49-4.81 times wider than in the year of the event. The resilience index was around 1 or even higher in most cases, meaning that ring-width indices were equal or higher in t_{+2} compared to t_{-2}. Only at ACU, the resilience index showed low values, in high- and mid-elevation plots after the 2016 LSF.

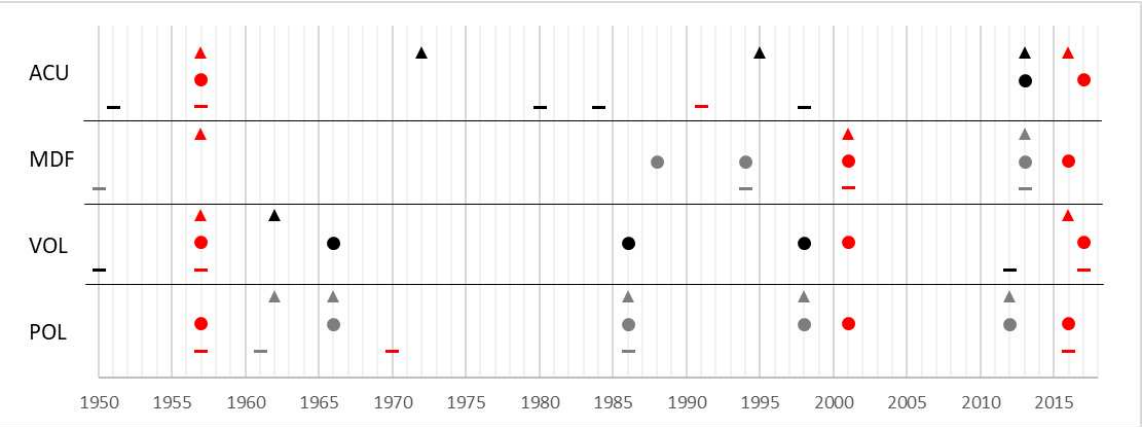

Figure 4. Negative pointer years (nPYs) detected at high (▲), mid (•) and low (-) elevation plots of the four study sites in the period 1950–2019. In red the nPYs occurred in LSF years when ΔT and ΣT exceeded the third quartile threshold.

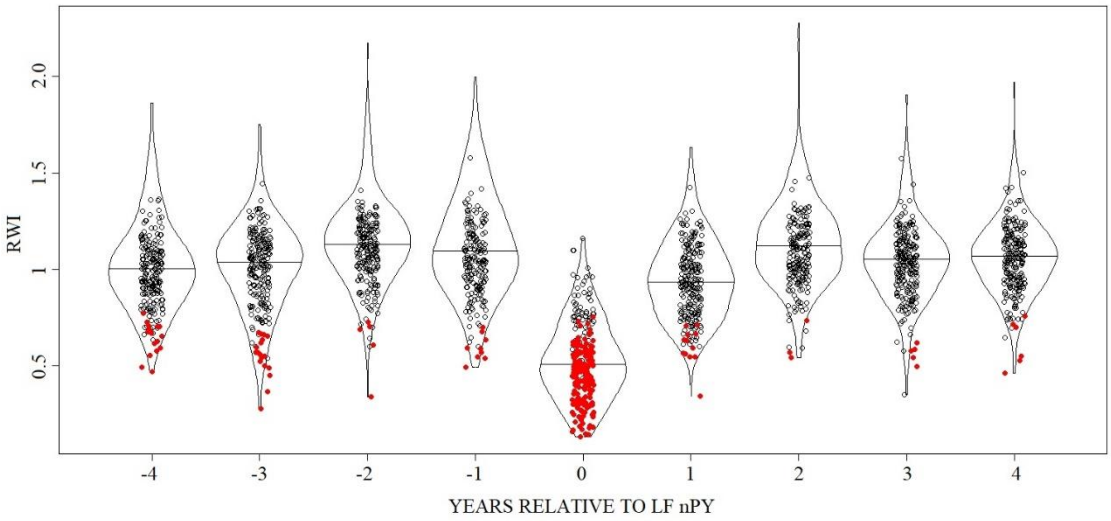

Figure 5. SEA beech growth response to spring late frosts (LSFs) in 1950-2019 time interval. The y axis shows the number of years before and after LSF negative pointer years (nPY). Horizontal lines inside the "violins" indicate median ring-width indices (RWI), whereas red dots a significant ($p < 0.05$) RWI reduction.

3.5. Variability factors in growth sensitivity to LSFs

Several trees featured some narrow rings related to spring frost (LSF rings). The frequency of LSF rings ranged from zero to five in the period 1960–2019, with most trees (41.8%) showing two LSF rings in their tree-ring series (Figure S5). The estimated number of LSF rings tends to be higher at mid- than at low- and high-elevation plots

(Figure S6), but between-plot differences were higher at MDF site despite no significant ($p = 0.11$). We did not find any significant contribution of tree parameters such as age, mean TRW, MS, Gini, and BAI trend as predictors of the LSF rings number using the GLMs modelling approach (Table S8). We only found two significant predictors using binomial models with random effects (GLMERs) to predict presence/absence of frost in 1957 (Age) and 2016 (Gini). For the 1957 events, the sites explained 66% of variance, while plot elevation only 6% (Table S6).

3.6 Late frost detection from remote sensing data

We computed vegetation indices (NDVI, EVI and LAI) at each elevation plot in ACU and VOL sites to assess the canopy reflectance trend throughout the growing seasons in 2016 and 2017 (years with LSF) as compared with 2018 a -LSF free year (Figs. 6 and 7). At ACU, the 2016 frost occurred on April 26th (DOY 116) and affected only the high-elevation plot. NDVI and EVI values were respectively 25% and 43% lower than undisturbed plots at DOY 147. EVI and NDVI values recovered over two months (DOY 180). At the same site, in 2017 the LSF occurred on April 22nd (DOY 112) and affected only the mid-elevation plot, with NDVI and EVI values 65% and 51% lower, respectively, then undisturbed plots at DOY 151. At ACU in 2017 beech canopies fully recovered the LSF event after 79 days (DOY 191), when spectral vegetation indices assume the same levels as the unaffected plots. The LSF occurred at VOL in 2016 (DOY 116) affected the high-elevation plot, with NDVI and EVI values respectively 34% and 54% lower than undamaged plots at DOY 144. On the contrary, the 2017 LSF (DOY 111) affected only the low- and mid-elevation VOL plots, with NDVI and EVI values respectively 17% and 23% lower than at unaffected high-

elevation plot at DOY 134. At VOL LSF in affected plots EVI and NDVI reached normal values after 88 days in 2016 and after 67 days in 2017.

Figure 6. The averaged NDVI and EVI trend curves throughout the growing seasons in 2016 and 2017 (LSF years) and 2018 (no-LSF year) at the three elevation plots at ACU and VOL sites. DOY (day of the year) is reported in x axes.

Late spring frost effect on LAI_{eff} is evident at both ACU and VOL in 2016 and 2017. We found differences comparing mean values of affected and unaffected plots and between post-frost (DOY 140-160) and recovery periods (DOY 190-210). In affected plots, the LAI_{eff} values are nearly half of those recorded in unaffected plots (1.2 to 2.3 m^2 m^{-2} vs. 2.8 – 5.0 m^2 m^{-2}) (Figure 7). As expected, in the latter plots LAI_{eff} values of post-frost and recovery periods were very similar, whereas in affected plots LAI_{eff} increased

until mid-July and reached 3.2 – 4.0 m^2 m^{-2} values. However, in disturbed plots estimated LAI_{eff} in the recovery period are in most cases slightly lower than in undisturbed plots.

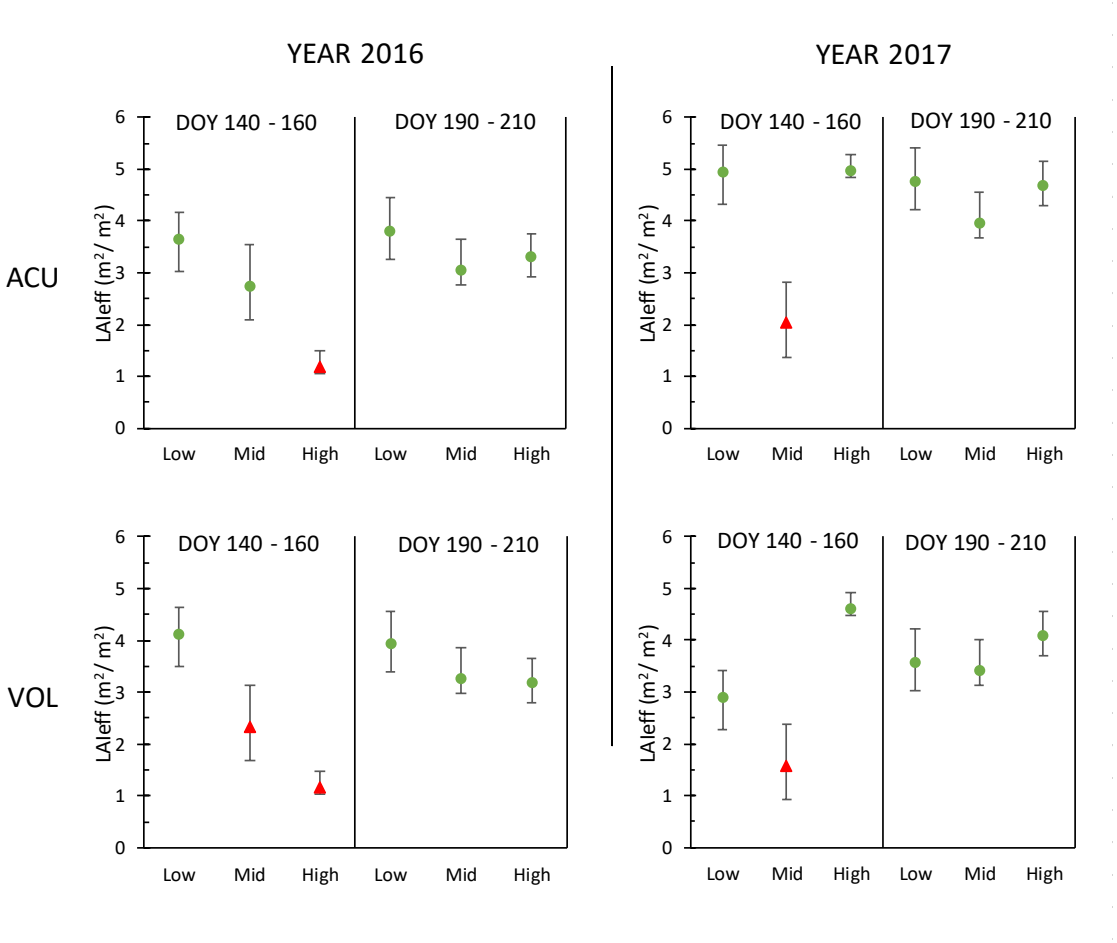

Figure 7. LAI_{eff} values at ACU and VOL sites in the two LSF years (2016 and 2017). The whiskers represent the minimum and maximum values within each plot. Mean LAI_{eff} values were compared between plots using a two-sided Wilcoxon test. Significant low LAI_{eff} values in affected plots are marked width a red triangle ($p<0.01$).

4. Discussion

The Apennines range, where beech shares more than 10% of the total forested area, is a transition zone where cold and wet air masses coming from Northern and Eastern Europe are merging with warmer masses from northern Africa. These conditions can induce important regional or local phenological variability of beech and increase its sensitivity to LSF events. Here we focused on detection and assessment of LSF effects on beech stands in Central and Southern Apennines. We used diverse but complementary

approaches to quantify, date, and spatially define the occurrence and the effects of major LSFs on beech forest productivity and growth. The results confirmed our hypothesis of the absence of a clear relationship between beech forest elevation and the incidence of LSF-induced defoliation. More severe growth reduction was found at mid-elevation plots (Figs. 4 and S6), although this can depend on LSF severity and time of occurrence. The POL-high plot (in southern Apennines) revealed the most resistant beech stand to LSFs without nPYs potentially associated to LSF impacts. In several cases, a defoliation-free portion of beech forest occurred above a defoliated one (e.g. at POL in 2016 or ACU and VOL in 2017). In these cases, the possibility of temperature inversions cannot be excluded, but the defoliation observed only at the intermediate zone of the slope suggested its relationship to the interannual thermal conditions and to the elevation dependent differences of bud burst timing.

Radial growth in beech forests depends on elevation, decreasing at higher elevation, given the shorter length of the growing season and the lower temperature (Pretzsch et al. 2021, Etzold et al. 2022). Nonetheless, at lower elevation or at sites with less summer precipitation, beech radial growth is more severely limited by water deficit (Dittmar et al 2003, Rozas et al. 2015, Rubio-Cuadrado et al. 2018, Serra-Maluquer et al. 2019). At lower elevation in Mediterranean mountains, growth and productivity of beech forests are also severely constrained by summer drought (Geßler et al. 2007, Piovesan et al. 2008, Gazol et al. 2019, Tognetti et al. 2019), a factor designing the southernmost xeric edge of beech distribution (Jump et al. 2006, Bolte et al. 2007, Serra-Maluquer et al. 2019).

Tree-ring analysis along the altitudinal gradients was the first step to detect the most exposed sites and the potential event years induced by LSF (Figure 2). In general, warm, and dry summer conditions were the main limiting factors of beech growth, in

agreement with other studies in the Apennines (Piovesan et al. 2003) and in the Iberian Peninsula (Rozas et al. 2015, Serra-Maluquer et al. 2019, Camarero et al. 2021). This reflects the beech tendence to avoid too dry and cold conditions.

At both central and southern sites beech growth was negatively affected by low summer precipitation, particularly at the two southernmost sites (POL and VOL) and at the MDF-low plot (Figure 3, Table 2). Significant relationships with April and May temperatures in some of the plots suggested a possible influence of spring frosts. Cold May temperatures could be an indicator of the LSF occurrence and warm temperature in April could anticipate the leaf emission and expose beech to LSF damage (Piovesan et al. 2003, Gazol et al. 2019, Sangüesa-Barreda et al. 2021).

At individual level, 32% of sampled trees were not significantly correlated with the selected climate parameters. Since in the sampled plots beech stands were or are still managed as coppice with standards, we assumed that the current dominant trees could be formerly in the intermediate or suppressed canopy layers, where trees possibly feature a lower climate sensitivity (Martín-Benito et al. 2008).

Using two climate indices, we detected warm springs followed by frost events in eleven years. However, plots' chronologies showed an abrupt growth decrease in only six of those years. Ten out of twelve plots were hit by at least two extreme events in the period 1950–2019 (Figure 4), with an average return time of 39 years, irregularly ranging from 13 to 60 years. Consecutive frost events occurred at the same site but causing damages at different elevations (e.g., ACU and VOL sites in 2016 and 2017 LSFs). No plots showed negative pointer years related to frosts in consecutive years; however, in the VOL-mid 67% of the series showed a negative event year in 2016 whilst 75% of series did it in 2017. The estimation of the return time is highly influenced by the thresholds used to define a pointer year in tree-ring chronologies. Sangüesa-Barreda et al. (2021)

calculated a reduced return time from 33 to 14 years before and after 1990 respectively. In our case, most LSFs also occurred after 1990 (in 1991, 2001, 2016 and 2017), excluding the 1957 event which affected all sites (Figure 4) and the 1970 event detected only at POL-low. In our studied stands the most severe LSFs occurred in 1957, 2016 and 2017, causing a radial growth reduction ranging from 36% to 84%. Even if in VOL-mid several trees were affected by consecutive frost events, their resilience values remained high even after the 2017 event.

LSFs can also occur at the beginning of dry growing seasons, a particular combination that occurred at the ACU site in 2017, with defoliation only at the mid elevation belt. ACU-middle trees show low resistance and resilience under the 2017 stressful conditions, with averaged values of 0.16 and 0.56 respectively (Tab. S7). Very dry summer periods can also reduce beech radial growth in the following years (Decuyper et al 2020, Hacket-Pain et al. 2016).

However, excluding this particular effect at ACU site, we did not find significant growth reductions in the years following the LSFs (Figure 5), suggesting a good recovery of beech to this disturbance, in accordance with recent studies (D'Andrea et al. 2019, Rubio-Cuadrado et al. 2021a, 2021b).

Not only LSF and drought events can cause negative pointer years in beech trees, but also masting years and insects' outbreaks (Hacket-Pain et al. 2015; Camarero et. al. 2018; Nussbaumer et al. 2021). The 2013 negative pointer year could be related to a mast year reported across beech forests of central Italy (Mancini et al. 2016), however the general lack of long-term, detailed data on seed production cannot confirm this hypothesis. In the same year in southern Apennine beech forests reduced radial growth in was attributed by unusually moister and colder conditions during the summer (Šimůnek et al. 2021).

GLMs show that the frequency of LSF rings is related to elevation rather than to individual tree parameters. Our mid-elevation beech plots (1245-1590 m asl) appeared the most sensitive to LSF on in terms of growth. This altitude range fits very well with the one (1250-1500 m asl) proposed for beech as the most exposed to LSFs in the southern Apennines (Nolè et al. 2018).

Detection and assessment of the LSFs impact on forest canopy cover and greenness can be efficiently conducted with remote sensing data and indices (Bascietto et al. 2018, 2019, Nolè et al. 2018, Rubio-Cuadrado et al. 2021a, Olano et al. 2021). At this regard we found EVI being a more sensitive index than NDVI to detect LSF effects on beech canopies (Figs. 6 and 7). In the affected beech stands of our study in 2016 the average NDVI and EVI were respectively 30% and 48% lower than unaffected forests, whereas in 2017 32% and 47% lower. The forest canopy on average recovered after 75 days from the frost events. However, the estimated recovery period can be biased by the time resolution of the used satellite data, and on cloud cover levels, challenging a correct daily resolution at population scale. The 2016 frost at VOL site was confirmed by the remoted sensed data, local meteorological records, and abrupt growth reductions, but not by the E-OBS gridded data that appeared to overestimate the minimum temperatures over the late frost period. The availability of suitable long-term *in situ* meteorological data would have helped the analysis. However, microclimatic conditions play an important role in regulating the budburst timing in spring while temperature of buds and leaves can be much lower than the temperature recorded by standard weather stations during clear nights due to radiative cooling (Vitasse et al., 2021).

Software applications based on artificial intelligence can estimate the biophysical components of vegetation such as LAI, but they could underestimate higher LAI values such as those observed over dense forests (Brown et al. 2021, Filipponi 2021). In our

beech forests, LAI_{eff} values ranged between 2.8 and 5.0 m^2 m^{-2} in relation to the stand structure. LSFs in ACU and VOL sites resulted in an estimated loss of LAI_{eff} values of 2.4-3.0 m^2 m^{-2} compared to undamaged neighbouring plots. In many cases, affected plots showed lower LAI_{eff} values until mid-July, probably due to the presence of smaller leaves (Rubio-Cuadrado et al. 2021a, 2021b). These findings demonstrate an intra-annual legacy effect which could be further investigated in terms of productivity or reduction in carbon uptake of the most affected stands by performing quantitative wood anatomy studies. Interestingly, such intra-annual legacy effects of reduced LAI_{eff} did not turn into inter-annual growth legacy effects. The use of both high-resolution satellite and aerial multispectral images and LiDAR based sensors could provide more information to study forest disturbances at finer spatial and temporal scales.

Our findings cannot confirm that LSF severity increased in the 1990s, given the widespread and great impact of the 1957 LSF across the Apennines. Nonetheless, we demonstrated the high resilience capacity of beech forests after LSFs. In addition, we cannot discard that an increasing frequency of LSFs could alter such resilience capacity, particularly in Mediterranean mountains prone to a forecasted warming but also to more variable precipitation which could increase the frequency of adverse weather extremes such as frost and drought events (Giorgi and Lionello 2008).

5. Conclusions

In European beech low growth rates caused by LSF-induced leaf shedding depend on site spring phenology and extreme temperature drop; both factors are closely related to elevation. However, beech trees affected by spring frost appeared to be resilient and rapidly recovering their growth rates, showing no year-to-year legacy or carryover effects. Satellite imagery was very useful to detect the most affected trees or stands and

to assess the LSFs impact and recovery time at intra-annual levels. Nonetheless, late frosts remain a threat in Apennine's beech forests, especially if followed within the same growing season by summer drought, another highly influential driver of climatic stress of trees. These extreme events and their potential synergy within globally warmer and climatically variable scenarios should be certainly considered in the future forest management and planning of mountain beech forests.

Acknowledgements

We acknowledge the E-OBS dataset from the EU-FP6 project UERRA (https://www.uerra.eu) and the Copernicus Climate Change Service, and the data providers in the ECA&D project (https://www.ecad.eu). JJC acknowledges funding by project RTI2018-096884-B-C31 of the Spanish Ministry of Economy, Industry and Competitiveness.

Supplementary material (Tree-ring and remote sensing analyses for assessing the role of elevation on European beech sensitivity to late spring frost)

Table S1. Mean climate parameters calculated in the four study sites from E-OBS gridded. Reported mean annual temperatures were interpolated at middle-plot elevation considering a mean lapse rate of −6.5 °C km^{-1} (see table 1 for details of plot elevations).

Site	Mean annual temperature (°C)	Total annual precipitation (mm)
ACU	8.4	1330
MDF	6.4	937
VOL	6.7	754
POL	5.0	985

Table S2. Spatial location of the climatic stations closest to the sites

Station	**Elevation (m a.s.l.)**	**Lat (°N)**	**Long (°E)**	**Nearest site**	**Distance from nearest site (km)**
Fonte Avellana	690	43.7411	12.7264	ACU	4.4
Umito	646	42.7374	13.4066	MDF	15.5
Marsicovetere	598	40.3389	15.8336	VOL	10.7
Rotonda	549	39.9493	16.0225	POL	12.1

Table S3. List of the Sentinel-2A and -2B images used to detect the canopy damage in beech forests during years 2016, 2017 and 2018. Dates as expressed as dd/mm/yyyy format.

2016			2017			2018		
Date	Satellite	Site	Date	Satellite	Site	Date	Satellite	Site
21/03/2016	Sentinel-2A	VOL	25/03/2017	Sentinel-2A	ACU	13/04/2018	Sentinel-2A	VOL
27/03/2016	Sentinel-2A	ACU	29/03/2017	Sentinel-2A	VOL	16/04/2018	Sentinel-2A	ACU
20/04/2016	Sentinel-2A	VOL	17/04/2017	Sentinel-2A	ACU	21/04/2018	Sentinel-2B	ACU
23/05/2016	Sentinel-2A	VOL	24/04/2017	Sentinel-2A	ACU	23/04/2018	Sentinel-2A	VOL
26/05/2016	Sentinel-2A	ACU	25/04/2017	Sentinel-2A	VOL	20/05/2018	Sentinel-2A	VOL
16/06/2016	Sentinel-2A	ACU	01/05/2017	Sentinel-2A	ACU	31/05/2018	Sentinel-2B	ACU
28/06/2016	Sentinel-2A	ACU	05/05/2017	Sentinel-2A	VOL	10/06/2018	Sentinel-2B	ACU
29/06/2016	Sentinel-2A	VOL	31/05/2017	Sentinel-2A	VOL	12/06/2018	Sentinel-2A	VOL
09/07/2016	Sentinel-2A	VOL	04/06/2017	Sentinel-2A	VOL	23/06/2018	Sentinel-2B	ACU
18/07/2016	Sentinel-2A	ACU	13/06/2017	Sentinel-2A	ACU	04/07/2018	Sentinel-2B	VOL
22/07/2016	Sentinel-2A	VOL	20/06/2017	Sentinel-2A	ACU	13/07/2018	Sentinel-2B	ACU
01/08/2016	Sentinel-2A	VOL	27/06/2017	Sentinel-2A	VOL	13/08/2018	Sentinel-2B	VOL
14/08/2016	Sentinel-2A	ACU	10/07/2017	Sentinel-2A	VOL	22/08/2018	Sentinel-2B	ACU
23/09/2016	Sentinel-2A	ACU	12/07/2017	Sentinel-2B	ACU	12/09/2018	Sentinel-2B	VOL
30/09/2016	Sentinel-2A	VOL	29/07/2017	Sentinel-2A	VOL	23/09/2018	Sentinel-2A	ACU
17/10/2016	Sentinel-2A	VOL	02/08/2017	Sentinel-2A	VOL	30/09/2018	Sentinel-2A	VOL
16/11/2016	Sentinel-2A	VOL	03/08/2017	Sentinel-2A	ACU	13/10/2018	Sentinel-2A	ACU
			26/08/2017	Sentinel-2A	VOL	25/10/2018	Sentinel-2B	VOL
			29/08/2017	Sentinel-2A	VOL	11/11/2018	Sentinel-2B	VOL
			15/09/2017	Sentinel-2A	ACU	12/11/2018	Sentinel-2A	ACU
			21/09/2017	Sentinel-2A	VOL			
			11/10/2017	Sentinel-2A	ACU			
			12/10/2017	Sentinel-2A	ACU			
			22/10/2017	Sentinel-2A	VOL			
			04/11/2017	Sentinel-2A	VOL			

Table S4. Correlation matrix between the standard chronologies of each sampled plot. Correlations were calculated for the common period 1950–2019. Correlation values above critical Pearson coefficients (one tail) at 95% or 99% confidence level were highlight with half stars or full stars respectively. Sites are ordered by latitude (north to south).

		ACU			MDF			VOL			POL		
		High	*Middle*	*Low*	*High*	*Middle*	*Low*	*High*	*Middle*	*Low*	*High*	*Middle*	*Low*
ACU	*High*	★ 1											
	Mid	★ 0.741	★ 1										
	Low	★ 0.531	★ 0.681	★ 1									
MDF	*High*	★ 0.600	★ 0.406	☆ 0.268	★ 1								
	Mid	★ 0.585	★ 0.342	☆ 0.176	★ 0.833	★ 1							
	Low	★ 0.414	★ 0.440	★ 0.361	★ 0.561	★ 0.631	★ 1						
VOL	*High*	★ 0.425	☆ 0.236	☆ 0.171	★ 0.396	★ 0.424	★ 0.321	★ 1					
	Mid	★ 0.602	★ 0.530	★ 0.305	★ 0.428	★ 0.475	★ 0.408	★ 0.700	★ 1				
	Low	★ 0.482	★ 0.596	★ 0.577	★ 0.299	☆ 0.205	★ 0.409	★ 0.453	★ 0.715	★ 1			
POL	*High*	☆ 0.219	☆ 0.194	☆ 0.229	★ 0.302	★ 0.295	☆ 0.232	★ 0.373	☆ 0.219	☆ 0.245	★ 1		
	Mid	★ 0.479	★ 0.351	☆ 0.241	★ 0.318	★ 0.385	☆ 0.087	★ 0.646	★ 0.633	★ 0.451	★ 0.559	★ 1	
	Low	☆ 0.208	☆ 0.082	☆ 0.023	☆ 0.109	☆ 0.120	☆ -0.102	★ 0.481	★ 0.446	★ 0.291	★ 0.609	★ 0.701	★ 1

Table S5. Accumulated degree days (ΣT) and spring temperature anomalies (ΔT) calculated from E-OBS gridded. Bold values are exceeding the 3rd quartile computed for the reference period 1951-1990 (Q3 1951–1990).

Parameter (°C)	Year						Q3 1951-1990
	1957	1970	1991	2001	2016	2017	
ΔT ACU	**6.7**	2.4	**4.8**	**6.3**	**4.8**	**5.3**	2.7
ΔT MDF	**5.4**	2.5	**4.1**	**5.1**	**5.8**	**5.6**	2.8
ΔT VOL	**5.9**	**3.9**	**3.8**	**5.5**	1.5	**5.2**	2.8
ΔT POL	**4.7**	**3.4**	**4.6**	**3.8**	1.2	**6.1**	2.6
ΣT ACU-Low	**450**	383	**471**	**558**	**518**	**445**	435
ΣT ACU-Mid	308	272	**383**	**432**	**409**	**336**	321
ΣT ACU-High	245	219	**313**	**347**	**344**	**277**	248
ΣT MDF-Low	**395**	278	338	**484**	**583**	**503**	345
ΣT MDF-Mid	**227**	182	205	**335**	**419**	**357**	215
ΣT MDF-High	130	130	123	**218**	**363**	**282**	163
ΣT VOL-Low	**497**	209	231	**427**	**835**	**463**	336
ΣT VOL-Mid	**419**	176	182	**319**	**745**	**414**	274
ΣT VOL-High	**302**	150	93	**206**	**581**	**302**	192
ΣT POL-Low	**410**	176	152	235	**822**	**364**	240
ΣT POL-Mid	**309**	144	120	**163**	**716**	**274**	171
ΣT POL-High	**115**	**81**	16	**69**	**468**	**137**	68

Table S6. Absolute minimum temperature and accumulated degree-days recorded in some LF events.

Station	Late frost date	Site plot	Interpolated absolute minimum temperatures (°C)	Accumulated degree-days (ΣT, °C)	Percentage of tree-ring series showing a narrow ring
F. Avellana	7 May 1957	ACU-High	-4.0	261	90.0
F. Avellana	7 May 1957	ACU-Mid	-3.1	354	100.0
F. Avellana	7 May 1957	ACU-Low	-2.0	492	94.1
F. Avellana	2 May 1970	ACU-High	-2.4	173	0.0
F. Avellana	2 May 1970	ACU-Mid	-1.5	223	16.7
F. Avellana	2 May 1970	ACU-Low	-0.4	315	5.9
F. Avellana	19 April 1991	ACU-High	-4.3	290	33.3
F. Avellana	19 April 1991	ACU-Mid	-3.4	367	61.1
F. Avellana	19 April 1991	ACU-Low	-2.3	476	76.5
F. Avellana	15 April 2001	ACU-High	-3.4	280	47.4
F. Avellana	15 April 2001	ACU-Mid	-2.5	369	38.9
F. Avellana	15 April 2001	ACU-Low	-1.4	476	47.1
Rotonda	8 May 2001	POL-High	-3.8	138	68.0
Rotonda	8 May 2001	POL-Mid	-1.9	215	88.9
Rotonda	8 May 2001	POL-Low	-1.0	297	40.9
Marsicovetere	8 May 2001	VOL-High	-5.1	154	19.2
Marsicovetere	8 May 2001	VOL-Mid	-3.8	227	33.3
Marsicovetere	8 May 2001	VOL-Low	-3.2	272	73.1
F. Avellana	22 April 2016	ACU-High	-3.0	260	81.0
F. Avellana	22 April 2016	ACU-Mid	-2.1	326	11.8
F. Avellana	22 April 2016	ACU-Low	-1.0	414	0.0
Umito	25 April 2016	MDF-High	-5.4	255	58.0
Umito	25 April 2016	MDF-Mid	-4.4	338	100.0
Umito	25 April 2016	MDF -Low	-2.6	479	0.0
Rotonda	26 April 2016	POL-High	-9.3	141	16.0

Rotonda	26 April 2016	POL-Mid	-7.4	255	96.2
Rotonda	26 April 2016	POL-Low	-6.5	318	95.2
Marsicovetere	25 April 2016	VOL-High	-3.2	284	80.8
Marsicovetere	25 April 2016	VOL-Mid	-1.9	411	66.7
Marsicovetere	25 April 2016	VOL-Low	-1.3	506	4.0
F. Avellana	19 April 2017	ACU-High	-4.9	186	68.8
F. Avellana	19 April 2017	ACU-Mid	-4.0	254	93.8
F. Avellana	19 April 2017	ACU-Low	-2.9	348	33.3
Rotonda	22 April 2017	POL-High	-8.2	11	25.0
Rotonda	22 April 2017	POL-Mid	-6.3	94	11.5
Rotonda	22 April 2017	POL-Low	-5.4	147	0.0
Marsicovetere	20 April 2017	VOL-High	-4.9	210	7.7
Marsicovetere	20 April 2017	VOL-Mid	-3.6	303	75.0
Marsicovetere	20 April 2017	VOL-Low	-3.0	361	91.7

Table S7. Percentage of series with negative event years (|zi| values > 0.75) and resilience indices after spring frosts occurred in 2016 and 2017 . Values are shown in bold when series with a negative year percentage exceed the 75% threshold.

Year	Site	Series with a negative event year (%)			Resistance (Rt) / Recovery (Rc) / Resilience (Rs) indices		
		High elevation plots	Mid elevation plots	Low elevation plots	High elevation plots	Mid elevation plots	Low elevation plots
2016	ACU	**81.0**	11.8	0.0	**0.31 / 2.49 / 0.78**	0.92 / 0.70 / 0.65	1.24 / 0.70 / 0.86
	MDF	58.8	**100.0**	0.0	0.53 / 1.39 / 0.73	**0.31 / 3.21 / 0.99**	1.38 / 0.65 / 0.90
	VOL	**80.8**	66.7	4.0	**0.41 / 4.76 / 1.93**	0.38 / 2.71 / 1.03	1.08 / 0.88 / 0.95
	POL	16.0	**96.2**	**95.2**	1.05 / 1.08 / 1.14	**0.27 / 4.81 / 1.29**	**0.46 / 2.27 / 1.05**
2017	ACU	33.3	**93.8**	68.8	0.44 / 1.11 / 0.49	**0.16 / 3.43 / 0.56**	0.62 / 1.31 / 0.82
	MDF	–	–	–	0.68 / – / –	0.61 / – / –	0.59 / – / –
	VOL	7.69	**75**	**91.7**	0.78 / 1.33 / 1.04	**0.27 / 3.45 / 0.94**	**0.41 / 2.68 / 1.11**
	POL	25.00	11.54	0.0	0.88 / 0.92 / 0.81	0.61 / 1.36 / 0.84	1.11 / 1.17 / 1.31

Table S8. Statistics based on four GLMs relative to each site and selected predictors. The "Estimate" values of "Low elevation" and "Mid elevation" predictors are the estimates respects to the High elevation plot in each of the four study sites. Abbreviations: TRW, mean tree-ring width; MS, mean sensitivity; Gini, Gini coefficient; BAI trend, basal area increment for the period 1990–2019.

Variable	ACU			MDF			VOL			POL		
	Estimate	SE	*p*	Estimate	SE	*p*	Estimate	SE	*p*	Estimate	SE	*p*
(Intercept)	0.28	0.83	0.74	0.05	0.98	0.96	1.13	0.72	0.12	0.93	0.70	0.19
Age	0.25	0.44	0.58	0.66	0.63	0.30	0.20	0.49	0.68	0.48	0.54	0.37
TRW	0.59	0.55	0.28	-0.25	0.65	0.70	-0.34	0.50	0.50	-0.24	0.69	0.72
MS	0.06	0.64	0.93	0.54	0.61	0.37	-0.01	0.47	0.98	0.00	0.52	1.00
Gini	0.39	0.58	0.50	-0.02	0.63	0.98	0.12	0.53	0.82	-1.11	0.81	0.17
BAI trend	0.04	0.60	0.95	-0.01	0.93	0.99	-0.31	0.61	0.62	-0.07	0.62	0.91
Mid-elevation plot	0.50	0.31	0.10	0.58	0.36	0.11	0.14	0.29	0.84	0.05	0.31	0.88
High-elevation plot	0.38	0.43	0.37	0.13	0.42	0.75	-0.25	0.26	0.24	-0.14	0.31	0.66

Table S9. Statistics based on two GLMEs relative to both 1957 and 2016 events. Plots are nested in sites and the variance explained by them is reported in the last row. Abbreviations: TRW, mean tree-ring width; MS, mean sensitivity; Gini, Gini coefficient. Significant predictors are highlighted with bold characters ($p \leq 0.05$).

Variable	1957			2016		
	Estimate	SE	*p*	Estimate	SE	*p*
(Intercept)	-0.73	0.96	0.45	-0.87	1.41	0.54
Age	6.33	1.79	**0.00**	1.97	1.50	0.19
TRW	0.46	1.07	0.67	1.41	1.47	0.34
MS	0.98	1.79	0.59	3.21	1.95	0.09
Gini	1.60	1.40	0.25	-3.66	1.85	**0.05**
Random effects	Variance					
Plot	0.06			0.00		
Site	0.66			0.00		

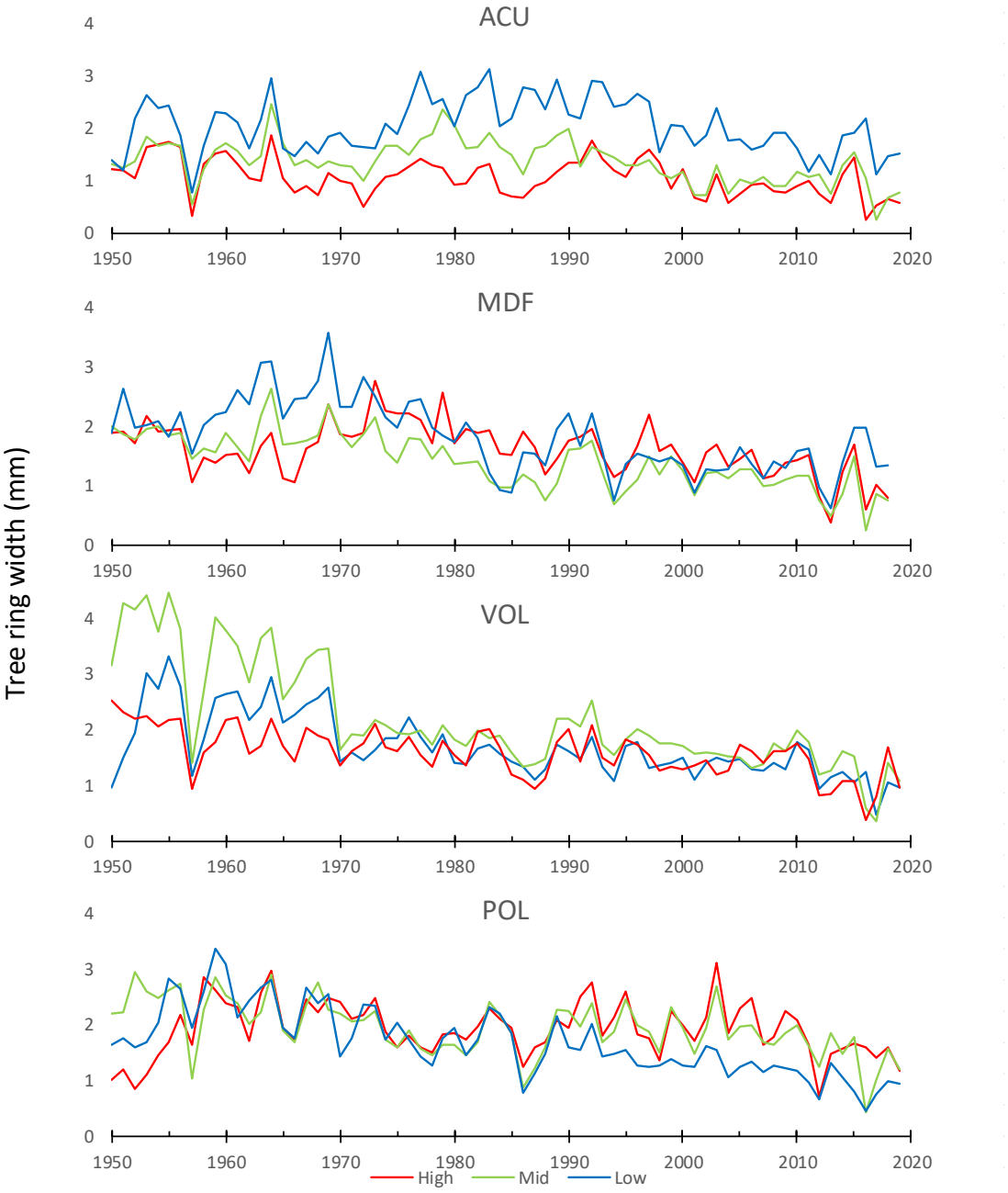

Figure S1. Mean ring-width series of the four study sites located at high (red lines), mid (green lines) and low (blue lines) elevation. Series are truncated in 1950, in accordance with the common time interval used for climate-growth analyses (1950-2019).

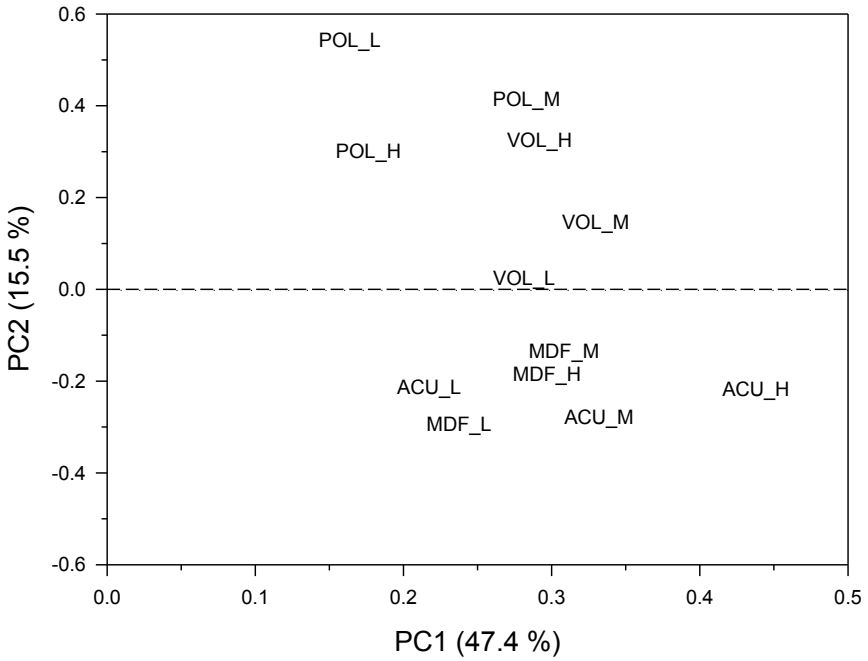

Figure S2. Principal component analysis biplot showing the plots' scores in the first (PC1) and second (PC2) principal components corresponding to four study sites (ACU, MDF, VOL and POL) and three elevations (_H, high; _M, mid; and _L, low).

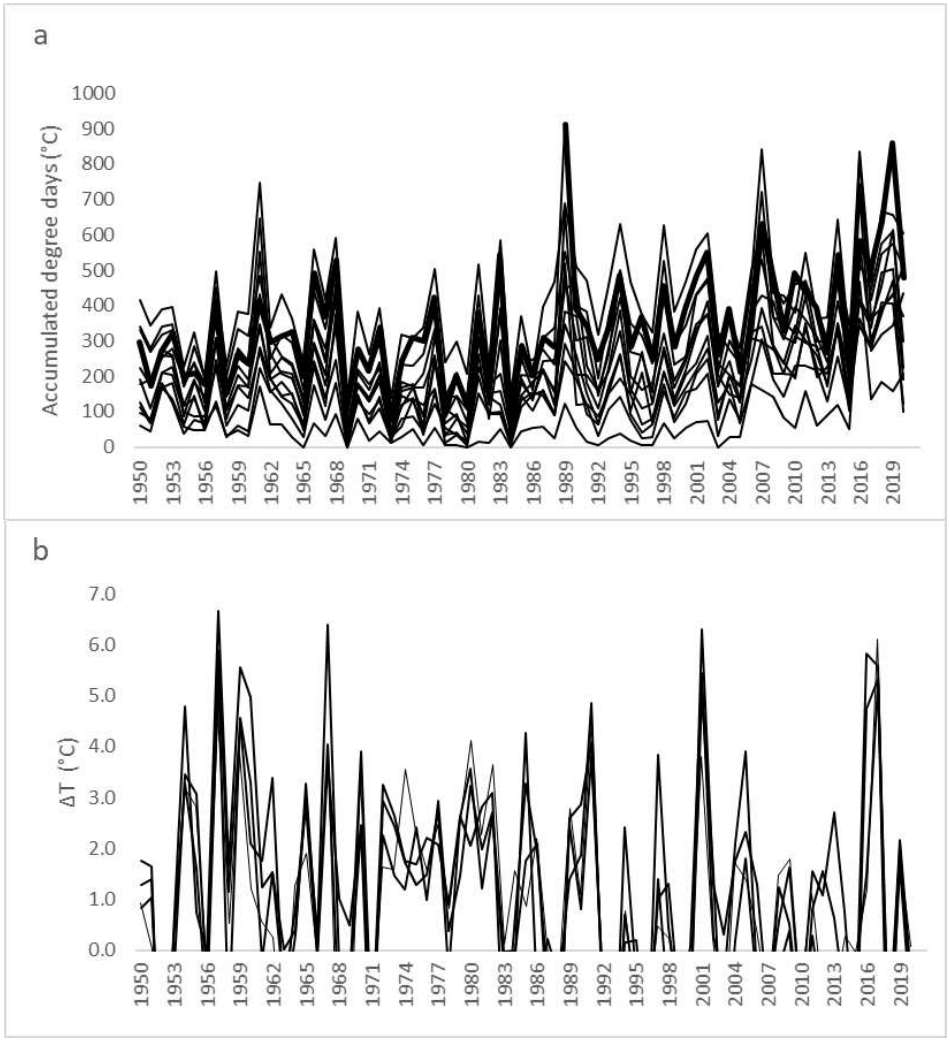

Figure S3. (a) Accumulated degree days (ΣT) and (b) spring temperature anomalies (ΔT) calculated in all study plots from E-OBS gridded climate data.

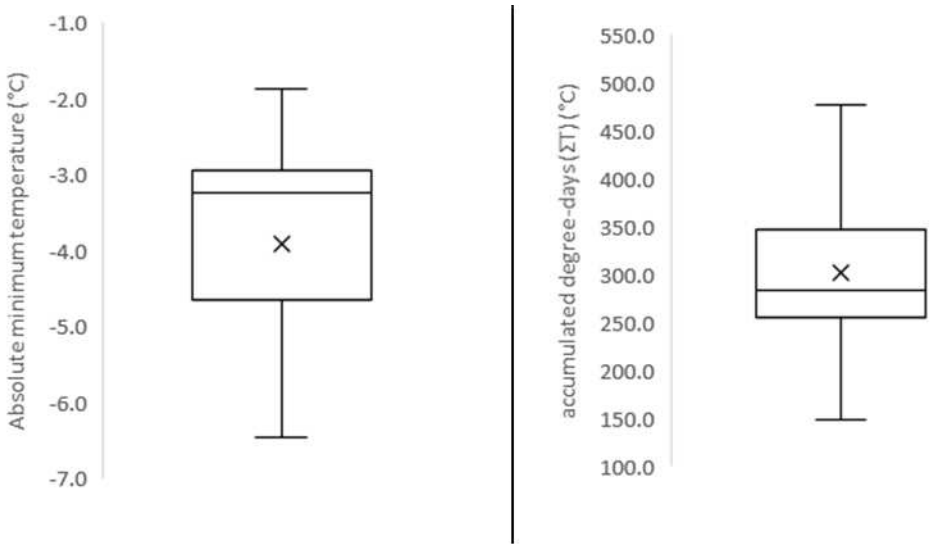

Figure S4. Absolute minimum temperature and accumulated degree-days (ΣT) in years with late frost negative pointer years. Data refer to local climate station records.

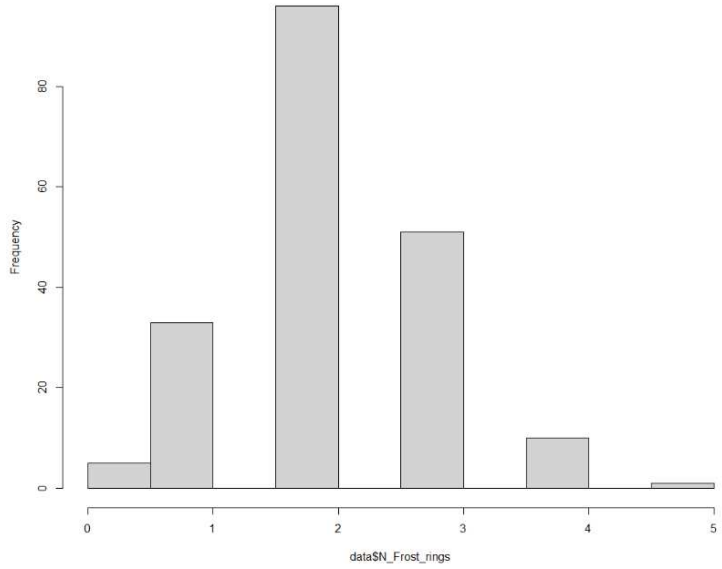

Figure S5. Number of trees (y axis) classified according to the number of produced LFnPYs (x axis).

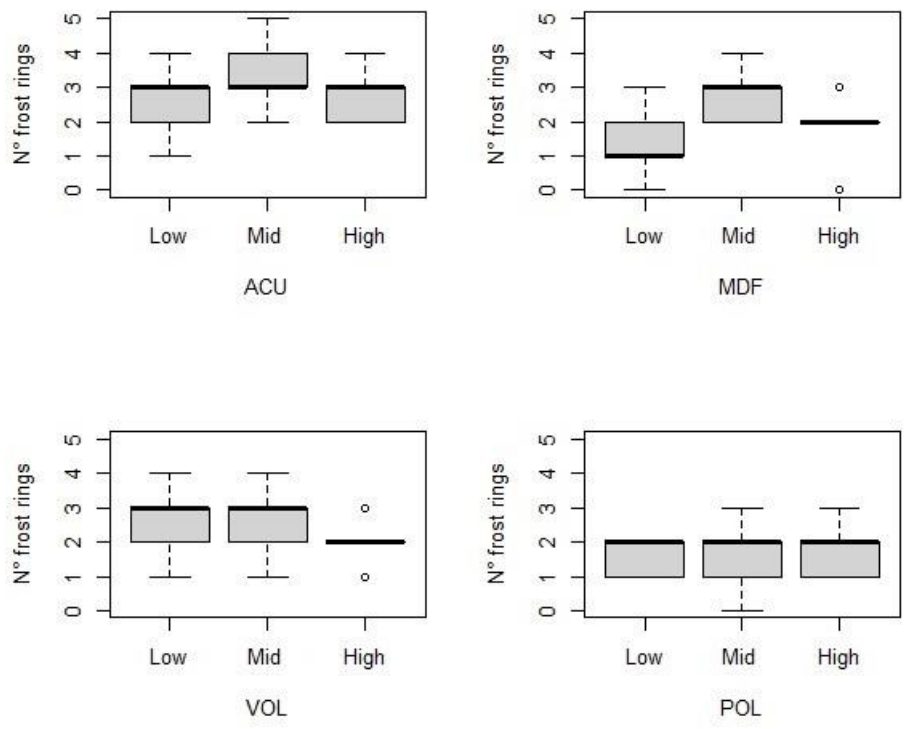

Figure S6. Estimated number of LFnPYs produced by trees at each of the four study sites and the three elevation plots.

Chapter 4

Do late frosts affect tree-ring growth and wood anatomical traits of European beech in Apennine forests (Italy)?

A printable version of this chapter in preparation and submitted to an international journal.

Authors: **Enrico Tonelli**[1], Marco Carrer[2], Alessandro Vitali[1]and Carlo Urbinati[1]

[1]Department of Agricultural, Food and Environmental Sciences, Marche Polytechnic University, Ancona, Italy.

[2] Universitá degli Studi di Padova, Dipartimento Territorio e Sistemi Agro-Forestali (TESAF), Viale dell'Università 16 - 35020 Legnaro, Italy

Abstract

Climate extremes such as spring frosts and droughts are the main meteorological disturbances affecting the European beech. Xylem anatomical features localized within an annual growth ring, allows to establish structure-function relationships and species sensitivity to environmental variability. In this study we aim i) to compare chronologies of tree-ring widths and vessel features of beech trees located along an elevation gradient and ii) to determine the variability of tree ring features before and after late frost disturbance. The study site, located in central Apennines, was hit by a severe spring frost in 2016. We investigated how vessel features vary in relation to indicators of spring frost occurrence, i.e., mean minimum temperatures (Tmin), accumulated degree days (ST) and temperatures anomalies (ΔT). Finally, we identify vessel features that formed immediately after frosts events and how they differ from those formed in non-affected trees. We found differences in vessel size along the altitudinal gradient, with high elevation stands showing smaller vessel diameter, vessel area and higher rates of vessel density. Vessel features do not provide significant added values in the evaluation of spring frost sensitivity. In fact, spring frosts cause the formation of very narrow tree rings but with no-significant differences in vessel features. However, these preliminary results need to be developed in other study sites to evaluate how climate extremes influence on beech wood anatomy along geographic gradients (elevation, latitude) and different forest structure (age, height, diameters, woodland management).

1. Introduction

Dendroanatomy is a relatively recent developed technique in dendroecology, that apply a quantitative wood anatomy (QWA) analysis of xylem-cell features along dated tree rings (von Arx et al. 2018, Pandey 2021). The aim is to obtain quantitative information with annual resolution, such as tracheid's features in conifers species or vessel features in broadleaf trees, providing better proxies than simple ring width. In broadleaf species, also wood fibres are as sensitive to environmental conditions as vessels in tree rings and can be useful for studying the responses of vegetation to stresses (De Micco et al. 2016, Prendin et al. 2020). The sample preparation is rather time consuming due to the various steps from the increment core sampling to the final image section to be used in the analysis (von Arx et al. 2016). However, the information extracted with QWA allows to better understand the influence of biotic and abiotic factors on the ecology of tree species and their adaptability under a climate change scenario. The analysis of the anatomical features and the construction of their time series represents a useful proxy for reconstructing disturbances that occurred in the past, before the availability of climatic data.

European beech (*Fagus sylvatica*) is one of the most widely distributed broadleaf species in Europe and is a key species in various protected habitats of Natura 2000 network. Several dendroecological studies describes European beech as a drought sensitive species, especially in its southern distribution edge and in the lowlands (Piovesan et al. 2008, Geßler et al. 2007, Gazol et al. 2019, Tognetti et al. 2019). Studies in beech QWA show that variation in vessel diameter, vessel area and vessel density are the main anatomical parameters for evaluating tree-drought relationship (Hajec et al. 2016, Arnič et al. 2021). However, vessel features in broadleaf species are also influenced by individual trees parameters such as tree total height and crown size which could mask the variability explained by climate factors when studying non-coetaneous stands (Rossel et al. 2017, Carrer et al., 2015).

Drought is not the only one climatic factor constraining European beech, which is also low tolerant to late frost (Dittmar et al. 2006; Menzel et al. 2015). In Europe the occurrence of late frost evets and associated defoliation is increasing in beech forests (Zohner et al. 2020; Sangüesa-Barreda et al. 2021), constraining their growth and productivity. Several studies described the effects of a recent spring frost occurred in Italy in 2016, which mostly involved the Apennines Mountain range where around one third of the Italian beech forests experinced defoliation (Nolè et al. 2018, Bascietto et al. 2018, 2019). Late frost influences the radial growth of beech in the years of occurrence, but in mature trees did not affect the growth in the following season (Príncipe et al. 2017; D'Andrea et al. 2019). Little is known on the relationship between spring frosts defoliations and the anatomical features in beech. Extreme frost events in European beech could be exceptionally marked by frost rings with

traumatic and distorted ray parenchyma (Braeuning et al. 2016), but in other cases no obvious peculiarities were observed (Príncipe et al. 2017).

In this study we aim to study how vessel features vary in relation to stand elevation in a pure beech stand in central Apennine. As the study area has recently been affected by a late frost event, we focussed on the role of this exceptional disturbance in determining the tree-ring features immediately after the event and the post disturbances legacies.

2. Materials and methods

2.1 Study site

The study area is located on the northern side of Montagna dei Fiori (MDF) the eastern most ridge (Fig.1) of the Monti della Laga orographic system. This massif is just 30 km westward of the Adriatic sea and its highest peak, Mount Girella, reaches the elevation of 1814 m a.s.l.. MDF is a N-S trending, regional anticline and soils are found on argillaceous marl bedrock (Di Francesco et al. 2010). The study area slopes are mainly covered by coppiced broadleaf forests (largely unmanaged), and to a lesser extent by coniferous plantation, whereas grasslands are concentrated at higher elevations above the current beech treeline located between 1570 and 1658 m a.s.l. (Biondi & Galdenzi 2012). Climate is temperate oceanic (submediterranean) with a mean annual temperature of 13.7°C and total precipitation of 790 mm. The study area was affected by a spring frost which occurred on April 25th, 2016, causing defoliation from 1300 m a.s.l. to the upper limit of the forest.

2.2 Sampling protocol

In the summer of 2019, three circular plots of 20 m radius were placed in pure beech forest stands along an elevational gradient, respectively at low (1080 m a.s.l.), mid (1245 m a.s.l.) and high elevation (1375 m a.s.l.). In each plot cores were extracted at breast height (1.30m) from five dominant randomly selected trees, using a 10-mm increment borer. All cores were mounted on wooden supports and thoroughly polished with progressively finer sandpaper. Tree-ring width measurements at 0.01 mm was provided by a semi-automatic system (LINTAB). Each measured series was visually crossdated and then checked with the COFECHA software (Holmes 1983).

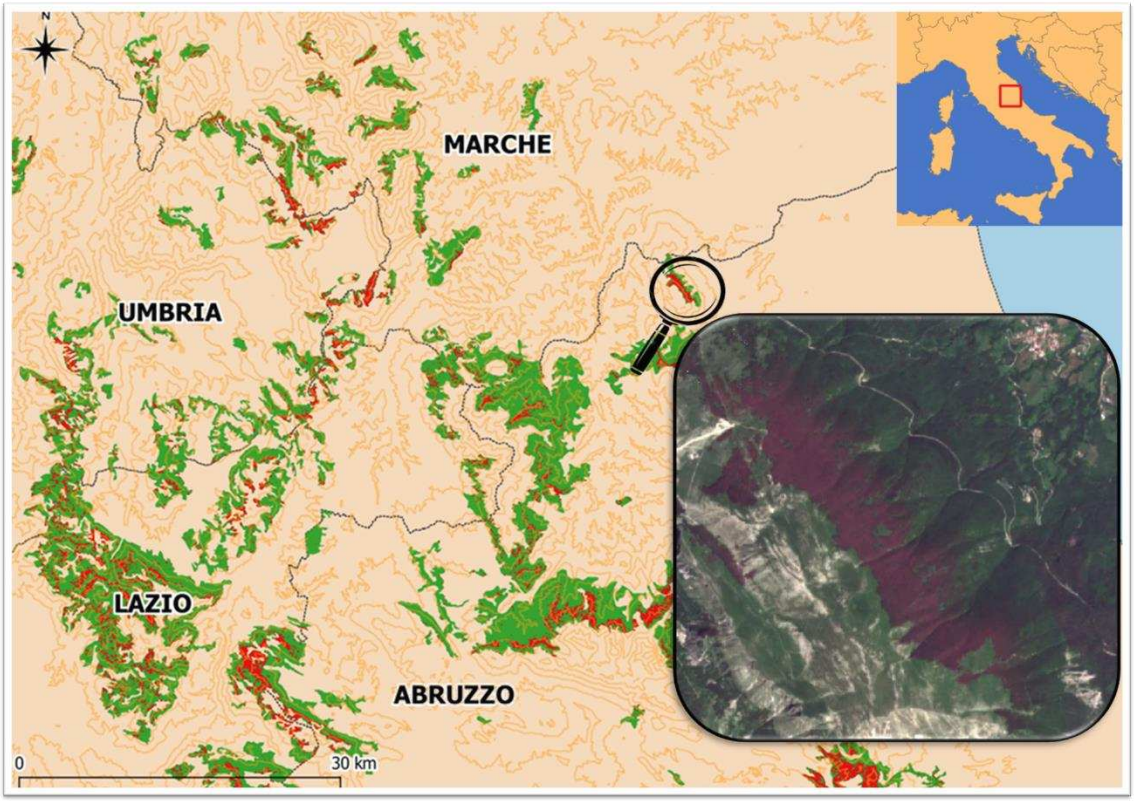

Figure 1 – In green, the area covered by beech forests in central Italy around the study site; while in red, distribution of beech forest affected by the late frost occurred on April 25th, 2016. In the frame a Sentinel-2 view (June 15th, 2016) at the site Montagna dei Fiori (Central Apennines).

2.3 Anatomical slide preparation

The wood cores were first divided in samples (≈ 4 cm in length) with oblique cuts, so that each contiguous portion shared one or more -rings with the following one. Wood samples were then boiled in water for 30 minutes to soften the wood and avoid damage to cell structures during cutting. Anatomical microsections of 12 µm thickness were cut with a rotary microtome (Leica RM2245) (Fig. 2a). Permanent slides were prepared staining with safranin and astrablue. Safranin is an indicator of lignin concentrations colouring cell walls in red, whereas astrablue enhance the presence of cellulose and reaction wood colouring cell walls in blue. The slide preparation procedure requires sections dehydrating and permanent sections fixing between glass slide and a cover glass (resin used EUKITT® and EUKITT® UV). Slide were sandwiched between PVC strips with a magnet placed on the top of the slide on a metal plate to keep the microsection flat and avoid air bubbles formation during drying. Then, microslides were cleaned with alcohol to remove dried excess resin and optimize the quality of digital images (Fig. 2b). High-resolution digital images of anatomical sections were captured using a slide scanner (D-Sight, A. Menarini Diagnostics srl) at 200x magnification.

2.4 Quantitative wood anatomy

Scanned images were then analysed with the ROXAS v3.0.1 tool and the image-processing software Image-Pro Plus v6.1 to extract vessel features (von Arx and Carrer, 2014). ROXAS is a specialized image analysis tool designed to automatically recognize and measure conduit lumen area and calculate reliable anatomical statistics (Fig. 2c). Captured images were first dated using the tree-ring measurements previously obtained. Finally, the following parameters were extracted within each annual ring; *i*) vessel density (VD), *ii*) percentage of relative conductive area (RCTA), *iii*) mean vessel size (MVA), *iv*) mean hydraulic diameter (Dh), *v*) mean of three widest vessels (Max3VA), *vi*) relative position of three widest vessel (Pmax3VA) and *vii*) the xylem-specific potential hydraulic conductivity (Ks). Ks was calculated as the ratio between the accumulated potential hydraulic conductivity as approximated by Poiseuille's law and the total ring area (Scholzet al. 2013). The lower threshold for vessel detection was set to 40 μm^2.

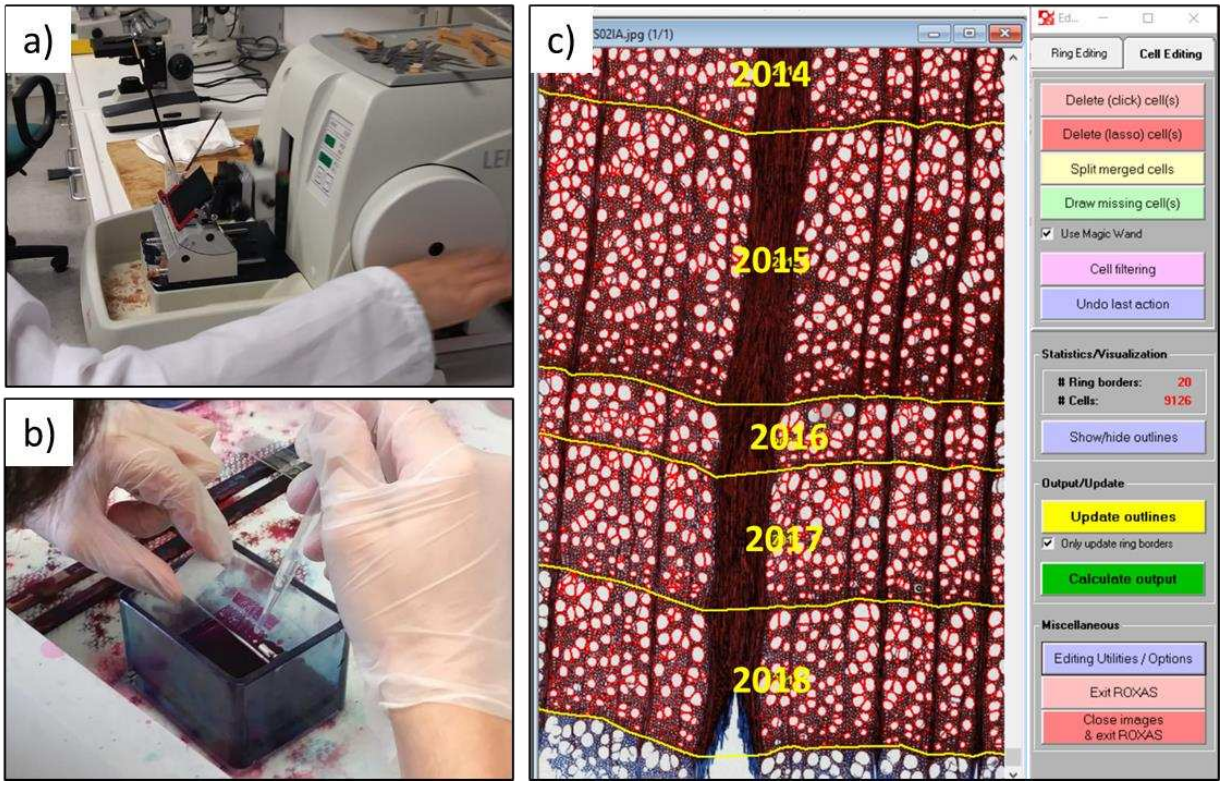

Figure 2: Various steps of samples processing. a) A rotary microtome used to prepare microsections. b) Staining process and preparation of permanent slides. c) Automatic vessels detection using Roxas tool.

2.5 Statistical analysis

Vessel parameters were first compared across the three plots to assess elevation-dependent trends. In this analysis, the null hypothesis of equal means in vessel features were verified through the one-way analysis of variance (ANOVA).

All the vessel's series of each tree were standardised by fitting cubic spline functions to remove to long-term variation in wood-anatomical features mostly related to tree height growth and to emphasize the high-frequency variability that contain climate information (Cook et al. 1990, Carrer et al. 2015). Smoothing spline's rigidity was set at 25 years and its wavelength cut-off value at 50%. All measured series were detrended dividing observed by fitted values to obtain dimensionless indices. Then, for each elevation plot, standardized series were averaged computing the robust bi-weight mean.

Standard series where therefore used to assess the climate sensitivity of beech vessel's features through the calculation of correlation coefficients (r-Pearson). This analysis focused on the relationship between the vessel's parameters and the late frost occurrence. The monthly minimum temperatures (Tmin) in January-September period, the accumulated degree-days (ΣT) and the spring daily temperature anomalies (ΔT) were used as climate series. The accumulated degree-days (ΣT) were used as a proxy of leaf phenology and the spring daily temperature anomalies (ΔT) were selected to quantify the severity of each event. ΣT was calculated as the cumulated daily mean temperature above a 5°C threshold from January 1st (Day Of the Year - DOY 1) to the date of the minimum temperature recorded between DOY 111 and 131 (approximately from April 20th to May 10th) while spring temperature anomalies (ΔT) as the difference between the mean minimum temperature from March 1st to April 30th (DOY 60 and 120) and the minimum temperature from April 20th to May 10th (DOY 110 and 130). As climate data, the daily E-OBS V 24.0e gridded datasets were used at 0.1° spatial resolution (Cornes et al 2018), selecting the climate time series at the closest grid point for the period 1950-2018. For the computation of ΣT index, temperatures records were interpolated from the grid elevation to the plot location considering a mean lapse rate of −6.5 °C km−1. Climate-growth correlations values and bootstrap confidence intervals (1000 samples) were analysed using the "dcc" function of the "treeclim" R package (Zang & Biondi, 2015). Finally, the impact of the 2016 frost on vessels features (indexed series) was estimated comparing the values in year 2016 with those in pre- disturbance period 2014-2015 while recovery was estimated considering the post-disturbance period 2017-2018. t-test was used to assess differences in indexed chronologies between values in frost-defoliated and unaffected plots and to assess significative year-to-years variation.

3.0 Results

3.1 Elevation related trends

Mean dendrometric values (Tab. 1) indicate a positive bottom-up trend for DBH and age and a negative one for tree height due to the decreasing soil fertility at higher elevation. Being a stored coppiced forest, trees are considerably older at hight elevation where management was withdrawn in earlier times.

Table1: Diameter at 1.30m (D), total tree heigh (H) and estimated age (Yrs) of the five beech trees sampled in each plot (at low, middle and high elevation).

	Low elevation			**Middle elevation**			**High elevation**		
Tree	**D**	**H**	**Yrs**	**D**	**H**	**Yrs**	**D**	**H**	**Yrs**
No.1	22	18.5	59	27	16.9	71	42	15.8	102
No.2	25	17.2	66	29	15.7	88	23	15.9	106
No.3	32	17.2	62	25	17.0	69	45	15.9	94
No.4	33	19.6	61	21	17.2	78	30	13.6	82
No.5	26	17.9	66	28	13.4	77	35	16.3	100
AVG	**27.6**	**18.1**	**62.8**	**26.0**	**16.0**	**76.6**	**35.0**	**15.5**	**96.8**

Sampled trees show mean TRW increments ranging from 2.04 mm at low elevation to 1.63/1.56 mm at both middle and high elevation with statistically statistically significant differences. Moreover, vessel parameters show statistical differences between plot elevation with p-values<0.001, except for mean Dh and Pmax3VA that show p-values<0.05 (Fig. 3). Tree rings at high elevation on a hand show higher VD and RCTA and consequently higher Ks values, on the other hand lower MVA, Dh and Max3VA. Trees at high elevation show higher PMaxVA.

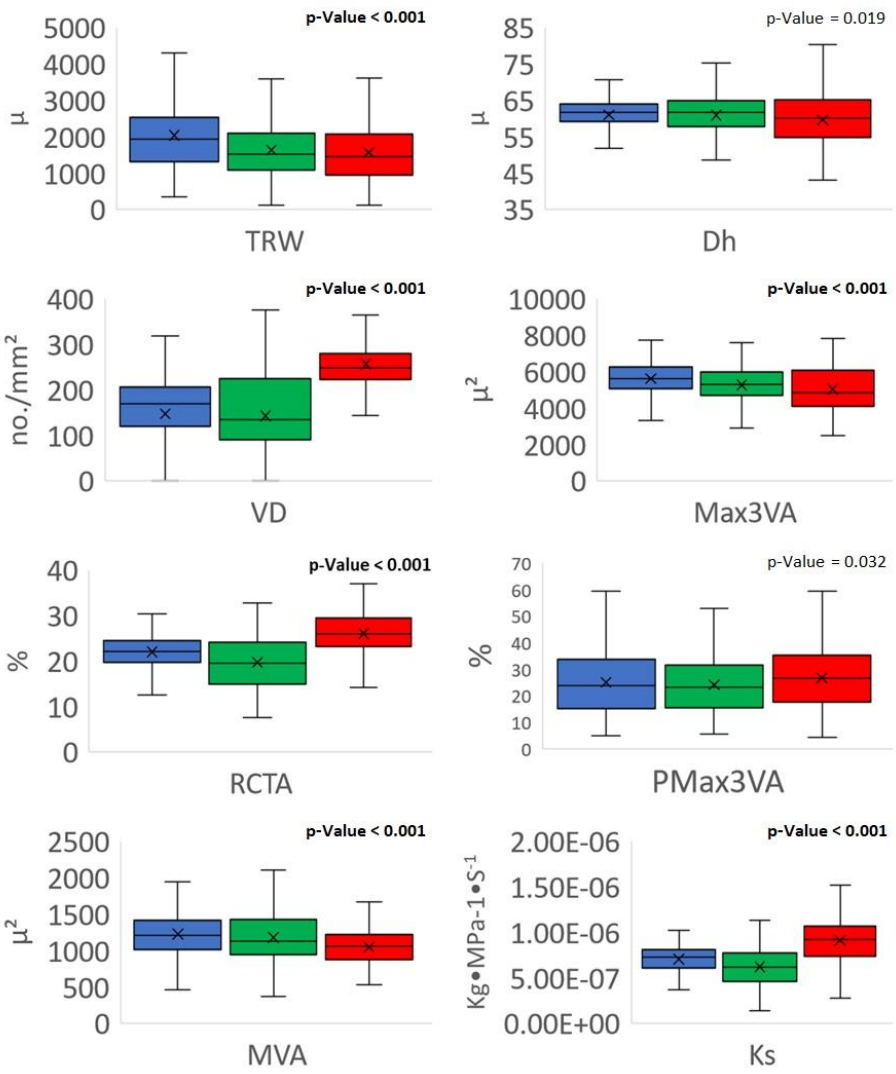

Figure 3: Differences among the elevation plots in tree ring width (TRW), vessel density (VD), relative conductive area (RCTA), mean vessel area (MVA), mean hydraulic diameter (Dh), mean of three widest vessels (Max3VA), VI) relative position of three widest vessels (Pmax3VA) and the xylem-specific potential hydraulic conductivity (Ks). *p-values* refers to the null hypothesis of equal means (ANOVA).

3.1 Beech sensitivity to late frosts

TRW and vessel's features are generally negative correlated with summer (June- September) minimum temperatures and the spring frost indices ΔT and ST (Fig. 4). Frost indices are never significantly correlated with VD, Dh, Max3VA and Ks. The highest significant correlation values were found in low-elevation chronology between Max3VA and minimum temperatures (Tmin) in September. The minimum temperatures of January and February in most cases do not limit the tree ring's anatomical characteristics, except for VD at low elevation and Dh at middle elevation. On the contrary, Tmin in the spring and late spring period (March, April, May) have an important effect on the studied parameters and traits, especially at middle and high elevation. TRW and Dh are negatively correlated with March Tmin at high and middle elevation, while RTCA is positively correlated. At high elevation, mild temperatures in April result in higher MVA and lower VD. May tmin positively influence the TRW at high elevation, the RCTA at low elevation and the MVA at middle elevation.

Spring frost events in 2016 cause an abrupt decrease in mean ring width at middle and high elevation (Fig.5-6). However, the parameters of the vessels were unaffected at the date of spring frost event and their indexed values in the period 2014-2018 remain close to 1. Mean values of PMac3VA show high rates in year-to -year variations in the period between 2014 and 2018, but the deviations are not related to the frost event. Both TRW and vessel parameters do not show evident carry-over effects after the late frost occurred in 2016. However, RCTA and Ks in 2017 are statistically lower at low elevation with p-values of 0.015 and 0.024 respectively.

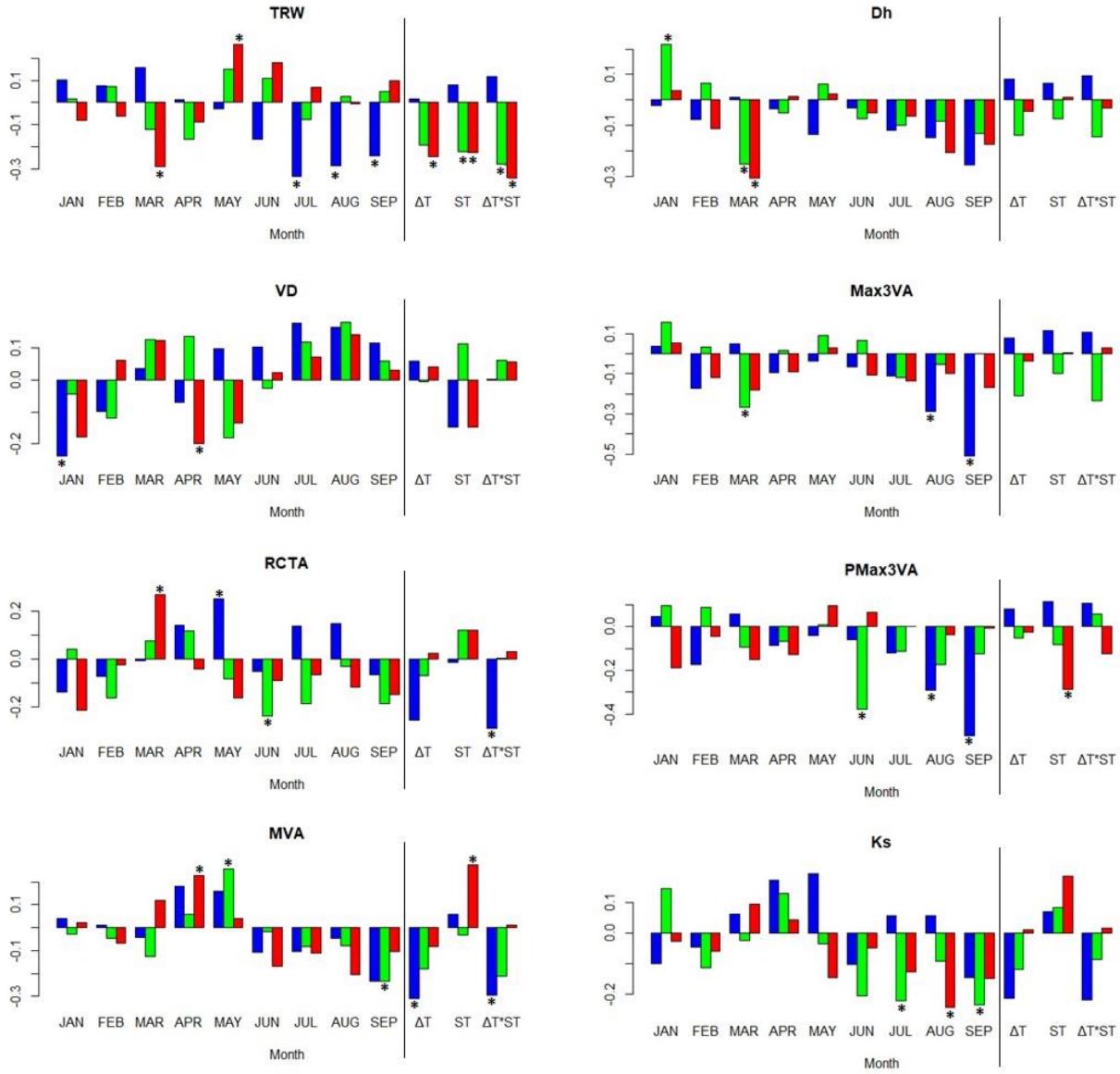

Figure 4: Correlation values between indexed plot chronologies (low in blue, middle in green and high in red) related to TRW and vessel features (VD, RCTA, MVA, Dh, Max3VA, Pmax3VA, Ks). Climate data considered in analysis are I) monthly minimum temperature from January to September, II) temperatures anomalies in spring (ΔT), III) accumulated degree-days (ST) IV) products between ΔT and ST. Correlation values with significative bootstrapped confidence intervals were marked with * symbols.

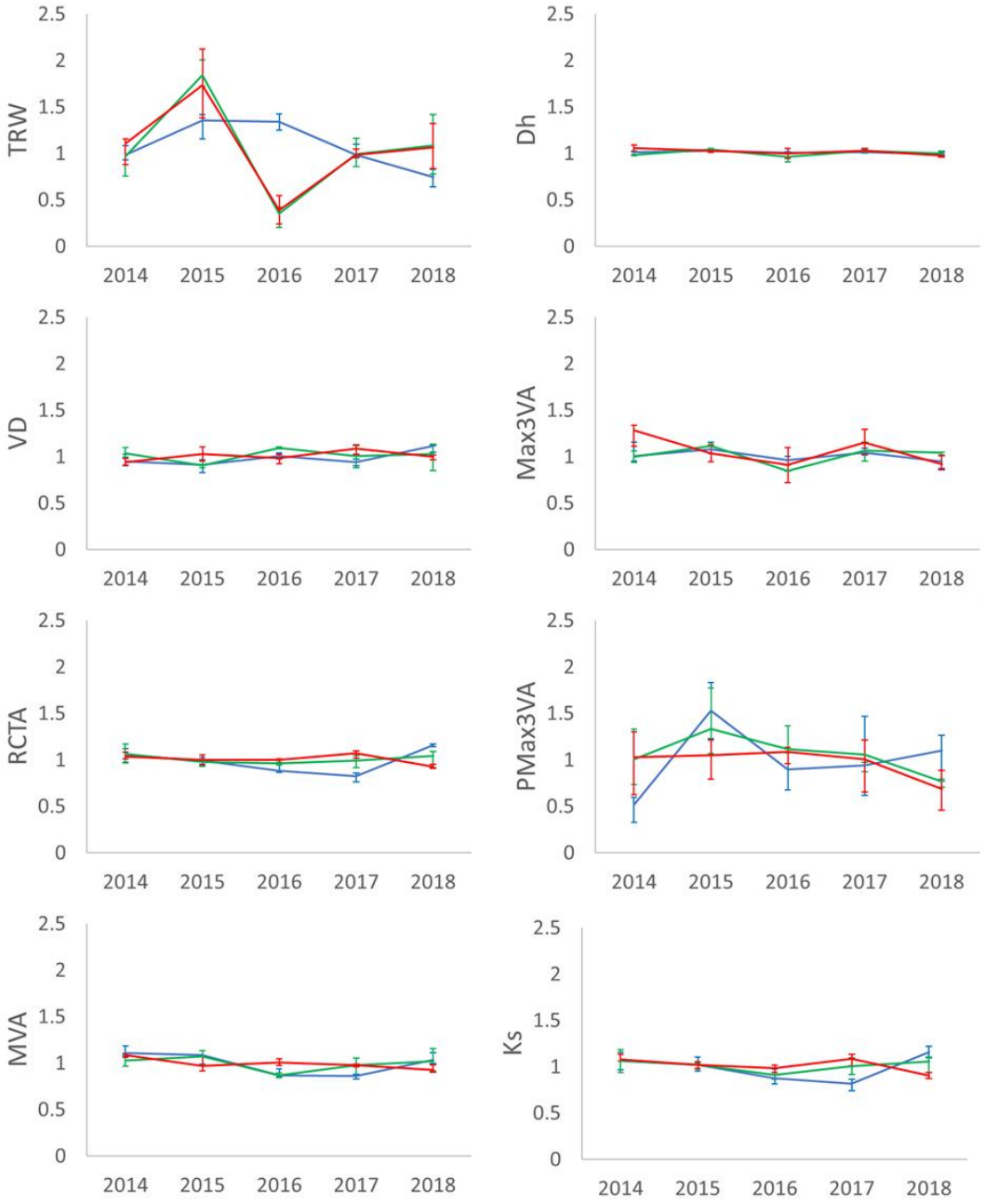

Figure 5: Indexed values of tree ring width (TRW) and vessel's parameters in the time period 2014-2018. Frost event occurred in 2016 and hit the middle elevation trees (green lines) and the high elevation trees (red lines) while the low-elevation trees (blue lines) were unaffected. Data are means ± IQR (whiskers).

Figure 6: Two beech wood anatomical section stained with astrablue and safranine captured at 200x magnification. On the left, a micro-section from the high elevation plot and on right one from low elevation plot). In 2016 a late frost defoliation occurred at high and middle elevation limiting tree ring growth.

4. Discussion

At MDF, beech trees at high elevation feature the smallest tree rings and vessel size while vessel density is significantly higher as indicated by the higher values of RCA and KS. In Slovenian beech forests similar studies detected smaller vessel diameter at high elevation (Prislan et al. 2018) and smaller MVA in late flushing beech populations (Arnič et al. 2021). Since leaf phenology of European beech is related to stand elevation (Čufar et al. 2012; Vitasse et al. 2013), we can hypothesize that also in our study area beech at high elevation has later flushing than at lower elevations. Although the entire beech forest in our study site was previously coppiced, beech at the three altitudinal plots have some structural and chronological differences. Beech trees at low elevation, although younger and with smaller diameters, are 2-2.5 meters taller than trees at middle/high elevation. Therefore, the differences found in the parameters of the extracted vessels are also partly due to the heterogeneity of the sampled stands.

TRW in trees at low elevation is mainly controlled by summer temperatures whereas at high elevation the main limiting factors are the spring temperatures (March and May), and the spring frost indices (Fig.3). This relationship could explain the greater drought influence in reducing radial growth at the low-elevation and a greater influence of late frosts at higher elevations. Both ΔT and ST show negative correlation with TRW showing that annular growth is reduced when early foliation is

immediately followed by frost events. Vessel parameters seems to be scarcely sensitive to minimum temperatures as well as ΔT and ST.

The 2016 spring frost did not cause differences in vessel traits between defoliated (at high and mid elevation) and unaffected trees (low elevation), whereas mean TRW is negatively affected as also reported in other studies (Príncipe et al. 2017; Gazol et al. 2019). In 2017 RCTA was significantly higher in the plots hit by the2016 frost, whereas TRW values recover at pre-disturbance levels at high and mid plots. However, this deviations of RCTA values are likely to be caused by the dry conditions recorded in 2017 rather than by the 2016 frost (Pollastrini et al. 2019; Rita et al. 2020). PMac3VA is the only vessel parameter showing large variations of mean values in the 2014-2018 interval, with wide variability even within the same plots (fig. 5). This condition could be attributed to the nature of beech xylem featuring a diffuse porosity that can switch to a semi-ring porosity only in dry years. PMac3VA values were relatively high at the mid plot in 2015, condition that could have contributed to increase the intensity of the 2016 late frost at this elevation. Indeed, the xylem vulnerability to embolism caused by frost events increases with the vessel size o, and small vessels in the last quarter of the growth ring could improve the resistance to late frost during the onset of the following growing season (Améglio et al. 2001; Cochard et al. 2001).

5. Conclusions

In the Apennines characteristics of vessel in European beech xylem can vary in populations located in relatively close areas but at different elevations. While TRW are sensitive to cold indices, vessel variables provide low added value in dendroecological works focusing on the sensitivity to spring frost events. In this contribution, the characteristics of the vessels on European beech in Central Apennines do not seem to provide exhaustive information for the reconstruction of frost events occurred in the past. The analyses will be developed on other beech stands in the Mediterranean area. In our site studied, the population includes relatively young trees, future analyses will also consider longer-lived populations. Furthermore, the type of management could affect the strength and plasticity of the anatomical features. It will therefore be interesting to compare high-forest stands with coppice-managed stands. Potential and limitation in using vessel features to study climate extremes such as late frost needs to be verified on other broadleaf tree species and over different climatic regions.

Chapter 5

Thinning improves growth while have disparate effects on post-drought resilience of Quercus subpyrenaica coppice forests in the Spanish Pre-Pyrenees

Enrico Tonelli[1]*. Alessandro Vitali[1], Federico Brega[1], Antonio Gazol[2], Michele Colangelo[2], Carlo Urbinati[1], J. Julio Camarero[2].

[1] Marche Polytechnic University, Department of Agricultural, Food and Environmental Sciences, 60131 Ancona, Italy.

[2] Instituto Pirenaico de Ecología (IPE-CSIC). Apdo. 202, 50192 Zaragoza, Spain.

*corresponding author

Abstract

During the past years, growth and productivity of different oak species have been constrained by water shortage in seasonally dry regions such as the Mediterranean Basin. Thinning could improve oak radial growth in these drought-prone regions through the reduction of tree competition for soil water in summer. However, we still lack adequate, long-term assessments on how lasting are thinning treatments and to what extent they contribute to oak growth recovery after drought. Here we aim: (i) to study the radial growth sensitivity to drought of *Quercus subpyrenaica* in the Spanish Pre-Pyrenees, and (ii) to verify if thinning represents a suitable option to enhance growth resistance to drought and post-drought growth recovery. We analysed basal area increment (BAI) trends in the period 1960-2020 of formerly coppiced oak stands thinned in 1984 and compared them with unthinned plots and also with coexisting Scots pine (*Pinus sylvestris*) growing in thinned and unthinned plots. We used the Standardized Precipitation Evapotranspiration Index (SPEI) to estimate the severity of droughts and we also assessed climate-growth relationships. Oaks in thinned plots showed higher BAI (369 mm^2) than those in unthinned plots (221 mm^2). Growth rates remained higher in thinned than in unthinned plots also under intense drought stress. An intense summer drought (SPEI < -1.28) occurred in 1984 caused abrupt BAI growth reductions in both oaks (- 40.5%) and pines (- 40.1%). The positive effect of thinning on BAI lasted for over 20 years and slightly declined as canopies closed. In the thinned plots, trees with smaller diameter showed the greatest growth release. Oaks in unthinned plots and Scot pine were more sensitive to short-term droughts in terms of growth reduction than oaks in thinned plots, while long term droughts have similar effects on oaks from both thinned and unthinned plots. Oaks were resilient to drought, showing recovery periods lasting from 1 to 2 years in both thinned and unthinned plots. However, intense and prolonged droughts could strongly reverse the expected growth enhancement of thinned plots, and a greater frequency of droughts would limit coppice growth and productivity thus lengthening the rotation periods.

Key words: Mediterranean oaks, dendroecology, SPEI, release, resilience.

Highlights:

- Thinning improves oak's basal area increments for over 20 years.
- The growth release following thinning is more marked in small diameter oaks.
- Thinning reduces oaks sensitivity to short-term droughts.
- Oaks recover pre-drought growth rates in 1 to 2 years.
- The impact of drought on growth is transitorily alleviated through thinning.

1. Introduction

Under a climate warming scenario, there is a greater likelihood of air temperatures and evapotranspiration rate exceeding the optimum range for many tree species, leading to range contractions in drought-prone regions (Thuiller 2004, Wang et. Al 2018). In seasonally dry Mediterranean regions, models predict greater susceptibility to climate warming and drought for winter deciduous, ring-porous oaks, often dominant in mesic sites (Benito Garzón et al. 2008, Sánchez de Dios et al. 2009, Acácio et al. 2017, Vila-Viçosa et al. 2020). However, we lack field data to test these predictions and to assess the sensitivity to drought of oaks given their ecological and socio-economic relevance in Mediterranean regions.

In recent years, dieback and mortality related to drought events have been reported in southern European deciduous oak forests, mainly in Spain and Italy (Amorini et al. 1996, Camarero et al. 2016, Colangelo et al. 2017, Gentilesca et al. 2017, Lloret et al. 2022). Under drought stress, deciduous, ring-porous oaks may osmotically adjust their tissues to continue to draw water into the leaves and keep high photosynthesis rates (anisohydry), increasing the risk of damage due to hydraulic failure since most of the stem conductivity depends on vessels located in the last-formed ring (Novick et al. 2002, Kaproth and Cavender-Bares 2016). In these species, stem radial increment is reduced in drought years, as well as mean lumen area of earlywood vessels thus decreasing hydraulic conductivity (Eilmann et al. 2006).

The effects of drought events on trees and forests can be assessed through the analysis of resilience components, and tree-ring data constitute one of the main valuable proxies for this purpose (Lloret et al 2011). Resilience is defined as the capacity of ecosystems, communities, or individuals to recover after disturbance and regain its pre-disturbance structure and function (Scheffer et al. 2001, Folke et al. 2004). Several dendroecological studies have shown how drought severity is the major factor influencing radial growth resilience to drought (e.g., Gazol et al. 2018). How oaks respond to climate (drought) also depend on both, external and internal constrains. For example, site characteristics may modify soil water availability resulting in a persisting environmental constraint for tree growth, as demonstrated in *Quercus pubescens* Willd. On limestone bedrock (Vodnik et al. 2019). In addition,

the risk of drought-induced dieback may be size-dependent, with canopy defoliation and mortality risk increasing with decreasing height and radial growth rate as found in *Quercus faginea* Lam. (Camarero et al. 2016). Drought-induced dieback leads to cascading effects on oak forests and associated species because it not only reduces tree growth but vitality since it may also increase tree vulnerability to biotic stressors such as insect defoliators and fungal pathogens (Wargo 2006; Thomaset al. 2002; Canelo et al. 2021).

In Spain, winter-deciduous oaks such as *Q. faginea*, *Q. pubescens* and *Quercus pyrenaica* Willd. Dominate many formerly coppiced forests, which comprise about 20% of the total forest area (Serrada et al. 1992, Cañellas et al. 2004). In the past, these oak coppices played relevant socio-economic roles in Mediterranean countries, primarily providing firewood and charcoal but also ensuring grazing for livestock in wood-pasture mixed systems. However, the abandonment of their traditional use and regular coppicing has reduced stem radial growth rate making these overaged stands prone to drought-induced dieback (Corcuera et al. 2006). The management of such coppice forests is a key forestry issue, especially in the Mediterranean countries where scenarios of warmer and drier climate conditions are forecasted (Vila-Viçosa et al. 2020).

Thinning could reduce the impact of drought in coppiced forests that enter the stem exclusion stage, reducing intra- and inter-species competition between trees for water (Cabon et al. 2018; Gavinet et al. 2020). Canopy openings following thinning improve light conditions and enhance coppice above-ground growth with an abrupt increase in tree growth (Müllerová et al. 2016; Hepner et al. 2020). Furthermore, comparing growth responses to climate variability between thinned and unthinned stands would provide a reliable assessment on post-thinning resilience to drought. However, we still lack suitable assessments of post-drought growth responses after thinning and drought to discern if post-thinning growth enhancement is transitory and linked to drought alleviation.

In this work we aimed: (*i*) to evaluate the effects of thinning on radial growth in thinned and unthinned *Q. subpyrenaica* formerly coppiced stands; and (*ii*) to assess if thinning can enhance growth and improve resilience by alleviating drought stress. Our hypothesis is that thinning can increase resistance to drought impact and improve resilience (post-drought recovery) of trees to severe water deficit by reducing tree-to-tree competition for soil water and light. We compare oak growth responses to thinning and drought and use as reference Scots pine (*Pinus sylvestris* L). trees inhabiting thinned and unthinned stands.

2. Material and methods

2.1 Study area and species

In North-eastern Spain, *Q. pubescens* and *Q. faginea* form a major biogeographic transition between the northern Eurosiberian and southern Mediterranean regions subjected to seasonal summer drought (Loidi and Herrera 1990). *Q. pubescens* is a sub-Mediterranean species present in sites with summer precipitation higher than 150 mm and altitude range between 400 and 1500 m (Ceballos and Ruiz de la Torre 1979). *Q. faginea* is a Mediterranean oak restricted to Morocco and Iberian Peninsula, mostly in sites with basic soils, summer precipitation higher than 100 mm and altitudes between 600-1200 m a.s.l. (Ceballos and Ruiz de la Torre 1979; Rivas-Martínez and Sáenz 1991). The contact areas between both species allowed their mixing and the resulting hybrid was named *Quercus subpyrenaica* E.H. del Villar (Huguet del Villar 1935, Amaral Franco 1990), which may be also regarded as *Q. pubescens* subspecies (Govaerts and Frodin 1998). Currently, *Q. subpyrenaica* populations are mainly found in the Central and Western Spanish Pre-Pyrenees, where usually form mixed forests with Scots pine.

The study site is located in one of these Spanish Pre-Pyrenean ranges (Sierra de Luesia-Sto. Domingo) near the "Puy Moné" peak (1302 m a.s.l.), Aragón region (**Fig. 1a**). The main forest type is a *Q. subpyrenaica* (*Qs*) mixed forest, whit *Acer campestris* L., *Acer opalus* Mill., *P. sylvestris* L. and *Fagus sylvatica* L. in the most mesic sites (valley bottoms, N-oriented slopes) and *Arbutus unedo* L. in warm-dry sites (S-oriented slopes). Other less abundant woody species are the trees *Ilex aquifolium* L., *Crataegus monogyna* Jacq., *Sorbus torminalis* L., the shrubs *Buxus sempervirens* L. and *Juniperus communis* L., and the vine *Amelanchier ovalis* Medik. Bioclimate in this region is temperate oceanic (Sub-Mediterranean variant). The, mean annual temperature is 10.4 °C while mean annual precipitation is 795 mm, with a mean annual water balance of -16 mm (Spanish Meteorological Agency AEMET, period 1961-2020 period). Weekly values of the Standardized Precipitation Evapotranspiration Index (SPEI; Vicente-Serrano et al., 2017), calculated on 48-month long scales, were high in 1978–1985 and low in 1985–1996 indicating wet and dry conditions, respectively (**Fig .1b**).

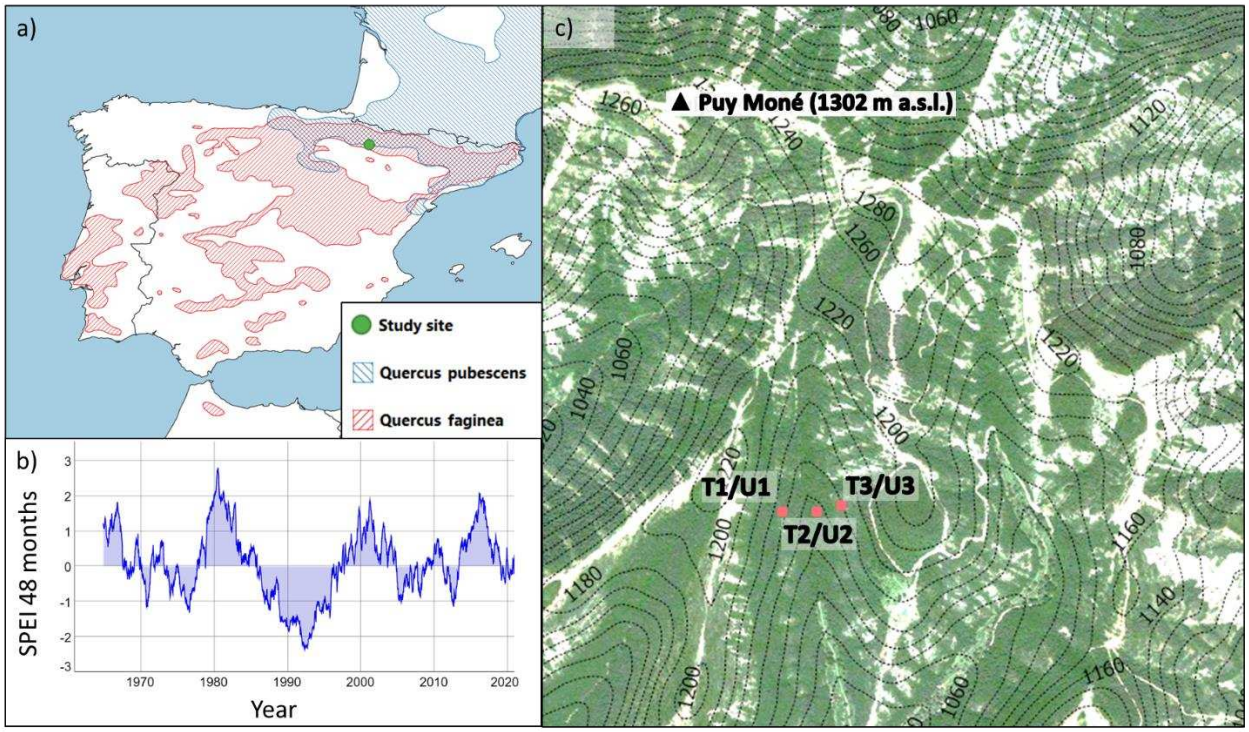

Figure 1. (a) Location of the study site and distribution range of *Q. pubescens* and *Q. faginea* in the Iberian Peninsula (Caudullo et al. 2017). (b) SPEI calculated on 48-month scale in study site area (Vicente-Serrano et al. 2017). (c) Location of sampled plots: east-facing side (T1/U1), valley floor (T2/U2) and west-facing side (T3/U3).

2.2 Field sampling

Thinning was carried out in 1984 on three squared plots of 100 m^2 in *Q. subpyrenaica* coppice stands. The basal area percentage removed in the thinning was 50%, corresponding to about 20-30 m^2ha^{-1}. The three thinned plots have different topographic features within the study area slope (SE and SW aspects, valley floor). In each thinned plot (T1, T2 and T3) structural parameters (dbh, diameter at breat height; height) were measured, and tree increment cores were collected. Cores and measurements were also collected in nearby unthinned plots (U1, U2, U3) of the same size and with similar topographic features than T1, T2 and T3, respectively. Sampling with the same protocol was repeated at all plots in 2003/2004 and 2021, except for the T3 plot which was surveyed only in 2003.

For each plot and woody species, we calculated mean dbh and height, tree density and total basal area (**Table 1**). We also calculated species richness (S) and species diversity (Shannon H' index) considering all woody plant species sampled within each plot.

2.3 Tree-ring data processing

All *Q. subpyrenaica* trees inside each plot were cored using a 0.5-mm increment borer (Haglof, Sweden). For each tree, 2 cores were extracted at breast height (1.3 m) from the thickest stems of each multi-stemmed individual. Additional cores were also collected from *P. sylvestris* trees located in T1 and U1 plots. In total, we sampled 145 oaks (71 trees in thinned plots and 74 trees in unthinned plots) and 12 pines. We considered the Scots pine series because pines were present in formerly thinned plots and could be used as a reference growth data to detect post-thinning growth enhancements.

We mounted all cores on wooden supports after air drying and polished them with progressively finer sandpapers. We visually cross-dated each core and then measured ring widths using a semi-automatic system (LINTAB-TSAP, Rinntech, Germany) at 0.01 mm accuracy. We used the COFECHA software to check the visual cross-dating (Holmes 1983). Next, tree-ring width series measured from the same tree were transformed into basal area increment (BAI) series and averaged for each tree using the *bai.in* function contained in *dplR* package (Bunn 2008) of R software (R Development Core Team, 2020).

2.4 Growth release detection

To detect potential growth releases following the 1984 thinning, BAI series were analysed. The 95% confidence interval of mean BAI series in thinned and unthinned plots was calculated using 1000 bootstrap resampling. Growth release following canopy opening in 1984 was estimated by calculating the percentage of BAI change (BC). For each individual tree, the BC was calculated comparing mean BAI values in the 1981–1984 and 1985–1988 periods using the following equation:

$$BC = [(M2-M1) / M1] \times 100 \qquad [1]$$

where M1 is the 4-year mean BAI including the thinning year (period 1981–1984) and M2 is the following 4-year mean (1985–1988 period). This approach is similar to the growth averaging method (Nowacki and Abrams 1997) based on comparing running 10-year ring-width means and used to detect growth releases or suppressions.

Table 1. Topographic and structural characteristics of thinned (T1, T2 and T3) and unthinned (U1, U2 and U3) sampled plots. Woody species abbreviations: *Ac, Acer campestre; Ao, Acer opalus; Au, Arbutus unedo; Av, Amelanchier ovalis; Bs, Buxus sempervirens; Cm, Crataegus monogyna; Ia, Ilex aquifolium; Jc, Juniperus communis; Ps, Pinus sylvestris; Qi, Quercus ilex; Qs, Quercus subpyrenaica.* Variables' abbreviations: S, species richness; H', diversity.

Plot	Elevation (m a.s.l.)	Slope (°)	Aspect	Density (No. stems ha^{1})	*Qs* density (No. stems ha^{1})	Total basal area (m^2ha^{1})	*Qs* basal area (m^2ha^{-1})	Woody species	S	H'
T1	1150	25	SE	3200	1800	44.35	41.74	*Qs, Bs, Av, St, Ia, Ac, Ps*	7	1.33
T2	1110	6	S	5900	1500	91.19	63.47	*Qs, Bs, Ao, Ia, Fs*	5	1.29
T3	1140	20	SW	2800	1500	21.75	14.31	*Qs, Qi, Au, Cm*	4	1.44
U1	1150	25	SE	7300	4400	56.92	53.45	*Qs, Bs, Jc, Cm, Ia*	5	0.82
U2	1110	6	S	6900	3200	52.78	48.15	*Qs, Bs, Jc, Ps*	4	0.87
U3	1140	20	SW	5900	3300	31.76	22.78	*Qs, Qi, Au, Cm*	4	1.60

2.5 Growth responses to drought

To analyse growth responses to drought we compared detrended BAI series and the SPEI drought index. First, the BAI series were detrended by fitting cubic spline functions to remove the age-, size- and disturbance-related trends and to emphasize the high-frequency growth variability (Cook et al. 1990). We set the smoothing spline rigidity at 10 years and its wavelength cut-off value at 50%. We detrended all measured series dividing observed by fitted values to obtain dimensionless BAI indices. Three mean site chronologies were developed with a minimum sample depth of 10 series: (i) *Q. subpyrenaica* chronology in thinned plots, (ii) *Q. subpyrenaica* chronology in unthinned plots, and (iii) *P. sylvestris* chronology. Mean standard chronologies were obtained averaging individual BAI indexed series using a bi-weight robust method (Fritts 1976).

For climate-growth analyses we used mean standard chronologies and monthly SPEI indices calculated on 1-, 3-, 6- and 9-months. SPEI data correspond to the 1.1-km^2 gridded SPEI dataset for Spain (Vicente-Serrano et al. 2017). Correlation values were calculated between monthly SPEI and indexed BAI for all the months of the vegetative period, April to October, in the post-thinning, common period 1984–2020. The stability of the strongest climate signals detected in this analysis was assessed by calculating moving response coefficients using 30-year moving windows and a 1-

year offset. Function parameters were bootstrapped to calculate their significance and confidence intervals. This analysis was done using the treeclim R package (Zang and Biondi 2015).

Finally, potential intense drought events were selected based on a SPEI threshold of −1.28. For these years (1967, 1986, 1989, 1995 and 2012) the Lloret resilience components (Lloret et al. 2011), i.e. resistance (Rt), recovery (Rc), resilience (Rs) and relative resilience (RRs) indices, and the growth recovery time (GRT, Thurm et al. 2016) were calculated on individual detrended BAI series using the "res.comp" fuction in "pointRes" R package (van der Maaten-Theunissen et al. 2015). We considered 4 years of pre- and post-disturbance for calculating resilience components and considered the maximum length of the recovery period equal to 10 years.

2.6 Variability of resilience components

Each tree indexed BAI series was correlated with the main climatic driver selected within the common period 1984–2002 using Pearson correlations. This 19-year interval follows the thinning and was selected to include most of the BAI series from trees sampled in 2003. Components of oak trees resilience (Rt, Rc, Rs and RRs) relative to drought events were used as response variables for each Generalized Linear Mixed-Effects (GLME) model applied, using the following predictors as fixed effects: (i) tree age, (ii) tree dbh, iii) mean ring-width increment (RW), iv) mean sensitivity (MS), a measure of the relative change in width between consecutive rings (Fritts 1976), and v) individual climate-growth correlation values (CorrSPEI). Treatment (unthinned /thinned) was used as dummy variable to search for response differences. Then, separate models for thinned and unthinned plots were fitted. Parameters (i), (ii), (iii) and (iv) refer to reconstructed values at the date of each drought events, based on ring-width measurements. The Variance Inflation Factor (VIF) was used to detect multicollinearity among predictors considering a threshold of VIF > 5 for presence of multicollinearity. All predictors were standardized to account for differences in measure units. The plot aspect was considered as random effect. Since the response variable (tree growth resistance) did not satisfy the normal distribution criterion (Shapiro–Wilk test), the gamma family was set in the GLMEs (**Fig. S1**). This analysis was carried out using the *glmer* function of the *lme4* R package (Bates et al. 2007). Marginal and conditional R^2 values (R^2m and R^2c, respectively), accounting for the variability due to fixed and fixed plus random factors, respectively, of fitted models were computed using "*r2_nakagawa*" function of the "*performance*" R package (Lüdecke et al. 2021). VIF was calculated using the *vif* function in the *car* R package (Fox et al. 2007).

3. Results

3.1 Quantification of release events in thinned plots

Sampled oak trees were relatively young, the average age was 43 years in thinned plot and 51 years in unthinned plots. In both thinned and untinned plots, oaks presented positive trends of mean BAI series up to the 1970s, representing the vigorous juvenile phase of growth during a wet-cool decade (**Fig. 2**). However, in this period growth rates were similar between thinned and unthinned plots. Scots pine showed higher growth rates than oaks, but also more interannual variability, with an exceptional BAI reduction in years 1992-1993 (**Fig. S2**). In 1989, both species and plots featured a drop in BAI due to an exceptional dry year.

After 1984, oaks in thinned plots showed a growth release. The oaks BAI series remained higher in thinned plots than in unthinned plots for the following 21 years, up to 2004. The mean BAI change (BC) of oaks in 1984 for thinned plots was 100%, while it was close to 0% for Scots pines and oaks in unthinned plots (**Fig. 3a**). The differences between the first and third quartiles in BC values were much larger in the thinned plots suggesting greater individual variability following the treatment. Trees that showed higher release levels were the individuals which, at the date of thinning, showed smaller diameters (**Fig. 3b**). Tree dbh in 1984 and BC were negatively related in thinned plots (r = -0.63, $p < 0.05$).

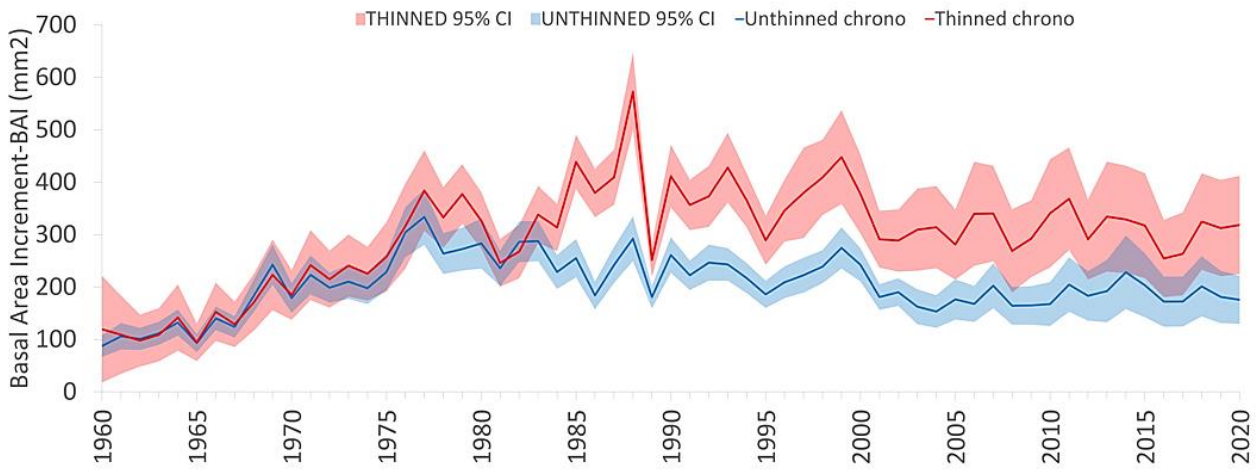

Figure 2. Basal area increment (BAI) series of oaks in thinned (red line) and unthinned (blue line) plots and bootstrapped confidence intervals (95% CIs). BAI series of Scots pine are plotted in Figure S2.

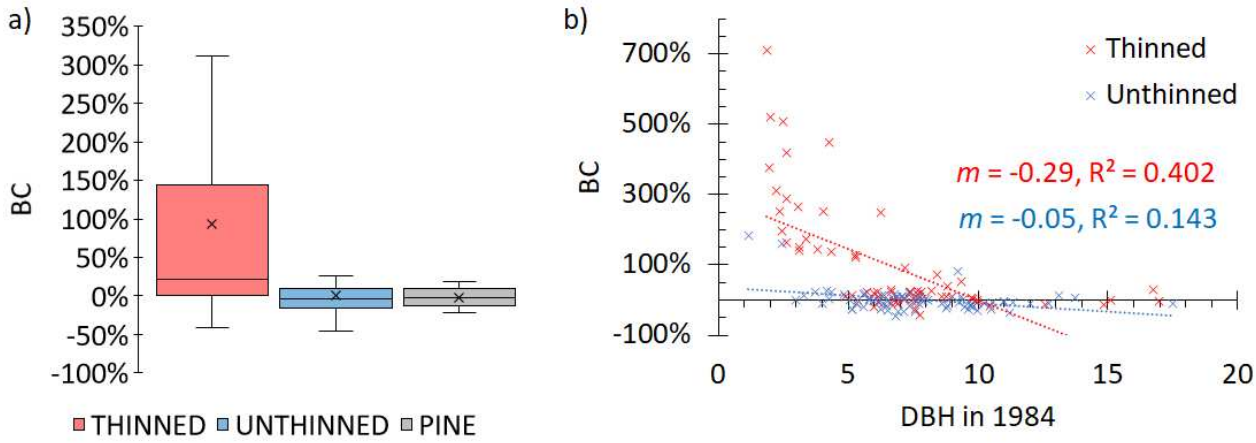

Figure 3: (a) Box plots of basal area increment (BAI) change (BC) after the thinning in 1984 in thinned and unthinned oak plots and in *P. sylvestris* (pine) series. (b) Scatter plot relating oak diameter (DBH) in 1984 with BAI change (BC) in thinned (red crosses) and unthinned (blue crosses) plots.

3.2 Growth response to droughts

In the post thinning interval (1984–2020), we found a significant BAI response to the 1-month SPEI values for June in unthinned plots, whereas no significant correlation was found for thinned plots indicating a low responsiveness to short term changes in soil water availability (**Fig. 4**). The highest and significant correlation coefficients in *P. sylvestris* trees were found between indexed BAI and July 1-month SPEI, indicating a higher sensitivity to shorter droughts than oaks in thinned plot and a response more similar to oaks that have not undergone the thinning treatment. The 3-month June, July and August SPEI showed positive relationships whit oak BAI for unthinned plots and only in August for thinned plots. Correlation coefficients for oaks in thinned and unthinned plots were high and significant for October 6- and 9-month long SPEIs. The moving correlation analyses revealed a progressive loss of significance of the correlations with the June 1-month SPEI, while the values remained higher and significant in the unthinned plots. However, no difference between thinned and unthinned plots for 6- and 9-month long SPEIs was found in moving correlation analyses (**Fig. 5**).

Exceptional dry growing season, with SPEI below the threshold of -1.28, occurred in 1967, 1986, 1989, 1995 and 2012 (**Fig. S3**). In terms of resistance, the 1989 drought more severely affected studied trees, causing abrupt BAI growth reductions in both oaks (-40.5%) and pines (-40.1%). Contrarily, the 2012 drought event did not severely constrain growth of oaks and pines. The *P. sylvestris* growth series showed remarkable differences with oaks in 1967 and 1995 (**Fig. S4**), when their resistance to drought was lower and higher than oaks, respectively.

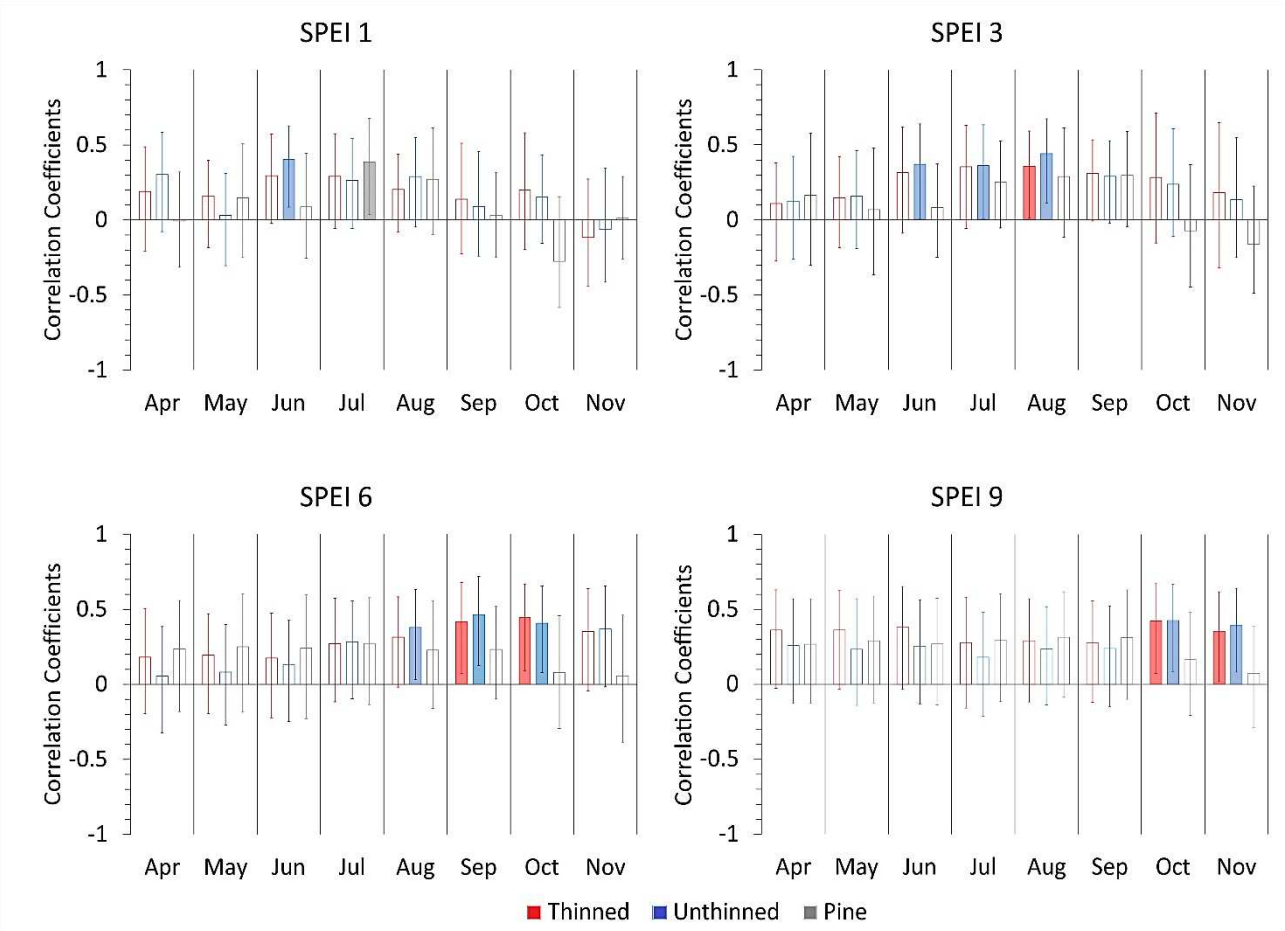

Figure 4. Correlation coefficients between mean indexed BAI standard chronologies and 1-, 3-, 6- and 9-month SPEI index. Bars were fill when 95% bootstrap confidence interval was significant. Period of analysis 1984-2020.

Generally, oaks and pines showed high recovery rates (Rc>1) after drought (**Figs. 6** and **S4**). Consequently, four years after drought events BAI was similar to pre-disturbance levels, with resilience values close to one. On average, recovery periods for both pine and oaks lasted between one and two years, with exception of 1967 when four years were required for pines and 1989 and 1995 droughts when growth took at least two years to recover in most oaks. Relative resilience indices showed distributions similarly to recovery indices (**Figs. 6** and **S5**), and they were inversely proportional to the resistance index.

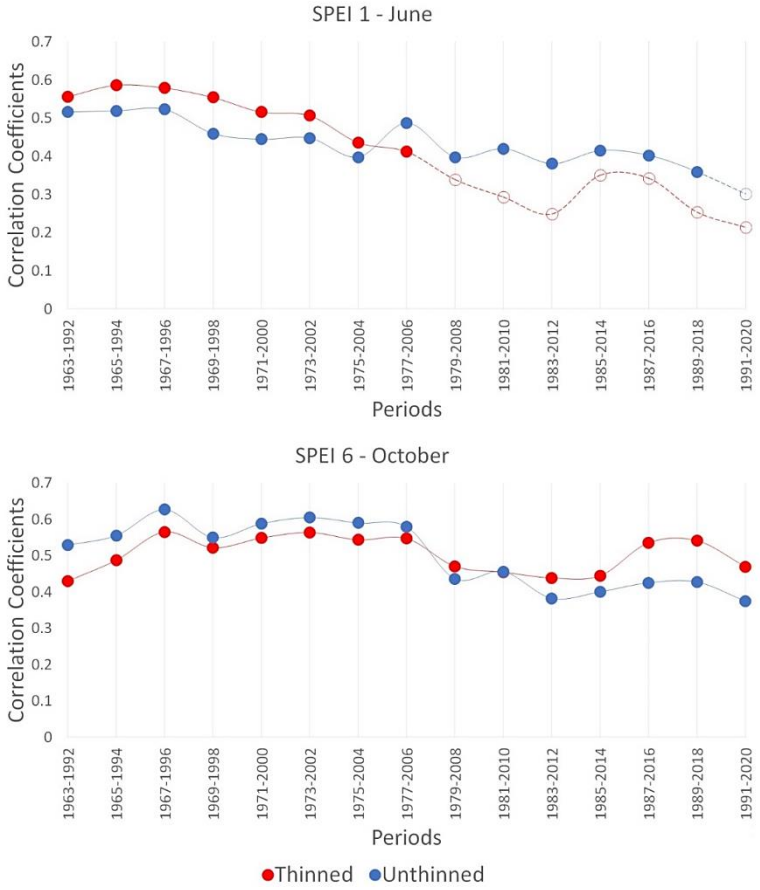

Figure 5. Pearson correlation coefficients calculated using 30-year moving windows between mean indexed BAI standard chronologies and June 1-month SPEI index (a) and October 6-month SPEI (b). Dots were filled when 95% bootstrap confidence interval was significant. Period of analysis is 1963-2020.

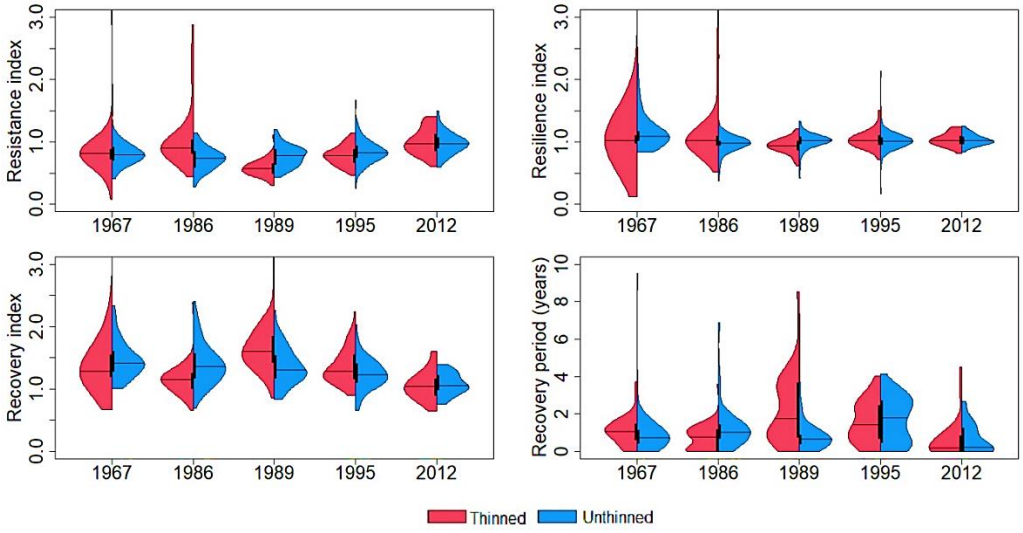

Figure 6. Violin plots showing resistance, recovery and resilience indices and recovery period (years) of *Q. subpyrenaica* trees in thinned (red) and unthinned (blue) plots for different drought events (see also Fig. S3). Scots pine values are plotted in Figure S4, whilst relative resilience indices calculated in *Q. subpyrenaica* trees in thinned and unthinned plots are plotted in Figures S4 and S5.

3.3 Variability of resilience components

The October 9-month SPEI index was selected as a main climatic driver of oak growth for the computation of climate growth correlation at individual tree level in the common period 1984–2002 (CorrSPEI). In this period, three exceptional droughts (1986, 1989 and 1995; cf. **Fig. S3**) were analysed using GLMEs.

Generally, thinned plots showed higher resistance values in 1986 and lower in 1989 than unthinned plots (**Table 2**). In 1986 and 1989, RW had a significant negative effect over resistance in unthinned stands. In the second event, MS and CorrSPEI parameters presented negative influences on growth resistance, especially for thinned plots. In the 1995 drought, there was not significant difference among thinned and unthinned plots, resistance was negatively related to RW and MS. For the same event, the only parameter with significant weight was the correlation coefficient between SPEI and BAI in unthinned plots (**Table S1**).

Thinned plots showed significant lower resilience only after the 1986 drought. However, larger oaks from thinned plots showed lower levels of relative resilience in the 1989 and higher in the 1995 drought. Mean sensitivity had a significant positive (1986) and negative (1989) weight on resilience, especially for thinned stands. CorrSPEI was often positively related to resilience, especially in 1989 and 1995. Finally, the relative resilience was not influenced by either tree dbh or tree age, but it depended more on CorrSPEI (positive relationship) and slightly on ring width and mean sensitivity (Tab.S1).

In all models performed, slope aspect always explained a very few portion of the variance. Moreover, the values of conditional and marginal R^2 were similar indicating that most variability in growth resistance to drought was accounted for by fixed factors (**Table 2**).

Table 2. Summary statistics (*t* values) of Generalized Linear Mixed-Effects models relating tree growth resistance and resilience to the three drought years studied (1986, 1989 and 1995) (for recovery and relative resilience see Tab.S1). Variables are abbreviated as: dbh, diameter at breath height; RW, mean ring width; MS, mean sensitivity; CorrSPEI, correlation coefficients of October 9-month SPEI index and the BAI chronology. In the case of fixed factors, NA indicates the parameter not included in the model, whereas in the case of the random factor (slope aspect. Bold values are statistically significant. Significance levels: * $p < 0.05$; ** $p < 0.01$; *** $p < 0.001$.

Resistance	1986			1989			1995		
	All	Thinned	Unthinned	All	Thinned	Unthinned	All	Thinned	Unthinned
Intercept	**+8.73*** **	**+11.15*** **	**+5.59*** **	**+15.51*** **	**+9.29*** **	**+11.16*** **	**+12.10*** **	**+11.16*** **	**+7.89*** **
Age	*NA*	*NA*	+0.31	*NA*	*NA*	**-1.81.**	*NA*	*NA*	+0.28
dbh	-1.26	-1.36	NA	**-2.15***	-0.18	NA	+1.00	**+2.04***	NA
RW	-0.81	-0.38	**-1.99***	-0.19	-0.83	**-2.30***	**-2.21***	**-2.92****	-0.99
MS	+0.40	+0.01	-0.44	**-3.65*** **	**-3.07****	-1.36	**-4.05*** **	**-3.81*** **	-0.92
CorrSPEI	-0.33	-1.12	+0.37	**-2.75****	**-1.69.**	**-2.60****	-1.43	-0.39	**-1.85.**
Thinning (dummy)	**+3.31*** **	*NA*	*NA*	**-5.47*** **	*NA*	*NA*	*-0.72*	*NA*	*NA*
Slope aspect variance	<0.01	0	<0.01	<0.01	0.01	0	<0.01	<0.01	<0.01
R^2m	0.07	0.04	0.03	0.18	0.05	0.15	0.13	0.21	0.06
R^2c	0.09	*NA*	0.07	0.19	0.07	*NA*	0.14	0.26	0.09

Resilience	1986			1989			1995		
	All	Thinned	Unthinned	All	Thinned	Unthinned	All	Thinned	Unthinned
Intercept	**+8.01*** **	**+6.01*** **	**+7.35*** **	**+18.35*** **	**+19.00*** **	**+11.44*** **	**+11.74*** **	**+11.76*** **	**+8.64*** **
Age	*NA*	*NA*	+1.29	*NA*	*NA*	-1.63	*NA*	*NA*	-1.07
dbh	**-2.35***	*-1.25*	*NA*	**-2.92****	***-1.94.***	*NA*	*-1.61*	**1.85.**	*NA*
RW	**+1.91.**	**+1.66.**	**-2.26***	+0.75	**+1.93.**	**-2.10***	-0.11	-0.04	**-2.34***
MS	**+3.77*** **	**+2.36***	+0.32	**-2.27***	**-3.28****	+0.72	-0.22	+0.04	-0.16
CorrSPEI	+0.71	-0.60	**+2.12***	**+2.28***	**+1.99***	**+1.73.**	**+4.38*** **	**+2.16***	**+3.88*** **
Thinning (dummy)	+0.47	*NA*	*NA*	**-2.65****	*NA*	*NA*	+0.53	*NA*	*NA*
Slope aspect variance	0.00	<0.01	<0.01	<0.01	0.00	<0.01	<0.01	<0.01	0.00
R^2m	0.293	0.319	0.106	0.176	0.188	0.147	0.147	0.129	0.243
R^2c	0.293	0.336	0.140	0.185	0.188	0.185	0.165	0.205	0.243

4. Discussion

4.1 Effects of thinning on oak radial growth

Thinning increased radial growth in *Q. subpyrenaica* trees, and this effect lasted for over 20 years and slightly tended to decrease probably as canopies closed. These results agree with other studies carried out on Iberian oak species showing a longer duration of the thinning positive effect on growth (Cutter et al. 1991; Mayor et al. 1993; Cañellas et al 2004). The *Q. subpyrenaica* response after these treatments depended on stem diameter, with smaller stems featuring more plastic response and showing a higher relative growth improvement than larger individuals. This could be related to the suppressed position of the dominated layer that promptly enhanced radial growth after the canopy opened by thinning. The larger trees that already reached a dominant or codominant position within the stand, exhibited fewer release effects which could be also due to higher competition among stems of the same individual which depend on the same stump, as reported by Corcuera et al. (2006) for *Quercus pyrenaica*. Juodvalkis et al. (2005) reported similar results demonstrating that an increase of tree volume could be achieved only when thinning 10-30 years-old oak (*Quercus robur*) stands, whereas at older ages the positive effect of thinning is buffered by overaging. On the other hand, in a study on *Q. pyrenaica* coppice stands in central Spain (Cañellas et al 2004), the larger trees were the most favoured by thinning due to their greater capacity of resource uptake (soil water and nutrients) and allocation occurring after thinning. However, an imbalance between stem diameter and parent root system size could occur after a thinning treatment in coppice stands, resulting in smaller trees not necessarily suppressed in root water uptake by bigger individuals.

4.2 Effects of thinning on climate-growth relationships

Since *Q. subpyrenaica* has shown a wide range of ecophysiological adjustments in response to drought stress in experiments based on seedlings, even wider than their parental taxa (Himrane et al. 2004), it is important to assess the growth responses to water shortage of adult trees inhabiting formerly coppiced forests as has been done in *Q. faginea* (Alla and Camarero 2012). In our study, climate-growth analysis confirmed the key role of water availability in limiting tree stem growth, in line with other studies on Mediterranean deciduous oaks (Corcuera et al. 2004, Camarero et al. 2016, Martínez-Sancho et al. 2021). Growth and productivity of oaks was linked to more consistently to longer (i.e 6 to 9 months) droughts. However, in unthinned plots growth was linked to early summer drought conditions in June, similarly to what Di Filippo et al. (2010) found in Turkey oak (*Quercus cerris* L.). Moving windows analysis revealed that this effect was also significant in oaks located in thinned plots, but it lost its significance following the thinning treatment. Correlations values between

oak growth and longer droughts (6- to 9-month SPEIs) did not show differences between thinned and unthinned plots and remained stable even after treatment.

Scots pine growth exhibited positive correlations to 1-month July SPEI, therefore being more sensitive to short-term droughts than *Q. subpyrenaica* in thinned plots. The different ecophysiological strategies of coexisting pines and oaks to withstand summer drought were well described by Martín-Gómez et al. (2017). They found that the anisohydric oaks presented a faster recovery of predawn water potential after summer drought than the pines, probably associated with more reliable and deeper soil water sources which could explain specific response to long droughts. These authors also reported a stronger negative effect of drought stress on long-term growth in pines, relying on shallower soil water sources, compared with oaks.

In our study, the exceptional growth reduction featured in Scots pine in 1992-1993 period (Fig. S2) was not related to intense drought conditions, suggesting an impact of other abiotic or biotic disturbances such as the defoliator pine processionary moth, *Thaumetopoea pityocampa* (Camarero et al. 2022). In addition, cold winter conditions (January and February were cold in 1992) could also have contributed to the sharp decrease in Scots pine growth as reported in Baltic area (Matisons et al. 2019, Cedro et al. 2022).

4.3 Impact of intense droughts on growth resilience

The oak *Q. subpyrenaica* is a ring-porous species with anisohydric behavior, maintaining higher transpiration and physiological activity under mild-to moderate drought conditions (Corcuera et al. 2004, Himrane et al. 2004, Tognetti et al. 2007). However, during extremely dry summer conditions, *Q. subpyrenaica* reduces transpiration rates showing high recovery rates after the first seasonal precipitation in early autumn (Martin-Gomez et al. 2017). The exceptionally and successive droughts detected in the study site from the 1980s onwards, also cited by other authors for nearby forested areas in Spain (Camarero et al. 2015, 2016, 2018; Manrique-Alba et al. 2022), could explain a stronger coupling between oak growth and water deficit. Differently from a study in a mixed coppice forests with *Q. ilex and Q. faginea* in the drier eastern Spain (Camarero et al. 2016), *Q. subpyrenaica* in our study site proved highly resistant to the 2012 drought event in both thinned and unthinned plots, perhaps because the 2012 drought was less severe in the wetter Spanish Pre-Pyrenees. The other selected droughts differently impact studied plots: the 1967 and 1995 events produced similar effects regardless thinning treatment, whereas in 1986 and 1989 the resistance values differed between thinned and unthinned plots. Specifically, in 1986 the drought impact on oak growth in the thinned plots was mitigated by the release post-thinning phase, while in the 1989 drought caused a more pronounced growth reduction in oaks from thinned plots. Nevertheless, also in concomitance of

intense droughts events absolute BAI values in thinned plots were significantly higher than those recorded in unthinned plots, in line with the results obtain by Aldea et al. (2017) in thinned pine-oak stands.

Most trees recovered pre-disturbance growth levels within one or two years, which concurs with global analyses of post-drought growth recovery (Anderegg et al. 2015), with wider interquartile ranges for the recovery periods after the 1989 drought, when some trees took up to six years to fully recover growth levels. Given the above-mentioned results, our starting hypothesis of greater resistance and resilience of the oaks inhabiting in thinned plots was not always verified.

The fitted GLMEs confirmed the influence of thinning on the resistance values during the 1986 and 1989 droughts, contrarily the other parameters included in the model were not significant. Tree-level drought sensitivity assessed with CorrSPEI generally had a higher weight than structural (dbh and age) and growth (RW and MS) parameters on resilience components (Rs, Rc, Rs and RR). As expected, CorrSPEI was negatively related to drought Rs but positively related to Rc, Rs and RR. Tree size (dbh) could enhance the oaks resilience against intense droughts and reduced the time to recover pre-drought growth rates (Camarero et al., 2016; Colangelo et al. 2017, Gonzalez de Andrés et al. 2021). However, our results did not show a clear role of stem size (dbh) on resilience components, with an opposite effect during 1995 drought as compared to 1986 and 1989 droughts.

Lithological and geomorphological features such as aspect and/or relative position of forest along the slope and could also determine the effect of the drought on tree growth (Lloret et al 2004). In our study case, slightly differences in slope aspects did not play a kay role in oaks resilience components, with no differences detected by GLMEs in sensitivity between SE- and wetter SW-oriented slopes. A greater number of plots distributed at different exposures may be necessary to better investigate this aspect.

5. Conclusions

We found that *Q. subpyrenaica* stem radial growth showed a moderate post-thinning release which preferentially benefitted small-diameter trees. Thinning resulted on long-lasting growth improvement which was reversed by severe droughts. Successive droughts reducing the amount of stored forest biomass, could lengthen the post-drought recovery time (usually lasting 1-2 years), postpone the turnover cycle and the timing of other silvicultural treatments. At the same time, thinning could reduce competition between individuals for soil water, causing dieback, especially in overaged coppice stands. We argue that future studies should carefully plan and monitor thinning treatments in similar seasonally dry oak coppices which probably respond more positively to thinning treatments carried out during wet decades and in regular intervals shorter than 20 years.

Supplementary materials

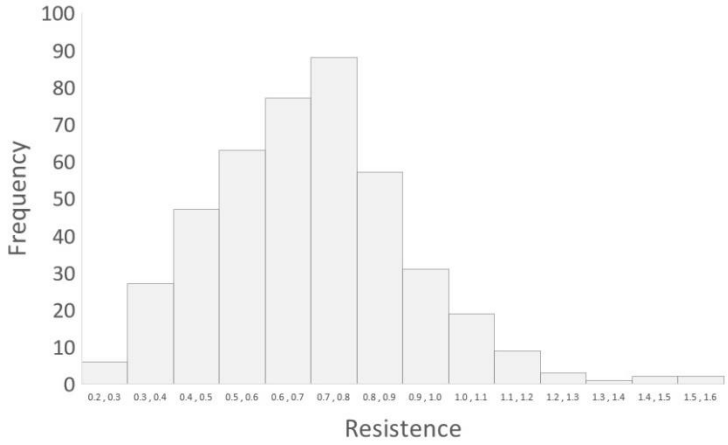

Figure S1. Histogram of the distribution of resistance values calculated in dry years (1967, 1986, 1989, 1995 and 2012; see also Fig. 1b).

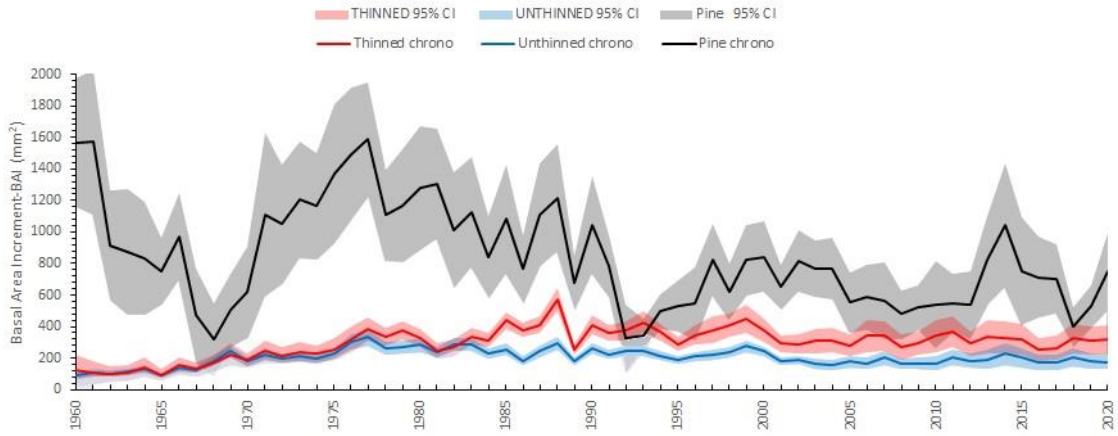

Figure S2. Mean basal area increment and bootstrapped 95% confidence intervals (CIs) of *Quercus subpyrenaica* trees in thinned and unthinned plots and *Pinus sylvestris* (Pine).

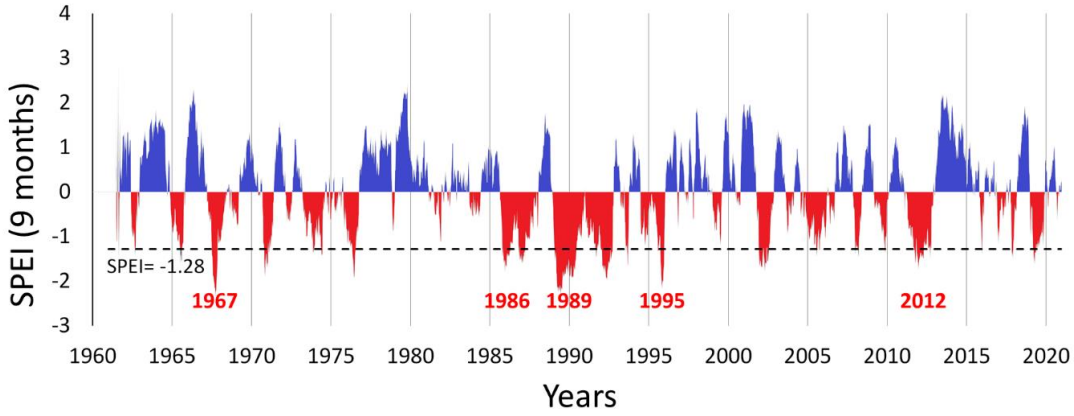

Figure S3. SPEI values calculated considering a 9-month September window, i.e. from January to September. Dry periods (negative values) were coloured in red, while wet periods (positive values) are in blue. Dry years are shown in red and refer to SPEI values lower than the -1.28 threshold for the growing season, i.e. from April to October.

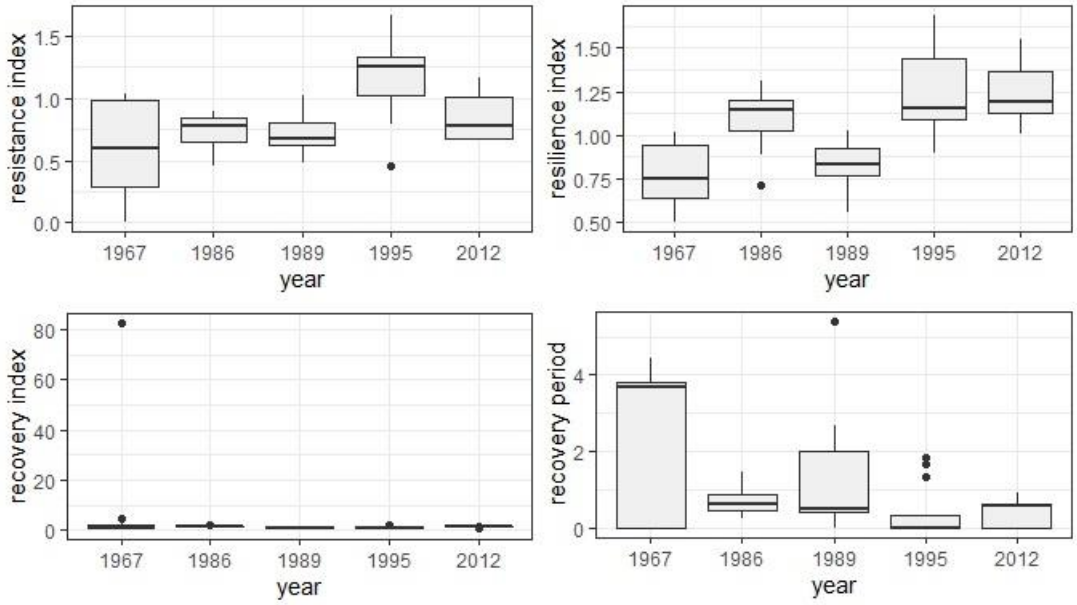

Figure S4. Resistance, recovery and resilience indices and recovery period (years) corresponding to severe drought events calculated in *P. sylvestris* trees.

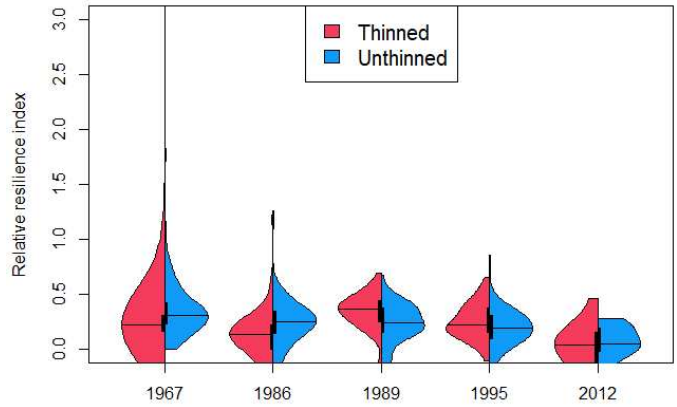

Figure S5. Relative resilience indices after drought events in oak trees showed distributions very similar to recovery indices (Fig. 6).

Table S1. Summary statistics (*t* values) of Generalized Linear Mixed-Effects models relating tree growth recovery and relative resilience to the three drought years studied (1986, 1989 and 1995). Variables are abbreviated as: dbh, diameter at breath height; RW, mean ring width; MS, mean sensitivity; CorrSPEI, correlation coefficients of October 9-month SPEI index and the BAI chronology. In the case of fixed factors NA indicated when the parameter was not included in the model, whereas in the case of the random factor (slope aspect) NA was used when the calculation of the conditional R^2 (R^2c) was not possible due to variance equal to 0. Bold values are significant ($p < 0.05$). Significance levels: * $p < 0.05$; ** $p < 0.01$; *** $p < 0.001$.

Recovery	1986			1989			1995		
	All	Thinned	Unthinned	All	Thinned	Unthinned	All	Thinned	Unthinned
Intercept	**+9.36*** **	**+8.50*** **	**+5.79*** **	**+8.082*** **	**+7.67*** **	**+5.69*** **	**+8.52*** **	**+9.72*** **	**+5.93*** **
Age	*NA*	*NA*	+0.53	*NA*	*NA*	+0.18	*NA*	*NA*	-0.73
dbh	+0.45	*+0.91*	*NA*	*-0.16*	-0.41	*NA*	**-1.69.**	-1.13	*NA*
RW	-1.61	**-1.67.**	-1.56	+1.25	+1.33	+0.57	**+2.19***	**+1.99***	+0.07
MS	+0.06	-0.50	+0.52	+1.13	+0.43	+0.93	**+3.62*** **	**+2.95** **	+1.49
CorrSPEI	+1.28	+0.98	+1.37	**+3.43** **	+1.62	**+2.89*** **	**+6.06*** **	**+2.45***	**+5.62*** **
Thinning (dummy)	**-4.41*** **	*NA*	*NA*	**+3.31** **	*NA*	*NA*	-0.18	*NA*	*NA*
Slope aspect variance	<0.01	<0.01	<0.01	<0.01	<0.01	<0.01	<0.01	0.00	<0.01
R^2m	0.268	0.107	0.090	0.426	0.247	0.189	0.446	0.457	0.352
R^2c	0.334	0.259	0.175	0.448	0.303	0.247	0.462	*NA*	0.410

Relative resilience	1986			1989			1995		
	All	Thinned	Unthinned	All	Thinned	Unthinned	All	Thinned	Unthinned
Intercept	**+20.00*** **	**+15.42**	**+13.73*** **	**+21.72*** **	**+18.49*** **	**+13.53*** **	**+21.72*** **	**+13.69*** **	**+13.84*** **
Age	*NA*	*NA*	+1.26	*NA*	*NA*	-0.37	*NA*	*NA*	-0.39
dbh	+0.06	+0.28	*NA*	*-1.48*	-1.32	*NA*	*-1.48*	-0.85	*NA*
RW	-1.43	-0.76	**-2.37***	+1.72.	**+1.76.**	**-1.69.**	*1.72*	**+2.23***	*-0.87*
MS	+1.29	+0.36	+1.00	**+3.28** **	-0.86	1.051	**+3.28** **	**+2.18***	**+1.88.**
CorrSPEI	**+1.70.**	+0.84	**+2.08***	**+6.67*** **	**1.65.**	**+3.12** **	**+6.67*** **	**+2.87** **	**+5.77*** **
Thinning (dummy)	**-3.10****	*NA*	*NA*	0.05	*NA*	*NA*	0.05	*NA*	*NA*
Slope aspect variance	<0.00	<0.01	<0.01	<0.01	0.00	<0.01	<0.01	0.00	<0.01
R^2m	0.169	0.024	0.219	0.176	0.188	0.147	0.529	0.484	0.503
R^2c	0.231	0.152	0.226	0.185	*NA*	0.185	0.530	*NA*	*0.505*

Chapter 6

General conclusions

This research was conducted during a three-year doctorate course and, even with some limitations imposed by the COVID pandemic, I had the chance to deepen my methodological skills attending the Dendrochronology and Wood Anatomy Laboratory at TESAF at University of Padova and at IPE in Zaragoza (Spain) under the supervision of prof. Marco Carrer and Dr. Julio Camarero respectively. My hope is to have contributed to shed some light on the effects of climate extremes (frost and drought) on Mediterranean deciduous forests and to develop suitable strategies to contrast effects of climate change, ensuring the products and ecosystem services provided by forests..

I've tried to integrate different methodologies analysing forest ecosystems at different spatial and temporal scales. Both remote sensing and tree-ring analyses requiring significant amounts of time, offering information at different spatial scales. Remote sensing allowed a synchronic approach for monitoring forest vegetation during the disturbance event, determining the surface of the affected area, estimating the intensity of the event and the time necessary for ecosystem recovery. Nevertheless, the *in-situ* data collection is essential for the validation of remote sensing outputs, as well as for investigating at more detailed scales how individual functioning is altered by disturbances. In this regard, the dendroecological analysis allowed to determine the impact of extreme events on growth at tree-level scale, in relation to the individual structural parameters and site geomorphological characteristics. Encouraging results were also obtained applying this analysis on short time series from young trees (*P. nigra*) that are usually associated with more individualistic growth trends but not for this reason unable to register climate signals, exhibiting growth increase or decrease in response to extreme (positive or negative) weather conditions. However, both remote sensing and tree-ring analyses have limitations. Remote sensing data are relatively recent source and high-quality images free of cloud interference are required for vegetational studies, factors that could limit the time series length and resolution used in analysis. In dendrochronology, limiting factors that cause narrow ring formations could be related to different disturbances as shown in beech populations in the Apennines (drought and late spring frost). Consequently, it could be difficult to determine the nature of the environmental factors that caused anomaly growth rates occurred before the available meteorological data. To solve this problem, a more refined analysis of the anatomical traits can be useful for studying the relationships between extreme events and growth. From our preliminary results, frost events do not seem to affect the plasticity of vessel traits in beech, which seem more related to the tree structural parameters (especially tree heights) and to the elevation of the stand. However, this analysis needs to be further investigated in future research both in other species and in

other populations and scales. In future studies, the application of isotope analysis can also serve to shed more light on the interactions between disturbances and tree growth. Not only impact but also resilience components could be successfully estimated from remote sensing measurements (vegetation indices) and tree-ring data with the same limitation previously discussed. In European beech resistance to late frost defoliations depend on spring leaf phenology timing and intensity of extreme minimum temperatures, both factors strictly related to forest stand elevation. However, frost affected beech trees were resilient and rapidly recovered their growth rates in one or two growing seasons, showing no year-to-year carryover or legacy effects. Satellite imagery was very useful to detect the most affected trees canopies and to assess the impact of late frost recovery time period at weekly resolution. Nonetheless, late frosts remain a threat in the Apennines beech forests, especially if followed within the same growing season by summer drought, another highly influential driver of climatic stress. This climate induced disturbance represents a threat to various Mediterranean species. Here, drought sensitivity has been studied in coppiced forests of *Quercus subpyrenaica*, an endemic species in the pre-Pyrenees, Spain. We have found a short-term positive effect of thinning on resistance to droughts, masked by the release phase due to the opening of the forest canopy cover. Following extreme summer drought events drastically reduce tree stem growth especially in thinned plots. However, both thinned and not unthinned plots do not show large differences in terms of resilience after severe

droughts. Future studies will have to consider the effects of thinning of varying intensity, and the effect of such practices on seed production, surface erosion and fire risk mitigation.

References

Acácio, V., Dias, F.S., Catry, F.X., Rocha, M., Moreira, F., 2017. Landscape dynamics in Mediterranean oak forests under global change: understanding the role of anthropogenic and environmental drivers across forest types. Glob. Chang. Biol. 23. https://doi.org/10.1111/gcb.13487

Aldea, J., Bravo, F., Bravo-Oviedo, A., Ruiz-Peinado, R., Rodríguez, F., del Río, M., 2017. Thinning enhances the species-specific radial increment response to drought in Mediterranean pine-oak stands. Agric. For. Meteorol. 237–238. https://doi.org/10.1016/j.agrformet.2017.02.009

Alla, A.Q., Camarero, J.J., 2012. Contrasting responses of radial growth and wood anatomy to climate in a Mediterranean ring-porous oak: Implications for its future persistence or why the variance matters more than the mean. Eur. J. For. Res. 131. https://doi.org/10.1007/s10342-012-0621-x

Allevato, E., Saulino, L., Cesarano, G., Chirico, G.B., D'Urso, G., Falanga Bolognesi, S., Rita, A., Rossi, S., Saracino, A., Bonanomi, G., 2019. Canopy damage by spring frost in European beech along the Apennines: effect of latitude, altitude and aspect. Remote Sens. Environ. 225, 431–440. https://doi.org/10.1016/j.rse.2019.03.023

Amaral Franco J, 1990. Quercus L. In: Castroviejo S, Laínz M, López G, Montserrat P, Muñoz F, Paiva J, Villar L (eds) Flora Ibérica. II. Plantas Vasculares de la Península Ibérica e Islas Baleares. RJBM-CSIC, Madrid, pp 16–36

Améglio, T., Cochard, H., & Ewers, F. W. , 2001. Stem diameter variations and cold hardiness in walnut trees. Journal of Experimental Botany, 52(364), 2135-2142.

Amorini, E., Biocca, M., Manetti, M.C., Motta, E., 1996. A dendroecological study in a declining oak coppice stand. Ann. des Sci. For. 53. https://doi.org/10.1051/forest:19960249

Anderegg, W.R.L., Schwalm, C., Biondi, F., Camarero, J.J., Koch, G., Litvak, M., Ogle, K., Shaw, J.D., Shevliakova, E., Williams, A.P., Wolf, A., Ziaco, E., Pacala, S., 2015. Pervasive drought legacies in forest ecosystems and their implications for carbon cycle models. Science (80-.). 349. https://doi.org/10.1126/science.aab1833

Andrews, C. M., D'Amato, A. W., Fraver, S., Palik, B., Battaglia, M. A., & Bradford, J. B. (2020). Low stand density moderates growth declines during hot droughts in semi-arid forests. Journal of Applied Ecology, 57(6), 1089-1102.

Arnič, D., Gričar, J., Jevšenak, J., Božič, G., von Arx, G., & Prislan, P., 2021. Different Wood Anatomical and Growth Responses in European Beech (Fagus sylvatica L.) at Three Forest Sites in Slovenia. Frontiers in plant science, 1551.

Auer, I., Böhm, R., Jurkovic, A., Lipa, W., Orlik, A., Potzmann, R., Schöner, W., Ungersböck, M., Matulla, C., Briffa, K., Jones, P., Efthymiadis, D., Brunetti, M., Nanni, T., Maugeri, M., Mercalli, L., Mestre, O.,

Moisselin, J.M., Begert, M., Müller-Westermeier, G., Kveton, V., Bochnicek, O., Stastny, P., Lapin, M., Szalai, S., Szentimrey, T., Cegnar, T., Dolinar, M., Gajic-Capka, M., Zaninovic, K., Majstorovic, Z., Nieplova, E., 2007. HISTALP - Historical instrumental climatological surface time series of the Greater Alpine Region. Int. J. Climatol. 27, 17–46. https://doi.org/10.1002/joc.1377

Augspurger, C.K., 2009. Spring 2007 warmth and frost: Phenology, damage and refoliation in a temperate deciduous forest. Funct. Ecol. 23, 1031–1039. https://doi.org/10.1111/j.1365-2435.2009.01587.x

Augspurger, C.K., 2013. Reconstructing patterns of temperature, phenology, and frost damage over 124 years: Spring damage risk is increasing. Ecology 94, 41–50. https://doi.org/10.1890/12-0200.1

Aussenac, G., 2000. Interactions between forest stands and microclimate: Ecophysiological aspects and consequences for silviculture. Ann. For. Sci., 57 (3), 287-301. https://doi.org/10.1051/forest:2000119Bätz, N., Colombini, P., Cherubini, P., Lane, S.N., 2016. Groundwater controls on biogeomorphic succession and river channel morphodynamics. J. Geophys. Res. Earth Surf. 121, 1763–1785. https://doi.org/10.1002/2016JF004009

Bajocco, S., Ferrara, C., Alivernini, A., Bascietto, M., Ricotta, C., 2019. Remotely-sensed phenology of Italian forests: Going beyond the species. Int. J. Appl. Earth Obs. Geoinf. 74, 314–321. https://doi.org/10.1016/j.jag.2018.10.003

Bascietto, M., Bajocco, S., Ferrara, C., Alivernini, A., Santangelo, E., 2019. Estimating late spring frost-induced growth anomalies in European beech forests in Italy. Int. J. Biometeorol. 63, 1039–1049. https://doi.org/10.1007/s00484-019-01718-w

Bascietto, M., Bajocco, S., Mazzenga, F., Matteucci, G., 2018. Assessing spring frost effects on beech forests in Central Apennines from remotely-sensed data. Agric. For. Meteorol. 248, 240–250. https://doi.org/10.1016/j.agrformet.2017.10.007

Bates, D., Mächler, M., Bolker, B.M., Walker, S.C., 2015. Fitting linear mixed-effects models using lme4. J. Stat. Softw. 67. https://doi.org/10.18637/jss.v067.i01

Bates, D., Sarkar, D., Bates, M.D., Matrix, L., 2007. The lme4 Package. October 2.

Bätz, N., Colombini, P., Cherubini, P., Lane, S.N., 2016. Groundwater controls on biogeomorphic succession and river channel morphodynamics. J. Geophys. Res. Earth Surf. 121, 1763–1785. https://doi.org/10.1002/2016JF004009

Benito Garzón, M., Sánchez De Dios, R., Sainz Ollero, H., 2008. Effects of climate change on the distribution of Iberian tree species. Appl. Veg. Sci. 11. https://doi.org/10.3170/2008-7-18348

Bigler, C., Bugmann, H., 2018. Climate-induced shifts in leaf unfolding and frost risk of European trees and shrubs. Sci. Rep. 8. https://doi.org/10.1038/s41598-018-27893-1

Biondi, E., & Galdenzi, D., 2012. Phytosociological analysis of the grasslands of Montagna dei Fiori (central Italy) and syntaxonomic review of the class Festuco-Brometea in the Apennines. Plant Sociology, 49(1), 91-112.

Biondi, F., Qeadan, F., 2008. Inequality in paleorecords. Ecology 89, 1056–1067. https://doi.org/10.1890/07-0783.1

Bolte, A., Czajkowski, T., Kompa, T., 2007. The north-eastern distribution range of European beech - A review. Forestry. https://doi.org/10.1093/forestry/cpm028

Bontemps, J. D., & Esper, J., 2011. Statistical modelling and RCS detrending methods provide similar estimates of long-term trend in radial growth of common beech in north-eastern France. Dendrochronologia, 29(2), 99-107.

Bose, A. K., Rohner, B., Bottero, A., Ferretti, M., & Forrester, D. I., 2021. Did the 2018 megadrought change the partitioning of growth between tree sizes and species? A Swiss case-study. Plant Biology.

Bottero, A., D'Amato, A. W., Palik, B. J., Bradford, J. B., Fraver, S., Battaglia, M. A., & Asherin, L. A., 2017. Density-dependent vulnerability of forest ecosystems to drought. Journal of Applied Ecology, 54(6), 1605-1614.

Braeuning, A., De Ridder, M., Zafirov, N., García-González, I., Dimitrov, D. P., & Gärtner, H. (2016). Tree-ring features: indicators of extreme event impacts. IAWA Journal, 37(2), 206-231.

Briffa, K. R., & Melvin, T. M., 2011. A closer look at regional curve standardization of tree-ring records: justification of the need, a warning of some pitfalls, and suggested improvements in its application. In Dendroclimatology (pp. 113-145). Springer, Dordrecht.

Briffa, K.R., Jones, D., 1990. Basic chronology statistics and assessment. Pages in E. , editors, in: Methods of Dendrochronology. pp. 137–153.

Brown, L.A., Fernandes, R., Djamai, N., Meier, C., Gobron, N., Morris, H., Canisius, F., Bai, G., Lerebourg, C., Lanconelli, C., Clerici, M., Dash, J., 2021. Validation of baseline and modified Sentinel-2 Level 2 Prototype Processor leaf area index retrievals over the United States. ISPRS J. Photogramm. Remote Sens. 175, 71–87. https://doi.org/10.1016/j.isprsjprs.2021.02.020

Bunn, A.G., 2008. TECHNICAL NOTE A dendrochronology program library in R (dplR). Dendrochronologia 26, 115–124. https://doi.org/10.1016/j.dendro.2008.01.002

Büntgen, U., 2019. Re-thinking the boundaries of dendrochronology. Dendrochronologia, 53, 1-4.

Bussotti, F., Grossoni, P., Bottacci, A., 1997. Sclerophylly in beech (Fagus sylvatica L.) trees: Its relationship with crown transparency, nutritional status and summer drought. Forestry 70, 267–271. https://doi.org/10.1093/forestry/70.3.267

Bussotti, F., Pollastrini, M., Holland, V., & Brüggemann, W., 2015. Functional traits and adaptive capacity of European forests to climate change. Environmental and Experimental Botany, 111, 91-113.

Cabon, A., Mouillot, F., Lempereur, M., Ourcival, J.M., Simioni, G., Limousin, J.M., 2018. Thinning increases tree growth by delaying drought-induced growth cessation in a Mediterranean evergreen oak coppice. For. Ecol. Manage. 409. https://doi.org/10.1016/j.foreco.2017.11.030

Camarero, J.J., Gazol, A., Sangüesa-Barreda, G., Cantero, A., Sánchez-Salguero, R., Sánchez-Miranda, A., Granda, E., Serra-Maluquer, X., Ibáñez, R., 2018. Forest growth responses to drought at short- and long-term scales in Spain: Squeezing the stress memory from tree rings. Front. Ecol. Evol. 6. https://doi.org/10.3389/fevo.2018.00009

Camarero, J.J., Gazol, A., Sangüesa-Barreda, G., Vergarechea, M., Alfaro-Sánchez, R., Cattaneo, N., Vicente-Serrano, S.M., 2021. Tree growth is more limited by drought in rear-edge forests most of the times. For. Ecosyst. 8. https://doi.org/10.1186/s40663-021-00303-1

Camarero, J.J., Sangüesa-Barreda, G., Vergarechea, M., 2016. Prior height, growth, and wood anatomy differently predispose to drought-induced dieback in two Mediterranean oak speciesk. Ann. For. Sci. 73. https://doi.org/10.1007/s13595-015-0523-4

Camarero, J.J., Tardif, J., Gazol, A., Conciatori, F., 2022. Pine processionary moth outbreaks cause longer growth legacies than drought and are linked to the North Atlantic Oscillation. Sci. Total Environ. 819. https://doi.org/10.1016/j.scitotenv.2022.153041

Campelo, F., Vieira, J., Nabais, C., 2013. Tree-ring growth and intra-annual density fluctuations of Pinus pinaster responses to climate: Does size matter? Trees - Struct. Funct. 27, 763–772. https://doi.org/10.1007/s00468-012-0831-3

Camuffo, D., Bertolin, C., Barriendos, M., Dominguez-Castro, F., Cocheo, C., Enzi, S., Sghedoni, M., della Valle, A., Garnier, E., Alcoforado, M.J., Xoplaki, E., Luterbacher, J., Diodato, N., Maugeri, M., Nunes, M.F., Rodriguez, R., 2010. 500-Year temperature reconstruction in the Mediterranean Basin by means of documentary data and instrumental observations. Clim. Change 101, 169–199. https://doi.org/10.1007/s10584-010-9815-8

Cañellas, I., Del Río, M., Roig, S., Montero, G., 2004. Growth response to thinning in Quercus pyrenaica Willd. coppice stands in Spanish central mountain. Ann. For. Sci. 61. https://doi.org/10.1051/forest:2004017

Canelo, T., Gaytán, Á., Pérez-Izquierdo, C., Bonal, R., 2021. Effects of longer droughts on holm oak quercus ilex l. Acorn pests: Consequences for infestation rates, seed biomass and embryo survival. Diversity 13. https://doi.org/10.3390/d13030110

Carnicer, J., Barbeta, A., Sperlich, D., Coll, M., Penuelas, J., 2013. Contrasting trait syndromes in angiosperms and conifers are associated with different responses of tree growth to temperature on a large scale. Front. Plant Sci. 4. https://doi.org/10.3389/fpls.2013.00409

Carrer, M., 2011. Individualistic and time-varying tree-ring growth to climate sensitivity. PLoS One, 6(7), e22813.

Carrer, M., Urbinati, C., 2004. Age-dependent tree-ring growth responses to climate in Larix decidua and Pinus cembra. Ecology 85, 730–740. https://doi.org/10.1890/02-0478

Carrer, M., von Arx, G., Castagneri, D., & Petit, G., 2015. Distilling allometric and environmental information from time series of conduit size: the standardization issue and its relationship to tree hydraulic architecture. Tree Physiology, 35(1), 27-33.

Castagneri, D., Vacchiano, G., Hacket-Pain, A., DeRose, R.J., Klein, T., Bottero, A., 2022. Meta-analysis Reveals Different Competition Effects on Tree Growth Resistance and Resilience to Drought. Ecosystems 25. https://doi.org/10.1007/s10021-021-00638-4

Caudullo, G., Welk, E., San-Miguel-Ayanz, J., 2017. Chorological maps for the main European woody species. Data Br. 12, 662–666. https://doi.org/10.1016/j.dib.2017.05.007

Cedro, A., Cedro, B., Podlasiński, M., 2022. Differences in Growth–Climate Relationships among Scots Pines Growing on Various Dune Generations on the Southern Baltic Coast. Forests 13. https://doi.org/10.3390/f13030470

Chamberlain, C.J., Cook, B.I., García de Cortázar-Atauri, I., Wolkovich, E.M., 2019. Rethinking false spring risk. Glob. Chang. Biol. 25. https://doi.org/10.1111/gcb.14642

Chhin, S., Wang, G.G., 2008. Climatic response of Picea glauca seedlings in a forest-prairie ecotone of western Canada. Ann. For. Sci. 65, 1–8. https://doi.org/10.1051/forest:2007090

Chianucci, F., Cutini, A., 2012. Digital hemispherical photography for estimating forest canopy properties: Current controversies and opportunities. IForest. https://doi.org/10.3832/ifor0775-005

Chianucci, F., Cutini, A., 2013. Estimation of canopy properties in deciduous forests with digital hemispherical and cover photography. Agric. For. Meteorol. 168, 130–139. https://doi.org/10.1016/j.agrformet.2012.09.002

Chianucci, F., Disperati, L., Guzzi, D., Bianchini, D., Nardino, V., Lastri, C., Rindinella, A., Corona, P., 2016. Estimation of canopy attributes in beech forests using true colour digital images from a small fixed-wing UAV. Int. J. Appl. Earth Obs. Geoinf. 47, 60–68. https://doi.org/10.1016/j.jag.2015.12.005

Cochard, H., Lemoine, D., Améglio, T., & Granier, A., 2001. Mechanisms of xylem recovery from winter embolism in Fagus sylvatica. Tree Physiology, 21(1), 27-33.

Colangelo, M., Camarero, J.J., Battipaglia, G., Borghetti, M., De Micco, V., Gentilesca, T., Ripullone, F., 2017. A multi-proxy assessment of dieback causes in a Mediterranean oak species. Tree Physiol. 37. https://doi.org/10.1093/treephys/tpx002

Colangelo, M., Camarero, J.J., Borghetti, M., Gazol, A., Gentilesca, T., Ripullone, F., 2017. Size matters a lot: Drought-affected Italian oaks are smaller and show lower growth prior to tree death. Front. Plant Sci. 8. https://doi.org/10.3389/fpls.2017.00135

Cook, E. R., Briffa, K. R., Shiyatov, S., Mazepa, V., 1990. Tree-ring standardization and growth-trend estimation. In Methods of dendrochronology: applications in the environmental sciences (pp. 104-123).

Copenheaver, C.A., Abrams, M.D., 2003. Dendroecology in young stands: case studies from jack pine in northern lower Michigan. For. Ecol. Manage. 182, 247–257. https://doi.org/10.1016/S0378-1127(03)00049-5

Corcuera, L., Camarero, J.J., Gil-Pelegrín, E., 2004. Effects of a severe drought on growth and wood anatomical properties of Quercus faginea. IAWA J. 25. https://doi.org/10.1163/22941932-90000360

Corcuera, L., Camarero, J.J., Sisó, S., Gil-Pelegrín, E., 2006. Radial-growth and wood-anatomical changes in overaged Quercus pyrenaica coppice stands: Functional responses in a new Mediterranean landscape. Trees - Struct. Funct. 20. https://doi.org/10.1007/s00468-005-0016-4

Cornes, R.C., van der Schrier, G., van den Besselaar, E.J.M., Jones, P.D., 2018. An Ensemble Version of the E-OBS Temperature and Precipitation Data Sets. J. Geophys. Res. Atmos. 123, 9391–9409. https://doi.org/10.1029/2017JD028200

Cropper, J.P., 1979. Tree-ring skeleton plotting by computer. Tree Ring Bull. 39, 47–59.

Čufar, K., De Luis, M., Saz, M. A., Črepinšek, Z., & Kajfež-Bogataj, L., 2012. Temporal shifts in leaf phenology of beech (Fagus sylvatica) depend on elevation. Trees, 26(4), 1091-1100.

Čufar, K., Prislan, P., De Luis, M., Gričar, J., 2008. Tree-ring variation, wood formation and phenology of beech (Fagus sylvatica) from a representative site in Slovenia, SE Central Europe. Trees - Struct. Funct. 22, 749–758. https://doi.org/10.1007/s00468-008-0235-6

Cutter, B.E., Lowell, K.E., Dwyer, J.P., 1991. Thinning effects on diameter growth in black and scarlet oak as shown by tree ring analyses. For. Ecol. Manage. 43. https://doi.org/10.1016/0378-1127(91)90071-3

D'Andrea, E., Rezaie, N., Battistelli, A., Gavrichkova, O., Kuhlmann, I., Matteucci, G., Moscatello, S., Proietti, S., Scartazza, A., Trumbore, S., Muhr, J., 2019. Winter's bite: beech trees survive complete defoliation due to spring late-frost damage by mobilizing old C reserves. New Phytol. 224, 625–631. https://doi.org/10.1111/nph.16047

D'Andrea, E., Rezaie, N., Battistelli, A., Gavrichkova, O., Kuhlmann, I., Matteucci, G., Moscatello, S., Proietti, S., Scartazza, A., Trumbore, S., Muhr, J., 2019. Winter's bite: beech trees survive complete defoliation

due to spring late-frost damage by mobilizing old C reserves. New Phytol. 224, 625–631. https://doi.org/10.1111/nph.16047

D'Andrea, E., Rezaie, N., Prislan, P., Gričar, J., Collalti, A., Muhr, J., Matteucci, G., 2020. Frost and drought: Effects of extreme weather events on stem carbon dynamics in a Mediterranean beech forest. Plant Cell Environ. 43. https://doi.org/10.1111/pce.13858

D'Orangeville, L., Houle, D., Duchesne, L., Phillips, R. P., Bergeron, Y., & Kneeshaw, D. , 2018. Beneficial effects of climate warming on boreal tree growth may be transitory. Nature communications, 9(1), 1-10.

D'Amato, A. W., Bradford, J. B., Fraver, S., & Palik, B. J., 2013. Effects of thinning on drought vulnerability and climate response in north temperate forest ecosystems. Ecological Applications, 23(8), 1735-1742.

de Dios, R.S., Benito-Garzón, M., Sainz-Ollero, H., 2009. Present and future extension of the Iberian submediterranean territories as determined from the distribution of marcescent oaks. Plant Ecol. 204. https://doi.org/10.1007/s11258-009-9584-5

De Frenne, P., Zellweger, F., Rodríguez-Sánchez, F. et al., 2019. Global buffering of temperatures under forest canopies. Nat. Ecol. Evol. 3, 744–749. https://doi.org/10.1038/s41559-019-0842-1

De Micco, V., Battipaglia, G., Balzano, A., Cherubini, P., & Aronne, G., 2016. Are wood fibres as sensitive to environmental conditions as vessels in tree rings with intra-annual density fluctuations (IADFs) in Mediterranean species?. Trees, 30(3), 971-983.

Decuyper, M., Chávez, R.O., Čufar, K., Estay, S.A., Clevers, J.G.P.W., Prislan, P., Gričar, J., Črepinšek, Z., Merela, M., de Luis, M., Notivoli, R.S., del Castillo, E.M., Rozendaal, D.M.A., Bongers, F., Herold, M., Sass-Klaassen, U., 2020. Spatio-temporal assessment of beech growth in relation to climate extremes in Slovenia – An integrated approach using remote sensing and tree-ring data. Agric. For. Meteorol. 287. https://doi.org/10.1016/j.agrformet.2020.107925

Di Filippo, A., Alessandrini, A., Biondi, F., Blasi, S., Portoghesi, L., Piovesan, G., 2010. Climate change and oak growth decline: Dendroecology and stand productivity of a Turkey oak (Quercus cerris L.) old stored coppice in Central Italy. Ann. For. Sci. 67. https://doi.org/10.1051/forest/2010031

Di Francesco, L., Fabbi, S., Santantonio, M., Bigi, S., & Poblet, J., 2010. Contribution of different kinematic models and a complex Jurassic stratigraphy in the construction of a forward model for the Montagna dei Fiori fault-related fold (Central Apennines, Italy). Geological Journal, 45(5-6), 489-505.

Dittmar, C., Fricke, W., Elling, W., 2006. Impact of late frost events on radial growth of common beech (Fagus sylvatica L.) in Southern Germany. Eur. J. For. Res. 125, 249–259. https://doi.org/10.1007/s10342-005-0098-y

Dittmar, C., Zech, W., Elling, W., 2003. Growth variations of Common beech (Fagus sylvatica L.) under different climatic and environmental conditions in Europe - A dendroecological study. For. Ecol. Manage. 173, 63–78. https://doi.org/10.1016/S0378-1127(01)00816-7

Drusch, M., Del Bello, U., Carlier, S., Colin, O., Fernandez, V., Gascon, F., Hoersch, B., Isola, C., Laberinti, P., Martimort, P., Meygret, A., Spoto, F., Sy, O., Marchese, F., Bargellini, P., 2012. Sentinel-2: ESA's Optical High-Resolution Mission for GMES Operational Services. Remote Sens. Environ. 120. https://doi.org/10.1016/j.rse.2011.11.026

Eilmann, B., Weber, P., Rigling, A., Eckstein, D., 2006. Growth reactions of Pinus sylvestris L. and Quercus pubescens Willd. to drought years at a xeric site in Valais, Switzerland. Dendrochronologia 23. https://doi.org/10.1016/j.dendro.2005.10.002

Falusi, M., Calamassi, R., 1996. Geographic variation and bud dormancy in beech seedlings (Fagus sylvatica L). Ann. des Sci. For. 53, 967–979. https://doi.org/10.1051/forest:19960505

Filipponi, F., 2021. Comparison LAI estimates from of high resolution satellite observations using different biophysical processors. In: Proceedings of the 1st International Electronic Conference on Agronomy, 3–17 May 2021. MDPI: Basel, Switzerland.

Folke, C., Carpenter, S., Walker, B., Scheffer, M., Elmqvist, T., Gunderson, L., & Holling, C. S., 2004. Regime shifts, resilience, and biodiversity in ecosystem management. Annu. Rev. Ecol. Evol. Syst., 35, 557-581.

Fox, J., Friendly, G. G., Graves, S., Heiberger, R., Monette, G., Nilsson, H., ... & Suggests, M. A. S. S., 2007. The car package. R Foundation for Statistical Computing, 1109.

Fritts, H. C., & Swetnam, T. W., 1989. Dendroecology: a tool for evaluating variations in past and present forest environments. Advances in ecological research, 19, 111-188.

Fritts, H. C., 1971. Dendroclimatology and dendroecology. Quaternary Research, 1(4), 419-449.

Fritts, H.C., 1976. Tree rings and climate. Academic Press, London.

Gavinet, J., Ourcival, J.M., Gauzere, J., García de Jalón, L., Limousin, J.M., 2020. Drought mitigation by thinning: Benefits from the stem to the stand along 15 years of experimental rainfall exclusion in a holm oak coppice. For. Ecol. Manage. 473. https://doi.org/10.1016/j.foreco.2020.118266

Gazol, A., Camarero, J.J., 2022. Compound climate events increase tree drought mortality across European forests. Sci. Total Environ. 816. https://doi.org/10.1016/j.scitotenv.2021.151604

Gazol, A., Camarero, J.J., Colangelo, M., de Luis, M., Martínez del Castillo, E., Serra-Maluquer, X., 2019. Summer drought and spring frost, but not their interaction, constrain European beech and Silver fir growth in their southern distribution limits. Agric. For. Meteorol. 278. https://doi.org/10.1016/j.agrformet.2019.107695

Gazol, A., Camarero, J.J., Vicente-Serrano, S.M., Sánchez-Salguero, R., Gutiérrez, E., de Luis, M., Sangüesa-Barreda, G., Novak, K., Rozas, V., Tíscar, P.A., Linares, J.C., Martín-Hernández, N., Martínez del Castillo, E., Ribas, M., García-González, I., Silla, F., Camisón, A., Génova, M., Olano, J.M., Longares, L.A., Hevia, A., Tomás-Burguera, M., Galván, J.D., 2018. Forest resilience to drought varies across biomes. Glob. Chang. Biol. 24. https://doi.org/10.1111/gcb.14082

Gentilesca, T., Camarero, J.J., Colangelo, M., Nolè, A., Ripullone, F., 2017. Drought-induced oak decline in the western mediterranean region: An overview on current evidences, mechanisms and management options to improve forest resilience. IForest 10. https://doi.org/10.3832/ifor2317-010

Geßler, A., Keitel, C., Kreuzwieser, J., Matyssek, R., Seiler, W., Rennenberg, H., 2007. Potential risks for European beech (Fagus sylvatica L.) in a changing climate. Trees - Struct. Funct. https://doi.org/10.1007/s00468-006-0107-x

Giorgi, F., Lionello, P., 2008. Climate change projections for the Mediterranean region. Glob. Planet. Change 63, 90–104. https://doi.org/10.1016/j.gloplacha.2007.09.005

González de Andrés, E., Rosas, T., Camarero, J.J., Martínez-Vilalta, J., 2021. The intraspecific variation of functional traits modulates drought resilience of European beech and pubescent oak. J. Ecol. 109. https://doi.org/10.1111/1365-2745.13743

Govaerts R, Frodin DG, 1998. World checklist and bibliography of Fagales (Betulaceae, Corylaceae, Fagaceae and Ticodendraceae). Royal Botanic Gardens, Kew

Grubb, P.J., 1977. The maintenance of species-richness in plant communities: the importance of the regeneration niche. Biol. Rev 52, 107–145. doi:10.1111/j.1469-185X.1977.tb01347.x

Guiot, J., 1991. The bootstrapped response function. Tree Ring Bull. 51.

Hacket-Pain, A.J., Cavin, L., Friend, A.D., Jump, A.S., 2016. Consistent limitation of growth by high temperature and low precipitation from range core to southern edge of European beech indicates widespread vulnerability to changing climate. Eur. J. For. Res. 135, 897–909. https://doi.org/10.1007/s10342-016-0982-7

Hacket-Pain, A.J., Friend, A.D., Lageard, J.G.A., Thomas, P.A., 2015. The influence of masting phenomenon on growth-climate relationships in trees: Explaining the influence of previous summers' climate on ring width. Tree Physiol. 35, 319–330. https://doi.org/10.1093/treephys/tpv007

Hagedorn, F., Shiyatov, S.G., Mazepa, V.S., Devi, N.M., Grigor'ev, A.A., Bartysh, A.A., Fomin, V. V., Kapralov, D.S., Terent'ev, M., Bugman, H., Rigling, A., Moiseev, P.A., 2014. Treeline advances along the Urals mountain range - driven by improved winter conditions? Glob. Chang. Biol. 20, 3530–3543. https://doi.org/10.1111/gcb.12613

Häkkinen, H., 1995. Does climatic warming increase the risk of frost damage in northern trees. Plant, Cell Environ.

Hanna, L., Kissick, A.L., McCroskey, E., Holland, J.D., 2019. Resilience to disturbance is a cross-scale phenomenon offering a solution to the disturbance paradox. Ecosphere 10. https://doi.org/10.1002/ecs2.2682

He, J.S., Zhang, Q. Bin, Bazzaz, F.A., 2005. Differential drought responses between saplings and adult trees in four co-occurring species of New England. Trees - Struct. Funct. 19, 442–450. https://doi.org/10.1007/s00468-004-0403-2

Heide, O.M., 1993. Dormancy release in beech buds (Fagus sylvatica) requires both chilling and long days. Physiol. Plant. 89, 187–191. https://doi.org/10.1111/j.1399-3054.1993.tb01804.x

Henrich, V., Jung, A., Götze, C., Sandow, C., Thürkow, D., Gläßer, C., 2009. Development of an online indices database: Motivation, concept and implementation, in: 6th EARSeL Imaging Spectroscopy SIG Workshop Innovative Tool for Scientific and Commercial Environment Applications. pp. 16–18.

Hepner, H., Lutter, R., Tullus, A., Kanal, A., Tullus, T., Tullus, H., 2020. Effect of Early Thinning Treatments on Above-Ground Growth, Biomass Production, Leaf Area Index and Leaf Growth Efficiency in a Hybrid Aspen Coppice Stand. Bioenergy Res. 13. https://doi.org/10.1007/s12155-020-10111-0

Himrane, H., Camarero, J.J., Gil-Pelegrín, E., 2004. Morphological and ecophysiological variation of the hybrid oak Quercus subpyrenaica (Q. faginea x Q. pubescens). Trees - Struct. Funct. 18. https://doi.org/10.1007/s00468-004-0340-0

Holmes, R., 1983. Computer-Assisted Quality Control in Tree-Ring Dating and Measurement. Tree-ring Bull.

Huete, A., Didan, K., Miura, T., Rodriguez, E.P., Gao, X., Ferreira, L.G., 2002. Overview of the radiometric and biophysical performance of the MODIS vegetation indices. Remote Sens. Environ. 83, 195–213. https://doi.org/10.1016/S0034-4257(02)00096-2

Huguet del Villar, E. H., 1935. Sur le nom de quelques Quercus et la systématique du faginea. Cavanillesia, 7, 57-70.

Isajev, V., Fady, B., Semerci, H., Andonovski, V., 2004. EUFORGEN Technical Guidelines for genetic conservation and use for European black pine (Pinus nigra). Bioversity Int.

Jetschke, G., van der Maaten, E., van der Maaten-Theunissen, M., 2019. Towards the extremes: A critical analysis of pointer year detection methods. Dendrochronologia. https://doi.org/10.1016/j.dendro.2018.11.004

Jump, A.S., Hunt, J.M., Peñuelas, J., 2006. Rapid climate change-related growth decline at the southern range edge of Fagus sylvatica. Glob. Chang. Biol. 12, 2163–2174. https://doi.org/10.1111/j.1365-2486.2006.01250.x

Jung, T., 2009. Beech decline in Central Europe driven by the interaction between Phytophthora infections and climatic extremes. For. Pathol. 39, 73–94. https://doi.org/10.1111/j.1439-0329.2008.00566.x

Juodvalkis, A., Kairiukstis, L., Vasiliauskas, R., 2005. Effects of thinning on growth of six tree species in north-temperate forests of Lithuania. Eur. J. For. Res. 124. https://doi.org/10.1007/s10342-005-0070-x

Kaproth, M., Cavender-Bares, J., 2016. Drought tolerance and climatic distributions of the American oaks. Int. Oaks 27.

Kirdyanov, A. V., Piermattei, A., Kolář, T., Rybníček, M., Krusic, P.J., Nikolaev, A.N., Reinig, F., Büntgen, U., 2018. Notes towards an optimal sampling strategy in dendroclimatology. Dendrochronologia 52, 162–166. https://doi.org/10.1016/j.dendro.2018.10.002

Kovács, B., Tinya, F., Ódor, P., 2017. Stand structural drivers of microclimate in mature temperate mixed forests. Agr. For. Met. 234–235, 11-21. https://doi.org/10.1016/j.agrformet.2016.11.268

Kreyling, J., Buhk, C., Backhaus, S., Hallinger, M., Huber, G., Huber, L., Jentsch, A., Konnert, M., Thiel, D., Wilmking, M., Beierkuhnlein, C., 2014. Local adaptations to frost in marginal and central populations of the dominant forest tree Fagus sylvatica L. as affected by temperature and extreme drought in common garden experiments. Ecol. Evol. 4, 594–605. https://doi.org/10.1002/ece3.971

Kullman, L., Öberg, L., 2009. Post-Little Ice Age tree line rise and climate warming in the Swedish Scandes: A landscape ecological perspective. J. Ecol. 97, 415–429. https://doi.org/10.1111/j.1365-2745.2009.01488.x

Lamichhane, J.R., 2021. Rising risks of late-spring frosts in a changing climate. Nat. Clim. Chang. https://doi.org/10.1038/s41558-021-01090-x

Lenz, A., Hoch, G., Vitasse, Y., Körner, C., 2013. European deciduous trees exhibit similar safety margins against damage by spring freeze events along elevational gradients. New Phytol. 200, 1166–1175. https://doi.org/10.1111/nph.12452

Liu, H.Q., Huete, A., 2019. A feedback based modification of the NDVI to minimize canopy background and atmospheric noise. IEEE Trans. Geosci. Remote Sens. 33, 457–465. https://doi.org/10.1109/tgrs.1995.8746027

Lloret, F., Jaime, L.A., Margalef-Marrase, J., Pérez-Navarro, M.A., Batllori, E., 2022. Short-term forest resilience after drought-induced die-off in Southwestern European forests. Sci. Total Environ. 806. https://doi.org/10.1016/j.scitotenv.2021.150940

Lloret, F., Keeling, E.G., Sala, A., 2011. Components of tree resilience: Effects of successive low-growth episodes in old ponderosa pine forests. Oikos 120, 1909–1920. https://doi.org/10.1111/j.1600-0706.2011.19372.x

Lloret, F., Siscart, D., Dalmases, C., 2004. Canopy recovery after drought dieback in holm-oak Mediterranean forests of Catalonia (NE Spain). Glob. Chang. Biol. 10. https://doi.org/10.1111/j.1365-2486.2004.00870.x

Lough, J.M., Fritts, H.C., 1987. An assessment of the possible effects of volcanic eruptions on North American climate using tree-ring data, 1602 to 1900 A.D. Clim. Change 10, 219–239. https://doi.org/10.1007/BF00143903

Lüdecke, D., Ben-Shachar, M., Patil, I., Waggoner, P., Makowski, D., 2021. performance: An R Package for Assessment, Comparison and Testing of Statistical Models. J. Open Source Softw. 6. https://doi.org/10.21105/joss.03139

Malandra, F., Vitali, A., Urbinati, C., Weisberg, P.J., Garbarino, M., 2019. Patterns and drivers of forest landscape change in the Apennines range, Italy. Reg. Environ. Chang. 19, 1973–1985. https://doi.org/10.1007/s10113-019-01531-6

Mancini, N.M., Mancini, G.M., Travaglini, D., Nocentini, S., Giannini, R., 2016. First results on the structure and seed production of beech stands at the timberline in the Monti della Laga (Gran Sasso and Monti della Laga National Park). l'italia For. e Mont. 31–47. https://doi.org/10.4129/ifm.2016.1.02

Manrique-Alba, À., Beguería, S., Camarero, J.J., 2022. Long-term effects of forest management on post-drought growth resilience: An analytical framework. Sci. Total Environ. 810. https://doi.org/10.1016/j.scitotenv.2021.152374

Maracchi, G., Sirotenko, O., & Bindi, M., 2005. Impacts of present and future climate variability on agriculture and forestry in the temperate regions: Europe. Climatic change, 70(1), 117-135.

Markonis, Y., Kumar, R., Hanel, M., Rakovec, O., Máca, P., & AghaKouchak, A., 2021. The rise of compound warm-season droughts in Europe. Science advances, 7(6), eabb9668.

Martín-Benito, D., Cherubini, P., Del Río, M., Cañellas, I., 2008. Growth response to climate and drought in Pinus nigra Arn. trees of different crown classes. Trees - Struct. Funct. 22. https://doi.org/10.1007/s00468-007-0191-6

Martínez-Sancho, E., Gutiérrez, E., Valeriano, C., Ribas, M., Popkova, M.I., Shishov, V. V., Dorado-Liñán, I., 2021. Intra-and inter-annual growth patterns of a mixed pine-oak forest under mediterranean climate. Forests 12. https://doi.org/10.3390/f12121746

Martín-Gómez, P., Aguilera, M., Pemán, J., Gil-Pelegrín, E., Ferrio, J.P., 2017. Contrasting ecophysiological strategies related to drought: the case of a mixed stand of Scots pine (Pinus sylvestris) and a submediterranean oak (Quercus subpyrenaica). Tree Physiol. 37. https://doi.org/10.1093/treephys/tpx101

Matisons, R., Jansone, D., Elferts, D., Adamovičs, A., Schneck, V., Jansons, Ā., 2019. fiPlasticity of response of tree-ring width of Scots pine provenances to weather extremes in Latvia. Dendrochronologia 54. https://doi.org/10.1016/j.dendro.2019.01.002

Mayor, X., Roda, F., 1993. Growth response of holm oak (Quercus ilex L) to commercial thinning in the Montseny Mountains (NE Spain). Ann. des Sci. For. 50. https://doi.org/10.1051/forest:19930303

Menzel, A., Helm, R., & Zang, C., 2015. Patterns of late spring frost leaf damage and recovery in a European beech (Fagus sylvatica L.) stand in south-eastern Germany based on repeated digital photographs. Frontiers in Plant Science, 6, 110.

Menzel, A., Seifert, H., Estrella, N., 2011. Effects of recent warm and cold spells on European plant phenology. Int. J. Biometeorol. 55, 921–932. https://doi.org/10.1007/s00484-011-0466-x

Moreno-Gutiérrez, C., Battipaglia, G., Cherubini, P., Saurer, M., Nicolas, E., Contreras, S., & Querejeta, J. I., 2012. Stand structure modulates the long-term vulnerability of Pinus halepensis to climatic drought in a semiarid Mediterranean ecosystem. Plant, Cell & Environment, 35(6), 1026-1039.

Müllerová, J., Pejcha, V., Altman, J., Plener, T., Dörner, P., Doleal, J., 2016. Detecting Coppice Legacies from Tree Growth. PLoS One 11. https://doi.org/10.1371/journal.pone.0147205

Nolè, A., Rita, A., Ferrara, A.M.S., Borghetti, M., 2018. Effects of a large-scale late spring frost on a beech (Fagus sylvatica L.) dominated Mediterranean mountain forest derived from the spatio-temporal variations of NDVI. Ann. For. Sci. 75, 1–11. https://doi.org/10.1007/s13595-018-0763-1

Novick, K., Jo, I., D'Orangeville, L., Benson, M., Au, T.F., Barnes, M., Denham, S., Fei, S., Heilman, K., Hwang, T., Keyser, T., Maxwell, J., Miniat, C., McLachlan, J., Pederson, N., Wang, L., Wood, J.D., Phillips, R.P., 2022. The Drought Response of Eastern US Oaks in the Context of Their Declining Abundance. Bioscience 72. https://doi.org/10.1093/biosci/biab135

Nowacki, G.J., Abrams, M.D., 1997. Radial-growth averaging criteria for reconstructing disturbance histories from presettlement-origin oaks. Ecol. Monogr. 67. https://doi.org/10.1890/0012-9615(1997)067[0225:RGACFR]2.0.CO;2

Nussbaumer, A., Gessler, A., Benham, S., de Cinti, B., Etzold, S., Ingerslev, M., Jacob, F., Lebourgeois, F., Levanic, T., Marjanović, H., Nicolas, M., Ostrogović Sever, M.Z., Priwitzer, T., Rautio, P., Roskams, P., Sanders, T.G.M., Schmitt, M., Šrámek, V., Thimonier, A., Ukonmaanaho, L., Verstraeten, A., Vesterdal, L., Wagner, M., Waldner, P., Rigling, A., 2021. Contrasting Resource Dynamics in Mast Years for European Beech and Oak—A Continental Scale Analysis. Front. For. Glob. Chang. 4. https://doi.org/10.3389/ffgc.2021.689836

Olano, J.M., García-Cervigón, A.I., Sangüesa-Barreda, G., Rozas, V., Muñoz-Garachana, D., García-Hidalgo, M., García-Pedrero, Á., 2021. Satellite data and machine learning reveal the incidence of late frost defoliations on Iberian beech forests. Ecol. Appl. 31. https://doi.org/10.1002/eap.2288

Piermattei, A., 2013. Climate Influence on the Expansion and Tree-Ring Growth of Pinus nigra L. at High Altitude in the Central Apennines. Open For. Sci. J. 6, 54–56. https://doi.org/10.2174/1874398601306010054

Piermattei, A., Campelo, F., Büntgen, U., Crivellaro, A., Garbarino, M., Urbinati, C., 2020. Intra-annual density fluctuations (IADFs) in Pinus nigra (JF Arnold) at high-elevation in the central Apennines (Italy). Trees, 1-11. https://doi.org/10.1007/s00468-020-01956-1R Core Team, 2018. A language and environment for statistical computing. R Foundation for Statistical Computing. http://www.R-project.org/

Piermattei, A., Garbarino, M., Urbinati, C., 2014. Structural attributes, tree-ring growth and climate sensitivity of Pinusnigra Arn. at high altitude: Common patterns of a possible treeline shift in the central Apennines (Italy). Dendrochronologia 32, 210–219. https://doi.org/10.1016/j.dendro.2014.05.002

Piermattei, A., Lingua, E., Urbinati, C., Garbarino, M., 2016. Pinus nigra anthropogenic treelines in the central Apennines show common pattern of tree recruitment. Eur. J. For. Res. 135, 1119–1130. https://doi.org/10.1007/s10342-016-0999-y

Piovesan, G., Bernabei, M., Di Filippo, A., Romagnoli, M., Schirone, B., 2003. A long-term tree ring beech chronology from a high-elevation old-growth forest of Central Italy. Dendrochronologia 21, 13–22. https://doi.org/10.1078/1125-7865-00036

Piovesan, G., Biondi, F., Di Filippo, A., Alessandrini, A., Maugeri, M., 2008. Drought-driven growth reduction in old beech (Fagus sylvatica L.) forests of the central Apennines, Italy. Glob. Chang. Biol. 14, 1265–1281. https://doi.org/10.1111/j.1365-2486.2008.01570.x

Politis, D.N., Romano, J.P., 1994. The stationary bootstrap. J. Am. Stat. Assoc. 89, 1303–1313. https://doi.org/10.1080/01621459.1994.10476870

Pollastrini, M., Puletti, N., Selvi, F., Iacopetti, G., Bussotti, F., 2019. Widespread Crown Defoliation After a Drought and Heat Wave in the Forests of Tuscany (Central Italy) and Their Recovery—A Case Study From Summer 2017. Front. For. Glob. Chang. 2. https://doi.org/10.3389/ffgc.2019.00074

Pott, R., 2000. Palaeoclimate and vegetation - long-term vegetation dynamics in central Europe with particular reference to beech. Phytocoenologia 30, 285–333. https://doi.org/10.1127/phyto/30/2000/285

Prendin, A.L., Carrer, M., Karami, M., Hollesen, J., Bjerregaard Pedersen, N., Pividori, M., Treier, U.A., Westergaard-Nielsen, A., Elberling, B., Normand, S., 2020. Immediate and carry-over effects of insect outbreaks on vegetation growth in West Greenland assessed from cells to satellite. J. Biogeogr. 47. https://doi.org/10.1111/jbi.13644

Pretzsch, H., Hilmers, T., Uhl, E., Bielak, K., Bosela, M., del Rio, M., Dobor, L., Forrester, D.I., Nagel, T.A., Pach, M., Avdagić, A., Bellan, M., Binder, F., Bončina, A., Bravo, F., De-Dios-García, J., Dinca, L., Drozdowski, S., Giammarchi, F., Hoehn, M., Ibrahimspahić, A., Jaworski, A., Klopčič, M., Kurylyak, V., Lévesque, M., Lombardi, F., Matović, B., Ordóñez, C., Petráš, R., Rubio-Cuadrado, A., Stojanovic, D., Skrzyszewski, J., Stajić, B., Svoboda, M., Versace, S., Zlatanov, T., Tognetti, R., 2021. European beech stem diameter grows better in mixed than in mono-specific stands at the edge of its distribution in mountain forests. Eur. J. For. Res. 140, 127–145. https://doi.org/10.1007/s10342-020-01319-y

Príncipe, A., van der Maaten, E., van der Maaten-Theunissen, M., Struwe, T., Wilmking, M., & Kreyling, J., 2017. Low resistance but high resilience in growth of a major deciduous forest tree (Fagus sylvatica L.) in response to late spring frost in southern Germany. Trees, 31(2), 743-751.

Prislan, P., Čufar, K., De Luis, M., & Gričar, J., 2018. Precipitation is not limiting for xylem formation dynamics and vessel development in European beech from two temperate forest sites. Tree Physiology, 38(2), 186-197.

Rao, M. P., Cook, E. R., Cook, B. I., Anchukaitis, K. J., D'Arrigo, R. D., Krusic, P. J., & LeGrande, A. N., 2019. A double bootstrap approach to Superposed Epoch Analysis to evaluate response uncertainty. Dendrochronologia, 55, 119-124.

Rita, A., Camarero, J.J., Nolè, A., Borghetti, M., Brunetti, M., Pergola, N., Serio, C., Vicente-Serrano, S.M., Tramutoli, V., Ripullone, F., 2020. The impact of drought spells on forests depends on site conditions: The case of 2017 summer heat wave in southern Europe. Glob. Chang. Biol. 26, 851–863. https://doi.org/10.1111/gcb.14825

Rivas-Martínez, S., & Saenz Lain, C., 1991. Enumeration of Quercus of the Iberian Peninsula. Rivasgodaya (Spain).

Rouse, J.W., Haas, R.H., Schell, J.A., Deeering, D.., 1973. Monitoring vegetation systems in the Great Plains with ERTS (Earth Resources Technology Satellite)., in: Third Earth Resources Technology Satellite-1 Symposium. pp. 309–317.

Rozas, V., Camarero, J.J., Sangüesa-Barreda, G., Souto, M., García-González, I., 2015. Summer drought and ENSO-related cloudiness distinctly drive Fagus sylvatica growth near the species rear-edge in northern Spain. Agric. For. Meteorol. 201, 153–164. https://doi.org/10.1016/j.agrformet.2014.11.012

Rubio-Cuadrado, Á., Camarero, J.J., del Río, M., Sánchez-González, M., Ruiz-Peinado, R., Bravo-Oviedo, A., Gil, L., Montes, F., 2018. Long-term impacts of drought on growth and forest dynamics in a temperate beech-oak-birch forest. Agric. For. Meteorol. 259, 48–59. https://doi.org/10.1016/j.agrformet.2018.04.015

Rubio-Cuadrado, Á., Camarero, J.J., Rodríguez-Calcerrada, J., Perea, R., Gómez, C., Montes, F., Gil, L., 2021. Impact of successive spring frosts on leaf phenology and radial growth in three deciduous tree species with contrasting climate requirements in central Spain. Tree Physiol. https://doi.org/10.1093/treephys/tpab076

Rubio-Cuadrado, Á., Gómez, C., Rodríguez-Calcerrada, J., Perea, R., Gordaliza, G.G., Camarero, J.J., Montes, F., Gil, L., 2021. Differential response of oak and beech to late frost damage: an integrated analysis from organ to forest. Agric. For. Meteorol. 297. https://doi.org/10.1016/j.agrformet.2020.108243

Sanchez-Salguero, R., Camarero, J.J., Gutiérrez, E., Gazol, A., Sangüesa-Barreda, G., Moiseev, P., Linares, J.C., 2018. Climate warming alters age-dependent growth sensitivity to temperature in eurasian alpine treelines. Forests 9, 688. https://doi.org/10.3390/f9110688

Sangüesa-Barreda, G., Di Filippo, A., Piovesan, G., Rozas, V., Di Fiore, L., García-Hidalgo, M., García-Cervigón, A.I., Muñoz-Garachana, D., Baliva, M., Olano, J.M., 2021. Warmer springs have increased the

frequency and extension of late-frost defoliations in southern European beech forests. Sci. Total Environ. 775. https://doi.org/10.1016/j.scitotenv.2021.145860

Scheffer, M., Carpenter, S., Foley, J. A., Folke, C., & Walker, B. 2001. Catastrophic shifts in ecosystems. Nature, 413(6856), 591-596.

Scholz, A., Klepsch, M., Karimi, Z., & Jansen, S., 2013. How to quantify conduits in wood?. Frontiers in plant science, 4, 56.

Schwarz, J. A., & Bauhus, J., 2019. Benefits of mixtures on growth performance of silver fir (Abies alba) and European beech (Fagus sylvatica) increase with tree size without reducing drought tolerance. Frontiers in Forests and Global Change, 79.

Schweingruber, F.H., 1996. Tree Rings and Environment Dendroecology. Paul Haupt.

Schweingruber, F.H., Eckstein, D., Serre-Bachet, F., 1990. Identification, Presentation and Interpretation of Event Years and Pointer Years in Dendrochronology. Dendrochronologia 8, 9–38.

Serrada, R., Allué, M., & San Miguel, A., 1992. The coppice system in Spain. Current situation, state of art and major areas to be investigated. Ann Ist Sper Selv, 23, 266-275.

Serra-Maluquer, X., Gazol, A., Sangüesa-Barreda, G., Sánchez-Salguero, R., Rozas, V., Colangelo, M., Gutiérrez, E., Camarero, J.J., 2019. Geographically Structured Growth decline of Rear-Edge Iberian Fagus sylvatica Forests After the 1980s Shift Toward a Warmer Climate. Ecosystems 22, 1325–1337. https://doi.org/10.1007/s10021-019-00339-z

Šimůnek, V., Vacek, Z., Vacek, S., Ripullone, F., Hájek, V., D'andrea, G., 2021. Tree rings of european beech (Fagus sylvatica l.) indicate the relationship with solar cycles during climate change in central and southern europe. Forests 12. https://doi.org/10.3390/f12030259

Speer, J.H., 2010. Fundamentals of tree-ring research. University of Arizona Press.

Spinoni, J., Vogt, J. V., Naumann, G., Barbosa, P., Dosio, A., 2018. Will drought events become more frequent and severe in Europe? Int. J. Climatol. 38. https://doi.org/10.1002/joc.5291

Szeicz, J.M., MacDonald, G.M., 1994. Age-dependent tree-ring growth responses of subarctic white spruce to climate. Can. J. For. Res. 24, 120–132. https://doi.org/10.1139/x94-017

Thomas, F.M., Blank, R., Hartmann, G., 2002. Abiotic and biotic factors and their interactions as causes of oak decline in Central Europe. For. Pathol. 32, 277–307. https://doi.org/10.1046/j.1439-0329.2002.00291.x

Thuiller, W., 2004. Patterns and uncertainties of species' range shifts under climate change. Glob. Chang. Biol. 10. https://doi.org/10.1111/j.1365-2486.2004.00859.x

Thurm, E.A., Uhl, E., Pretzsch, H., 2016. Mixture reduces climate sensitivity of Douglas-fir stem growth. For. Ecol. Manage. 376. https://doi.org/10.1016/j.foreco.2016.06.020

Tognetti, R., Cherubini, P., Marchi, S., Raschi, A., 2007. Leaf traits and tree rings suggest different water-use and carbon assimilation strategies by two co-occurring Quercus species in a Mediterranean mixed-forest stand in Tuscany, Italy. Tree Physiol. 27. https://doi.org/10.1093/treephys/27.12.1741

Tognetti, R., Lasserre, B., Di Febbraro, M., Marchetti, M., 2019. Modeling regional drought-stress indices for beech forests in Mediterranean mountains based on tree-ring data. Agric. For. Meteorol. 265, 110–120. https://doi.org/10.1016/j.agrformet.2018.11.015

Tuel, A., & Eltahir, E. A., 2020. Why is the Mediterranean a climate change hot spot?. Journal of Climate, 33(14), 5829-5843.

Ünsalan, C., Boyer, K.L., 2004. Linearized vegetation indices based on a formal statistical framework. IEEE Trans. Geosci. Remote Sens. 42, 1575–1585. https://doi.org/10.1109/TGRS.2004.826787

van der Maaten-Theunissen, M., van der Maaten, E., Bouriaud, O., 2015. PointRes: An R package to analyze pointer years and components of resilience. Dendrochronologia 35, 34–38. https://doi.org/10.1016/j.dendro.2015.05.006

Vayreda, J., Martinez-Vilalta, J., Gracia, M., Canadell, J. G., & Retana, J., 2016. Anthropogenic-driven rapid shifts in tree distribution lead to increased dominance of broadleaf species. Global Change Biology, 22(12), 3984-3995.

Vicente-Serrano, S.M., Tomas-Burguera, M., Beguería, S., Reig, F., Latorre, B., Peña-Gallardo, M., Luna, M.Y., Morata, A., González-Hidalgo, J.C., 2017. A high resolution dataset of drought indices for Spain. Data 2. https://doi.org/10.3390/data2030022

Vila-Viçosa, C., Gonçalves, J., Honrado, J., Lomba, Â., Almeida, R.S., Vázquez, F.M., Garcia, C., 2020. Late Quaternary range shifts of marcescent oaks unveil the dynamics of a major biogeographic transition in southern Europe. Sci. Rep. 10. https://doi.org/10.1038/s41598-020-78576-9

Vitali, A., Camarero, J.J., Garbarino, M., Piermattei, A., Urbinati, C., 2017. Deconstructing human-shaped treelines: Microsite topography and distance to seed source control Pinus nigra colonization of treeless areas in the Italian Apennines. For. Ecol. Manage. 406, 37–45. https://doi.org/10.1016/j.foreco.2017.10.004

Vitali, A., Garbarino, M., Camarero, J.J., Malandra, F., Toromani, E., Spalevic, V., Čurović, M., Urbinati, C., 2019. Pine recolonization dynamics in Mediterranean human-disturbed treeline ecotones. For. Ecol. Manage. 435, 28–37. https://doi.org/10.1016/j.foreco.2018.12.039

Vitali, A., Urbinati, C., Weisberg, P.J., Urza, A.K., Garbarino, M., 2018. Effects of natural and anthropogenic drivers on land-cover change and treeline dynamics in the Apennines (Italy). J. Veg. Sci. 29, 189–199. https://doi.org/10.1111/jvs.12598

Vitasse, Y., Basler, D., 2013. What role for photoperiod in the bud burst phenology of European beech. Eur. J. For. Res. https://doi.org/10.1007/s10342-012-0661-2

Vitasse, Y., Baumgarten, F., Zohner, C.M., Kaewthongrach, R., Fu, Y.H., Walde, M.G., Moser, B., 2021. Impact of microclimatic conditions and resource availability on spring and autumn phenology of temperate tree seedlings. New Phytol. 232. https://doi.org/10.1111/nph.17606

Vitasse, Y., Bottero, A., Cailleret, M., Bigler, C., Fonti, P., Gessler, A., Lévesque, M., Rohner, B., Weber, P., Rigling, A., Wohlgemuth, T., 2019. Contrasting resistance and resilience to extreme drought and late spring frost in five major European tree species. Glob. Chang. Biol. 25. https://doi.org/10.1111/gcb.14803

Vitasse, Y., Lenz, A., Körner, C., 2014. The interaction between freezing tolerance and phenology in temperate deciduous trees. Front. Plant Sci. 5. https://doi.org/10.3389/fpls.2014.00541

Vodnik, D., Gričar, J., Lavrič, M., Ferlan, M., Hafner, P., Eler, K., 2019. Anatomical and physiological adjustments of pubescent oak (Quercus pubescens Willd.) from two adjacent sub-Mediterranean ecosites. Environ. Exp. Bot. 165. https://doi.org/10.1016/j.envexpbot.2019.06.010

von Arx, G., & Carrer, M., 2014. ROXAS–A new tool to build centuries-long tracheid-lumen chronologies in conifers. Dendrochronologia, 32(3), 290-293.

von Arx, G., Carrer, M., Björklund, J., & Fonti, P., 2018. Quantitative wood anatomy opens a weekly to millennial time window in tree-ring research. In EGU General Assembly Conference Abstracts (p. 18929).

von Arx, G., Crivellaro, A., Prendin, A. L., Čufar, K., & Carrer, M., 2016. Quantitative wood anatomy—practical guidelines. Frontiers in plant science, 7, 781.

Wang, W.J., He, H.S., Thompson, F.R., Spetich, M.A., Fraser, J.S., 2018. Effects of species biological traits and environmental heterogeneity on simulated tree species distribution shifts under climate change. Sci. Total Environ. 634. https://doi.org/10.1016/j.scitotenv.2018.03.353

Wargo, P. M., 1996. Consequences of environmental stress on oak: predisposition to pathogens. In Annales des sciences forestières (Vol. 53, No. 2-3, pp. 359-368). EDP Sciences.

Weiss, M., Baret, F., 2016. S2ToolBox Level 2 products: LAI, FAPAR, FCOVER - Version 1.1. Sentin. ToolBox Level2 Prod. 53.

Wigley, T.M.L., Briffa, K.R., Jones, P.D., 1984. On the average value of correlated time series with applications in dendroclimatology and hydrometeorology. J. Clim. Appl. Meteorol. 23, 201–213. https://doi.org/10.1175/1520-0450(1984)023<0201:OTAVOC>2.0.CO;2

Xue, J., Su, B., 2017. Significant remote sensing vegetation indices: A review of developments and applications. J. Sensors. https://doi.org/10.1155/2017/1353691

Zalloni, E., Battipaglia, G., Cherubini, P., Saurer, M., & De Micco, V., 2019. Wood growth in pure and mixed Quercus ilex L. forests: Drought influence depends on site conditions. Frontiers in Plant Science, 10, 397.

Zang, C., Biondi, F., 2015. Treeclim: An R package for the numerical calibration of proxy-climate relationships. Ecography (Cop.). 38, 431–436. https://doi.org/10.1111/ecog.01335

Zellweger, F., Coomes, D., Jonathan Lenoir J., Depauw, L., Maes, S.L., Wulf, M., Kirby, K.J., Brunet, J., Kopecký, M., Máliš, F., Schmidt, W., et al., 2019. Seasonal drivers of understory temperature buffering in temperate deciduous forests across Europe. Glob. Ecol. Biog. 28 (12), 1774-1786. doi/full/10.1111/geb.12991

Zhang, Z., 2015. Tree-rings, a key ecological indicator of environment and climate change. Ecol. Indic. 51, 107–116. https://doi.org/10.1016/j.ecolind.2014.07.042

Zohner, C.M., Mo, L., Renner, S.S., Svenning, J.C., Vitasse, Y., Benito, B.M., Ordonez, A., Baumgarten, F., Bastin, J.F., Sebald, V., Reich, P.B., Liang, J., Nabuurs, G.J., De-Migueln, S., Alberti, G., Antón-Fernández, C., Balazy, R., Brändli, U.B., Chen, H.Y.H., Chisholm, C., Cienciala, E., Dayanandan, S., Fayle, T.M., Frizzera, L., Gianelle, D., Jagodzinski, A.M., Jaroszewicz, B., Jucker, T., Kepfer-Rojas, S., Khan, M.L., Kim, H.S., Korjus, H., Johannsen, V.K., Laarmann, D., Langn, M., Zawila-Niedzwiecki, T., Niklaus, P.A., Paquette, A., Pretzsch, H., Saikia, P., Schall, P., Seben, V., Svoboda, M., Tikhonova, E., Viana, H., Zhang, C., Zhao, X., Crowther, T.W., 2020. Late-spring frost risk between 1959 and 2017 decreased in North America but increased in Europe and Asia. Proc. Natl. Acad. Sci. U. S. A. 117. https://doi.org/10.1073/pnas.1920816117

Zohner, C.M., Rockinger, A., Renner, S.S., 2019. Increased autumn productivity permits temperate trees to compensate for spring frost damage. New Phytol. 221, 789–795. https://doi.org/10.1111/nph.15445